MASTERARBEIT / MASTER'S THESIS

Titel der Masterarbeit / Title of the Master's Thesis

„Semisynthesis of a lipidated bank vole prion protein"

verfasst von / submitted by

Alexander Buchner BSc

angestrebter akademischer Grad / in partial fulfilment of the requirements for the degree of

Master of Science (MSc)

Wien, 2022 / Vienna 2022

Acknowledgements

First of all, I want to immensely thank my supervisor and the head of the institute of biological chemistry Univ.-Prof. Dr. Christian F. W. Becker, for giving me the opportunity to work on this exciting master's thesis project. Through his interesting lectures during my studies, I was able to get motivated about this topic in advance. Whenever I had questions, I could always count on advice from him and I am thankful that he did a proof-reading of my written thesis.

Special thanks to my Co-supervisor Mag. Gerhard Niederacher, who guided me through the practical work in the first weeks and if there occurred any problems, he had always an open ear for me. I was able to learn a lot from him, since he is familiar with many molecular biology methods. Additionally, he also did a proof-reading of my work.

Besides my supervisors, I want to mention Mag. Manuel Felkl and Alanca Schmid, MSc., as they both introduced me to the world of solid phase peptide synthesis. Especially Alanca shared a lot of her experience regarding SPPS and the purification procedure with me. I am very grateful for their help, as I was quite unexperienced in the area of SPPS – thank you.

Furthermore, I would like to thank all the members of the Becker group for their scientific support, any motivating words if something did not go according to plan and for the great time I had during my apprenticeship in the research group. It was a pleasure to get to know everyone and I will not forget a lot of great moments we shared at lunch, in the big office or at the outing.

Many thanks to the administration staff at the University of Vienna for handling the submission of my master thesis.

Last, I am very thankful for all the support I received from my family – my mother Petra and my brother Martin - during the last steps of my studies. Further thanks, to all my friends which kept me motivated and accompanied me during my time at university.

Abstract

In this work a semisynthetic modified bank vole prion protein was produced. It is known that the cellular prion protein (PrP^C) is linked to the glycosylphosphatidylinositol-anchor (GPI-anchor) *in vivo* and therefore the prion protein is connected to the cellular membrane. It is difficult to purify homogenous cellular prion proteins, which include posttranslational modifications (PTM), such as the GPI-anchor, in sufficient amounts. However, robust access to homogenously modified prion proteins is required to advance research in the area of prion diseases. Therefore, new ways to overcome the challenging task to produce modified prion proteins were explored. One of these methods is called "semisynthesis of proteins". In this approach a recombinantly expressed protein and a chemically synthesized peptide are chemoselectively and regioselectively joined together. For example, this method is commonly used in the field of protein engineering to incorporate non-coded amino acids into proteins. The first steps of this master thesis included the recombinant expression of full-length bank vole prion protein (amino acids 23-231) in *E. coli*. The full-length construct was purified using a preparative high performance liquid chromatography (HPLC) system. In a second step, a GPI-anchor mimicking peptide was chemically synthesized via solid phase peptide synthesis (SPPS). Once the purification was done, the two segments were joined together via a reaction called "Expressed Protein Ligation (EPL)". Semisynthetic bank vole prion protein was then purified and folded to obtain the correct tertiary structure. Correct folding of the lipidated bank vole prion protein (bvPrP) was proven by performing circular dichroism (CD) measurements. Human (hPrP) and murine prion protein was previously produced by semisynthesis and subsequent usage in *in vitro* experiments has led to a better insight in the emergence of prion diseases, such as the Creuzfeldt-Jakob disease (CJD) in humans. The bank vole prion protein that was obtained in this work will be further used to perform *in vivo* experiments in the bank vole model organism by collaborators in the US. Due to the sequence similarities of the bvPrP with the hPrP the expected results can also provide insights on prion diseases in general.

Zusammenfassung

Das Ziel dieser Arbeit war es ein semisynthetisches, modifiziertes Rötelmaus Prion Protein herzustellen. Es ist bekannt, dass das zelluläre Prion Protein *in vivo* mit einem Glykosylphosphatidylinositol-Anker (GPI-Anker) verbunden und dadurch in der zellulären Membran verankert ist. Dies erschwert eine direkte Aufreinigung von homogenen Prion-Proteinen, welche eine posttranslationale Modifikation (PTM) wie den GPI-Anker aufweisen. Es wäre jedoch notwendig solch homogene, modifizierte Prion Proteine einfach und vor allem in ausreichenden Mengen produzieren zu können, um im Forschungsbereich der Prion-Erkrankungen voranzuschreiten. Diesbezüglich wurde nach Wegen gesucht, um diese herausfordernde Aufgabe leichter zu bewältigen. Mittlerweile gibt es verschiedene Möglichkeiten Prion Proteine mit PTMs herzustellen. Eine Methode ist die sogenannte „Semisynthese von Proteinen". Diese beruht auf der Strategie, zwei Polypeptidfragmente des Proteins separat herzustellen und diese sowohl chemoselektiv als auch regioselektiv miteinander zu verbinden. Ein Teil ist das rekombinant exprimierte Protein und der andere ein chemisch-synthetisiertes Peptid. Die Methode der Semisynthese wird zum Beispiel häufig im Bereich des „Protein-Engineering" eingesetzt, um nicht-kodierte Aminosäuren in Proteine einzubauen. Die ersten Schritte dieser Masterarbeit beinhalteten die rekombinante Expression des vollständigen Rötelmaus Prion Proteins (Aminosäuren 23-231) in *E. coli*. Das Rötelmaus Prion Protein wurde über präparative Hochdruckflüssigkeitschromatographie (HPLC) aufgereinigt. Ein peptidisches GPI-Anker Mimetikum wurde über die Methode der Festphasenpeptidsynthese hergestellt. Im Zuge der Ligation der beiden Peptidsegmente, genannt „Expressed Protein Ligation", wurde das GPI-Anker-Mimetikum mit dem vollständigen Rötelmaus Prion Protein verknüpft. Das aufgereinigte Ligationsprodukt wurde im letzten Schritt gefaltet, um die biologische Funktionsfähigkeit für weitere Experimente zu gewährleisten. Die Faltung wurde durch eine Messung mit einem zirkularen Dichroismus (CD) Spektrometer nachgewiesen. Unter der Anwendung dieser Methode, konnte man schon erfolgreich semisynthetische humane und murine Prion Proteine herstellen. Diese modifizierten humanen Prion Proteine werden für *in vitro* Experimente zur Untersuchung der Entstehung von Prion-Krankheiten, wie z.B.: die Creuzfeldt-Jakob-Krankheit im Menschen, verwendet. Das im Zuge dieser Masterarbeit hergestellte Rötelmaus Prion Protein kann von einem Partner, welchem die Rötelmaus als Modell Organismus zur Verfügung steht, für *in vivo*

Experimente genützt werden, um die Entstehung von Prion Krankheiten genauer untersuchen zu können. Die Kombination aus der Möglichkeit Rötelmaus Prion Proteine einfacher herzustellen und die Verfügbarkeit von Modellorganismen bietet eine Grundlage für die Untersuchung von Prion Krankheiten. Die daraus gewonnenen Erkenntnisse können eventuell einen Aufschluss über Prion Erkrankungen im Allgemeinen geben.

Table of Contents

List of Figures

Index of Tables

List of Schemes

1 Introduction

1.1 Prion Diseases

The host encoded cellular prion protein is closely linked to an infectious, progressive, and neurodegenerative condition which is called prion disease or transmissible spongiform encephalopathy (TSE).[1,2] Although the pathophysiological processes that trigger the disease are not well understood yet, it is known that incorrect folding and aggregation of the cellular prion protein play an important role in the development of prion illnesses. Prion diseases can affect humans as well as animals. These different manifestations of the disease include for example Scrapie in sheep, BSE in cattle, FSE in cats and Kuru, Gerstman-Sträussler-Scheinker (GSS) disease, fatal familial insomnia (FFI) and Creuzfeldt-Jakob disease (CJD) in humans.[3] The most common human prion disease is CJD and there are three different possibilities of how it can arise. First, the disease can be acquired by infection, second it can arise sporadically (sCJD) and third CJD can be inherited as autosomal dominant mutation of the PrP^c encoding gene. The symptoms of the Creuzfeldt-Jakob disease first manifest themselves in rapidly increasing dementia. This is accompanied by problems with the muscle coordination, sudden changes in personality and impaired vision. As the disease progresses these mental disorders become severe for the organism and eventually will be lethal.[4] Nowadays human prion diseases are rare, although this was not always the case. Back in the 1950s, Kuru drew the attention to Papa New Guinea due to a spread within a primitive tribe. It was a ritual for kinship groups of the fore tribe to consume the deceased relatives at mortuary feasts, which triggered the spread among the community. The transmission of kuru was eventually stopped by ending cannibalism.[3,5] To proof the hypothesis that Kuru is infectious, chimpanzees were inoculated with brain-derived tissues of infected humans. In turn the monkeys also became ill, making Kuru the first proven transmissible human prion disease.[6] At that time, it was believed that transmissible diseases are only transmitted and triggered by genetic material, more precisely by nucleic acids (DNA or RNA). In 1982, this assumption was questioned by Stanley Prusiner and co-workers. They claimed that infectious diseases can be caused by proteinaceous infectious particles. Prusiner suggested that these particles, or as he named them "prions", are not only transmissible but also heritable.[7,8] In 1984, they identified 15 characteristic amino acids at the end of the protein, which allowed them to find the corresponding gene. In collaboration with other scientists working in the field, they were able to show that several

mammalian organisms carry the PrP gene in their genome. To their surprise, for example, the mice expressed the prion protein without getting sick. With these new findings, the question arose whether the prion protein is not involved in the infectious disease or whether two different types of the prion protein are present in a sick organism.[3] Shortly thereafter, they created a cDNA-library from scrapie-infected hamster brain tissues by testing various oligonucleotides for complementarity with the N-terminus. This revealed a gene encoding PrP 27-30. Ultimately, they were able to show that these scrapie prion proteins with a molecular mass within the range of 27-30 kDa were not degraded by protein-degrading enzymes.[7,9] As a result, it became clear that the TSE-causing prion protein is a variant of the benign prion protein. Following the results the nomenclature PrP^c for the cellular prion protein and PrP^{Sc} for the scrape prion protein has been defined.[3,7] Since the scrapie prion protein is significantly involved in pathogenesis and is also responsible for infectivity, the focus of today's research is on PrP^{Sc}.[10] The molecular process in which PrP^{Sc} induces a conformational change in PrP^C and the significance of the post-translational modifications, that make the interaction between these two PrP variants possible in the first place, are important questions that cannot yet be answered completely.[13] Accurate new knowledge derived from the study of scrapie prion proteins and their influence on the pathophysiological process could also provide essential information for other neurodegenerative diseases such as Alzheimer's Disease, amyotrophic lateral sclerosis, Huntington's disease or other similar prion-like diseases. Prion-like diseases show similar aspects as there are also misfolded proteins present in the brain with the potential to aggregate. These proteins are called prionoids. In some cases even prionoids can be transmissible, as it could be shown for α-synuclein prionoids that are present in multiple system atrophy (MSA).[11,12] These coherences are highlighting the importance of an accurate understanding of prion diseases.

1.2 Cellular Prion Protein

The cellular prion protein is a cell surface protein which is mainly expressed in the central nervous system, but can be found in other cell types or tissues as well.[14-16,30] The human PrP gene, which consists of two exons and one intron, is located on the short arm of chromosome 20. However, exon 1 is a non-coding exon and thus probably functions more as a transcription site. In contrast to PrP genes from other organisms, it includes only a single transcriptional

start site.[17,18,31] In comparison, the *mus musculus* (house mouse) PrP gene includes four exons.[19] Studies on the human PrP gene revealed that the encoded protein is composed out of 254 amino acids.[18,20] The sequence of the cellular prion protein is separated into different sections. The first 22 amino acids serve as a N-terminal signaling sequence to enter the secretory pathway. Then there is the flexible N-terminal part, which includes the amino acids 23-120. The amino acids 121-231 define the C-terminal globular domain.[1] In order to learn more about the defined tertiary structure, cellular prion proteins were isolated from Syrian hamster (SHa) brains. By performing Fourier-transform infrared (FTIR) spectroscopy measurements mainly alpha helical fractions could be determined.[21] These results were in line with spectroscopic data of recombinant PrP. Due to their accessibility, recombinantly expressed prion proteins were used for further biochemical experiments[22-25], for example in solving nuclear magnetic resonance (NMR), to obtain a more realistic overview about the structure (*Figure 1*).[26-29] The unstructured and flexible N-terminal tail consists of two charged clusters (CC1 and CC2), a hydrophobic domain adjacent to a four octapeptide repeat (OR) which shows a high affinity to divalent cations, especially to copper(II).[30] The configuration of the copper binding region in the human prion protein (hPrP) was investigated in detail by using the full-length prion protein, synthetic octa- and tetra-peptides. It was found that different parameters have an influence on the binding affinity to divalent cations. It depends on the cation concentration and the pH, how many copper ions hPrP can bind.[32-34] In the globular domain three alpha-helices (residues 144-154, 173-194, 200-228), two of them connected via a disulfide bond (position 179 and 214), and a small antiparallel ß-sheet (residues 128-131 and 161-164) can be found (*Figure 1*). The C-terminal serine at position 231 is linked to the glycosylphosphatidylinositol-anchor (GPI-anchor) *in vivo*. The C-terminal part includes more posttranslational modifications as it contains two asparagine residues at position 181 and 197 as glycosylation sites.[1,30] This results in different forms of PrP^C: non-glycosylated, mono-glycosylated and di-glycosylated.[1,35,36] As shown by recent studies[37], these glycosylation patterns have a strong influence on the toxicity and the aggregation potential of the human prion protein. Different hPrP mutants (pathological PrP mutants V180I and F198S, mono-glycosylated mutants N181D, N197D and T199N/N181D/N197D, and a non-glycosylated mutant N181D/N197D) were developed to specifically predict the glycosylation pattern. The wild type hPrP and these mutants where then used in biochemical experiments to investigate the effect of the glycosylation pattern on the protein's subcellular localization. The method of

immunocytochemical staining was used to reveal that wild-type PrP and mono-glycosylated mutants are connected to the plasma membrane, whereas pathogenic and non-glycosylated mutants are primarily located in the cytoplasm. PrP mutants which were located in the cytoplasm showed increased proteinase K (PK) resistance and aggregation as it was confirmed by immunoblotting and flow cytometry. Furthermore, higher cellular reactive oxygen species (ROS) levels could be detected in the presence of the cytoplasm located mutants compared to when PrP is attached to the plasma membrane. The absence of N-glycosylation also indicates a higher cytotoxicity.[37] The C-terminal GPI-anchor is another decisive factor to tether both the PrP^C and the PrP^{Sc} to the cellular membrane.[38]
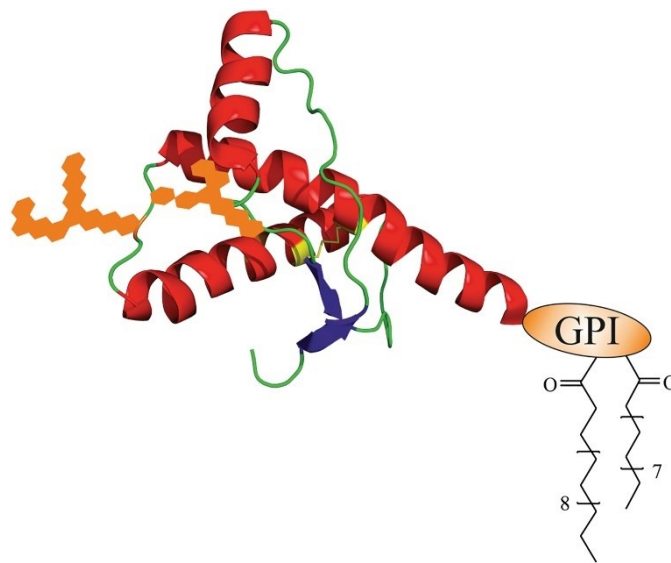
Figure 1: Tertiary Structure of human PrP derived from NMR measurements by Zahn *et al.*[29] Posttranslational Modifications such as the C-terminal GPI-anchor and the N-glycosylations (orange) are included. The figure was taken from Hackl & Becker.[1]

Approximately 10-15% of prion diseases are caused because of genetic mutations in the PRNP gene.[17,39] Mutations within the coding region of PRNP lead to changes in the tertiary structure, making the protein more prone to form pathogenic variants. These defective phenotypes do not directly trigger a neurodegenerative disease but increase the risk of developing it.[40] In addition, these pathogenic phenotypes could be observed in various prion diseases such as CJD, GSS or FFI. Unfortunately, it remains a challenge to accurately determine disease-causing mutations in the gene, as the pathogenic phenotype could be heterogenous. To name examples, for the mutations M129V and E219K several studies have demonstrated that the combination of these two might be disease modifying. Surprisingly, the combination is on the one hand a risk factor for vCJD but on the other hand also protective against sCJD.[17] The V180I

mutation was initially believed to be purely of pathogenic nature, but further studies showed that it could be also detected in healthy patients.[17,41]

1.3 Scrapie Prion Protein

The scrapie prion protein is the misfolded and toxic form of the cellular prion protein. A known property of the misfolded proteins is that they tend to aggregate. Just as the PrP^C, it is encoded by the PRNP gene and furthermore it is tagged with the same PTM's. However, the structure of the two variants is distinguishable and they differ in their biochemical and physiological properties.[9,42] It remains rather challenging to get a high-resolution structure of the PrP^{Sc} because of its aggregation potential and consequently its insolubility.[43] Nevertheless, a few methods were performed to get lucidity about the structure of the infectious protein. Based on cryo electron microscopy (Cryo-EM) and 3D modeling[45], a four-ring beta-solenoid structure was determined for the PrP^{Sc}. The 3D-reconstruction allowed to determine the average molecular height of a single PrP^{Sc} as 17,7 Å.[44,45] The presence of a four-ring ß-solenoid was identified by X-ray fiber diffraction of the brain-derived PrP 27-30 core as well, supporting the underlying structure even more.[44,46] Furthermore, the outcome of biophysical methods such as FTIR-spectroscopy and CD spectroscopy revealed a high ß-sheet content of PrP^{Sc}.[47-49] The output of all these experiments recommends a secondary structure content of 50% ß-sheet- and 50% random-coil loop for the PrP 27-30 core, which would fit to a four-ring ß-solenoid structure connected by unstructured loops.[44] In this model the ß-solenoid composition stretches from the N-terminus to the C-terminus, including the amino acids from position 90 to 230. As previously found, treatment of brain derived PrP 27-30 samples with PK results in degradation of amino acids up to the position 86-98 (depending on the strain).[7,44] These results support the local range of the four-ring ß-solenoid and in addition it indicates that the N-terminal region is not part of the prion domain, thus not infectious.[44,50] However, these claims are at odds with the assumption that the ß-solenoid rings are connected with unstructured random coils, since these could be targeted by nonspecific protein kinases. One possibility would be that the ß-solenoid structure is extremely compact and the intermediate spaces are not accessible to kinases.[7,51-54] However, this has been refuted since secondary cleavages of PrP^{Sc} have been determined by using a variety of binding antibodies. Thereby the cleaving fragments have been identified.[53,55-57] An unambiguous elucidation of the structure

of the infectious protein turns out to be difficult for another reason. There are obvious differences in terms of susceptibility to protein kinases between distinct prion strains. Prusiner and coworkers have found a bank vole prion strain (I109) which was overexpressed in transgenic mice and that ultimately led to a spontaneous neurological dysfunction. The transgenic mice showed common symptoms of prion disease, but to their surprise, the treatment of brain homogenates from the spontaneously ill, transgenic mice with PK induced digestion of the prion proteins.[58,59] Again, it was Prusiner who was able to identify structural variations and biochemical parameters that contribute to the diversity of prion strains. These variations include the extent of protease resistance, conformational stability, differences in glycosylation patterns and the electrophoretic mobility of proteolytic fragments.[60] This illustrates the difficulty of determining a uniform high-resolution structure once more, since a multitude of factors contribute to the structure of a specific prion strain.

The four-ring ß-solenoid structure gained much attention due to the detection via X-ray fiber diffraction and Cryo-EM, yet there are still other theories about the structure of the scrapie prion protein circulating among scientists. There exists a model which is called the parallel in-register intermolecular beta-sheet (PIRIBS). The name refers to the stacking behavior of the PrP molecules. Each prion protein stacks perfectly on top of the previous PrP molecule in register. The PIRIBS model shows similarities to the solved amyloid structures, however a single PrP molecule contributes 4,8 Å to the molecular height in this model, resulting in a deviation to the height measurements of the Cryo-EM and 3D-remodelling. Another weakness of this theoretical structure is that the described dense stacking of the PIRIBS model would not tolerate the bulky glycosyl side chains of PrP.[45-46,61]

With the underlying theories and the resulting possible structures of PrP^Sc, investigation of the propagation mechanism of PrP^Sc has been started. The four rings of the ß-solenoid show a contiguous pattern in composition with each the lowest- and the uppermost ring containing an unpaired ß-sheet. These unpaired sites can interact with any amyloidogenic peptide by hydrogen bonding. This allows an unfolded PrP molecule in close-proximity to interact with the lower- or uppermost rung of the ß-solenoid, thereby folding the protein and attaching another rung (*Figure 2*). This mechanism can then be repeated three more times resulting in a new ß-solenoid. The newly generated ß-solenoid may function as a further template for a new unfolded PrP molecule.
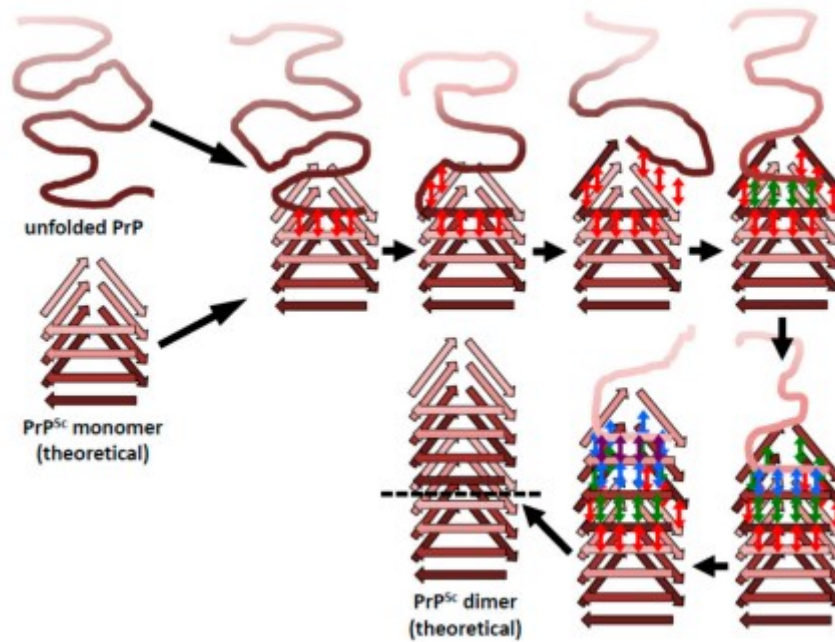
Figure 2: A theory model for the propagation mechanism of PrP[Sc] assuming that it forms a ß-solenoid four-ring structure. The image was taken from Wille & Requena.[44]

However, this should only give a brief insight into the studies on the conversion from PrP[C] to PrP[Sc].[62,63] The mechanism of the conformational change remains still needs to be elucidated and is discussed in more detail in the section 1.5.

1.4 Physiology of the cellular prion protein

As mentioned in the previous chapter, the prion protein is mostly known because of its connection to prion diseases, whereas the main biological function of the benign prion protein in the central nervous system remains enigmatic. To gain more knowledge about the physiological function of PrP[C], the expression levels in different cell types and the localization of the protein were examined.[1,30] Neurons and glial cells in the central nervous system (CNS) show increased expression in contrast to other cells. Immunocytochemical studies by light- and electron microscopy in primates, as well as the investigation of transgenic mice, which expressed an enhanced green fluorescent protein (EGFP)-tagged PrP[C], revealed that PrP[C] is primary located along axons and the pre-synaptic terminals of neurons.[64-68] To some extent it is also found in postsynaptic structures. These studies suggest that the function of PrP[C] might be to regulate the synaptic transmission and plasticity, thereby retaining the common synaptic structure. This is consistent with the early stages of prion diseases, in which synaptic dysfunction and synaptic loss are significant events in further disease progression.[69-73]

Therefore, experiments with PrP^C-deficient mice (ZH1, Edbg) were performed. It has been shown that these mice exhibit reduced long term potentiation (LTP) in hippocampal Schaffer collaterals and they displayed weakened inhibitory effects in the gamma-aminobutyric acid (GABA) dependent synaptic transmission.[74,75] The term synaptic plasticity describes the ability to respond to recent activities with a change in its strength. LTP is related to synaptic plasticity as this effect influences learning and memory in the hippocampus. Therefore, impaired or reduced LTP could lead to cognitive deficits and this in turn could assign PrP^C a role in memory formation.[76] However, this functional assignment is controversial, as previous experiments did not provide clear evidence for it.[77] The cellular prion protein is also linked to the regulation of the circadian rhythm. More precisely, the presence of PrP^C is connected to sleep homeostasis and sleep continuity. Thereby, the loss of function might lead to the disruption of the sleep pattern, which is a prominent symptom of neurodegenerative diseases such as FFI.[78,79] This was partially confirmed by experiments with $Prnp$Z$^{H1/ZH1}$ and co-isogenic $Prnp$$^{Edbg/Edbg}$ mice as they showed an altered circadian rhythm, increased sleep fragmentation and increased slow wave activity.[80]

There are other possible functions for PrP^C that may arise from its interaction with molecular partners.[30] For example, the cellular prion protein is involved in reducing the cellular excitability. The interaction with a subunit (DPP6) of the voltage-gated potassium channel 4.2 increases and prolongs the current of it.[81] Additionally, it has been reported that the wild-type PrP^C and a mutant PrP^C induce calcium homeostasis in neurons of transgenic mice by co-immunoprecipitation with a subunit (α2δ-1) of the voltage-gated calcium channel (VGCC). [82]It was reported that the triggered calcium homeostasis accompanied by deficits in the VGCC current led to reduced slow after hyperpolarization (sAHP) in the PrP^C-deficient mice. Furthermore, it was observed that the mutant PrP^C affects the trafficking and the binding of the auxiliary subunit α2δ-1 to the VGCC, whereas the physiology of the wild-type in this interaction is not identified yet. In this context with the sAHP induced neuronal firing, it was shown that increased neuronal excitability in the hippocampus of the transgenic mice also results in an increased vulnerability to kainate-induced seizures.[30,83-84] In PrP^C-deficient mice the interaction of PrP^C and the kainic acid (KA) receptor subunit GluR6/7 is missing, ultimately resulting in the upregulation of KA-receptors and enhanced neurotoxic signaling.[85-87] More detailed studies have demonstrated that the cleavage of PrP^C is enhanced under ischemic conditions. The resulting N- and C-terminal fragments show a neuroprotective function. For

example, the N-terminal cleaving fragment (N1) seems to inhibit the staurosporine-induced Caspase-3 activation as it was shown with pressure-induced ischemia in the rat retina.[88,89] In combination with further studies[90,91], these results propose a linkage of PrP^C to neuroprotection against excitotoxic occurrences.

In other studies, it has been observed that the cellular prion protein is already expressed in the early stages of murine embryonic development.[92,93] It was found that in PrP^C knockout mouse embryos, a wide variety of genes showed increased expression. In contrast the transcription rate of these genes was negligible in adult organisms.[94,95] Based on a transcriptome analysis, it seems that PrP^C is involved in development processes, as the increased transcription of several different genes apparently compensates the absence of PrP^C.[96]

In experiments with five different PrP^C-knockout strains (e.g., PrnpZH3/ZH3) it was demonstrated that PrP^C probably fulfills a function in the peripheral nervous system. The PrP^C-deficient mice developed a late-onset peripheral neuropathy, which is eventually triggered by disrupting the structure of the peripheral myelin. More particularly, the N-terminal polycationic cluster of PrP^C is cleaved in the neuronal system, which enables the binding of the fragment to the G-protein coupled receptor Adgrg6 (Gpr126) on Schwann cells. This fragment-receptor interaction induces promyelinating cAMP response. These findings suggest that the physiological function of the cellular prion protein includes the maintenance of peripheral myelin. Furthermore, the N-terminal fragment of PrP^C might serve as a clinical drug candidate for peripheral chronic demyelinating polyneuropathies. [94,97-98]

1.4.1 Trafficking of the cellular prion protein

During the synthesis of PrP^C, it is first translocated in the endoplasmic reticulum (ER). The N-terminal signal sequence enables the interaction with the signal recognition particles (SRP) in the ER. Once the signal sequence has served its purpose, it gets cleaved off and additionally a GPI-anchor is attached to the C-terminal serine.[99,100] Depending on the subsequent localization and associated biological function, four distinct isoforms of the cellular prion protein during synthesis are possible. These isoforms are denoted as ^{sec}PrP, ^{Ctm}PrP, ^{Ntm}PrP and cyPrP. The secretory prion protein (^{sec}PrP) is the predominant isoform thereby it is recognized

by the molecular transport machinery and directed to the plasma membrane. Rarely, not the N-terminal domain but the internal hydrophobic domain interacts with the translocon in the ER. This distinct domain interaction results in the [Ctm]PrP isoform, in which the N-terminal sequence is located in the cytosol with the GPI-anchor projecting into the ER membrane. If the domains are oriented in the exact opposite and the GPI-anchor is absent, it is stated as [Ntm]PrP isoform. The fourth isoform (cyPrP) is generated due to a flawed translocation into the ER, resulting in the accumulation of the protein in the cytosol during ER stress. If the processing of PrP[C] is properly finished in the ER, the protein is transported to the Golgi.[100,101] In this cell compartment, the side chains of two asparagine residues (position 181 and 197) get N-glycosylated.[31] Once these modifications are examined, the PrP[C] is further transported to the cell surface, where the GPI-anchor tethers the protein to the plasma membrane. It depends on the GPI domain to which region of the plasma membrane it is attached. For example, the GPI domain of PrP[C] can also be anchored to lipid rafts, which are known for containing a high amount of cholesterol and sphingolipids.[30,102] In this membrane-bound state, PrP[C] can undergo further modifications. It can be cleaved at three different target sites (α-, β- and γ- cleavage) by proteolytic enzymes or it is detached from the GPI-anchor in a molecular process called shedding. These cleavage processes may influence physiological and pathological events of the prion protein.[100,103]

The correct destination of PrP[C] is reached due to intracellular trafficking which is mediated by specific transport vesicles. These vesicles are mandatory for passing endocytic and secretory membrane systems.[104-106] Depending on the cell type and the associated modes of internalization, the cellular prion protein is part of various signal mechanisms.[107,108] The major pathway for PrP[C] internalization is called "Clathrin Mediated Endocytosis" (CME).[105,109] Clathrin is a large, oligomeric protein which can be incorporated into the inner surface of the plasma membrane. There the proteins assemble to a lattice structure, causing the membrane to invaginate, thus Clathrin-coated vesicles (CCV) are formed.[110] It was shown that the PrP[C] interacts with cellular membrane receptors and proteins such as the laminin receptor precursor (LRP) and the low-density lipoprotein receptor-related protein 1 (LRP1) via its C-terminal GPI-anchor. It was revealed that both LRP and LRP1 are essential components in the intracellular uptake of CME of the PrP[C], as these are internalized by CCV. Lipid rafts are in close contact with the PrP[C] vesicles during the whole CME process, suggesting that these regions are the major interaction sites.[100,111-113] In further studies it was shown that impaired clathrin

formation and the disruption of lipid rafts with drugs like filipin and nystatin results in a stop of the intracellular uptake of PrP^C.[114]
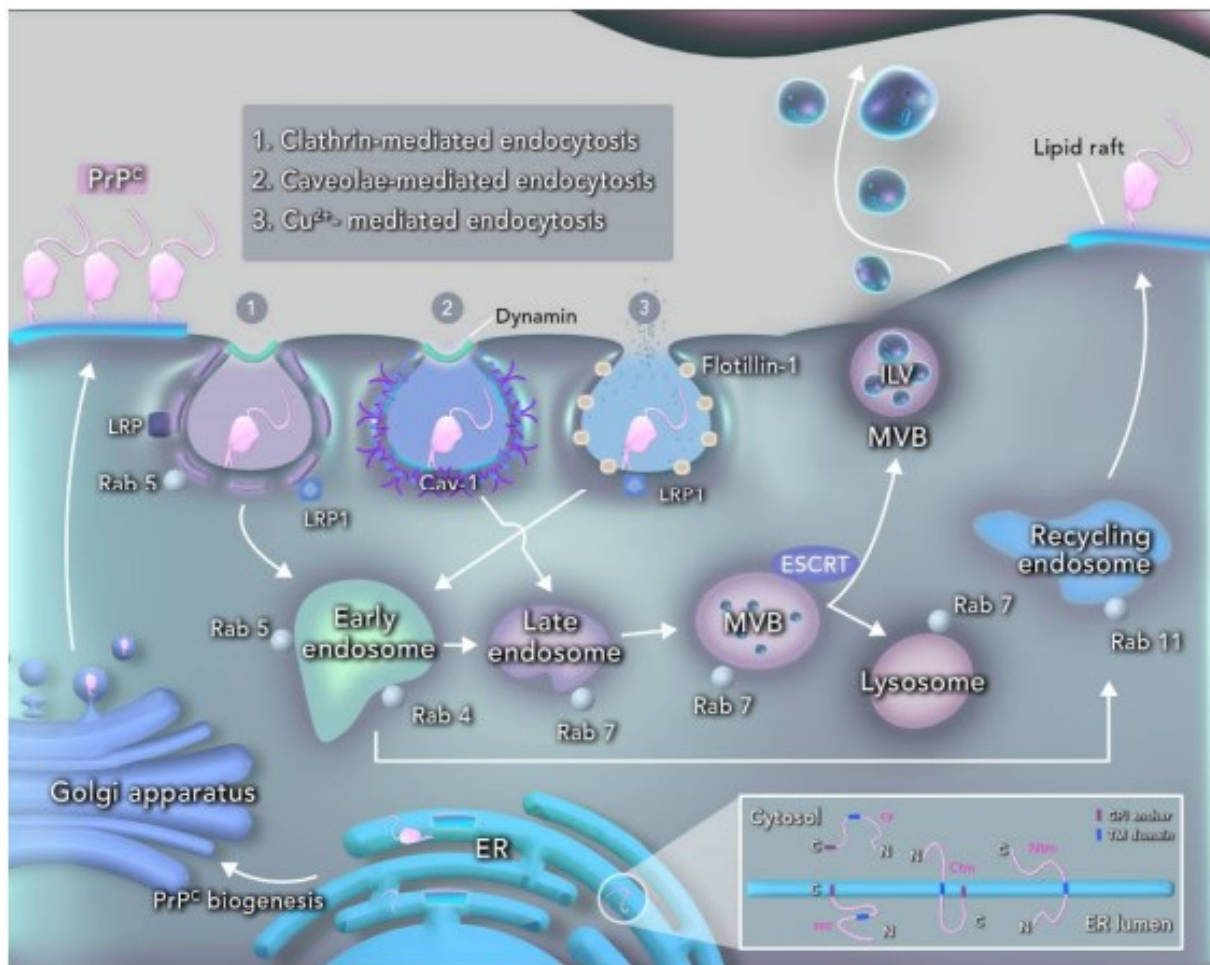
Figure 3: Synthesis, cellular location and endocytic transport of PrP^C.
The figure was taken from Alves *et al.*[100] The window in the lower right corner shows the four different isoforms (^{sec}PrP, ^{Ctm}PrP, ^{Ntm}PrP and cyPrP) that may form during the synthesis in the ER. Pathway 1 features the clathrin-mediated endocytosis in which the interaction of PrP^C and LRP or LRP1 takes place. Pathway 2 shows the caveolae-mediated endocytosis that includes the interaction with dynamin or caveolin-1. In pathway 3 the Cu^{2+}-mediated endocytosis can be observed. With the assistance of LRP1 the N-terminal domain of PrP^C can bind to copper ions, resulting in the internalization. Each endocytic pathway is related to a specific Rab protein (GTPase family). These proteins define, if PrP^C is either sorted to the early or late endosome.[100]

However, there are other studies, in which it was found that intracellular uptake of PrP^C is possible independently of clathrins. The internalization of PrP^C can occur in specific lipid rafts regions called caveolae. More precisely said, caveolae are membrane invaginations in which PrP^C is enriched. In this distinct pathway PrP^C is linked to dynamin or caveolin-1, two transmembrane proteins, which allow the internalization and further enable PrP^C to be delivered to the late endosomes and lysosomes.[109] It was shown that the interaction of endocytic PrP^C and the stress inducible protein 1 (STI1) play a key role in the activation of extracellular signal-regulated kinases 1/2 (ERK1/2) mediated signaling. This was demonstrated

by experiments involving hippocampal neurons, which carried a PrP^C-mutant that lacked endocytic activity. In these cells the ERK1/2 mediated signaling was perturbed.[115] In addition to the role of PrP^C in the signaling pathway of ERK1/2, it was reported that the interaction with the caveolin-1 activates the protein tyrosine kinase p59fyn in caveolae during neurite outgrowth.[116] However, this activation only works properly in cooperation with the p42/44-ERK1/2 mediated signaling, again highlighting the importance of PrP^C in these molecular pathways.[117] Furthermore, it is assumed that PrP^C guides the neuronal receptor NCAM to the lipid raft region, thereby supporting the p59fyn activation.[118] The major internalization pathways of PrP^C can be observed in *Figure 3*.

Summarized, the processing during the biosynthesis of PrP^C and the thereby resulting allocation of the domains is an essential step for the correct trafficking of PrP^C to the target location. The internalization, mediated by clathrin-coated vesicles, caveolae or Cu^{2+} ions leads to the interaction with various binding partners and triggers the activation of different signaling pathways.

1.5 Conformational change: PrP^C to PrP^{Sc} conversion

Even though a considerable amount of data on the cellular- and scrapie prion protein is now available, it has not yet been possible to determine the exact mechanism for the propagation of the infectious prion protein.[1] Back then in vitro experiments were performed, to learn more about the autocatalytic conversion from PrP^C to the protease-resistant form (PrP^{res}). By using the method of protein misfolding cyclic amplification (PMCA) it was tried to convert recombinant prion proteins. In comparison with the brain derived PrP^C the respective infectivity levels were lower since the recombinantly expressed prion proteins were lacking a GPI-anchor.[38] In further studies with transgenic mice similar results were observed. In turned out that the aggregated prion proteins in scrapie-infected transgenic mice were not a common protease-resistant form but an amyloid plague. These transgenic mice expressed prion proteins which lacked the GPI-anchor, proposing an important role of the PrP GPI-anchor in the development of prion diseases.[119] Prusiner and coworkers demonstrated by experiments with transgenic mice expressing Syrian hamster and mouse prion proteins, that the interaction of the homologous PrP^C and the scrapie prion protein induces prion synthesis.[120]

As it was shown that PrP knockout mice did not develop any signs of scrapie infectivity, the presumption that the rate of PrP[Sc] formation is directly proportional to PrP[C] expression seemed to be valid. These findings were in line with the "protein-only" hypothesis.[121-123] Based on this theory two models which should describe the conversion from PrP[C] to PrP[Sc] are discussed nowadays: The template-directed refolding model described by Prusiner[124] and the seeded nucleation model proposed by Jarret and Lansbury[125]. The mechanism of the conversion can be observed in *Figure 4* for both models.
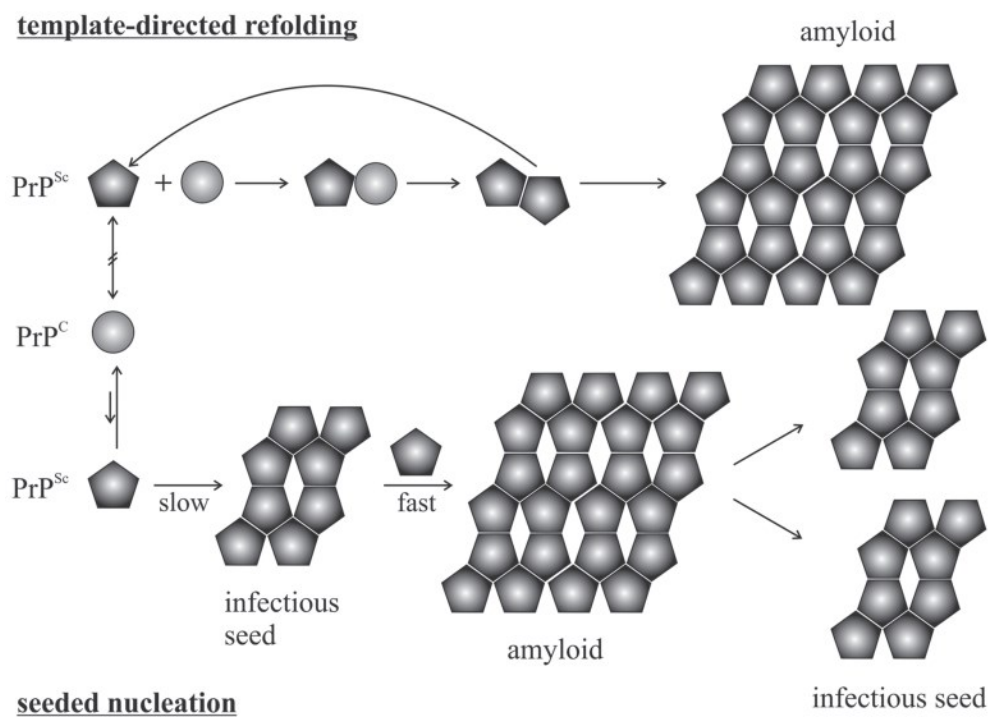
Figure 4: Theoretical model for the PrP[C]-PrP[Sc] conversion. The template-directed refolding mechanism can be observed at the top, whereas the seeded nucleation model is shown at the bottom. The figure was modified from Aguzzi and Callela[15] by Hackl & Becker[1].

In the template-directed refolding mechanism the spontaneous conversion of a cellular prion protein monomer to a PrP[Sc] monomer is prevented by a high-energy barrier. It is suggested, that for the conversion an interaction of an already stable PrP[Sc] monomer and PrP[C] is required. The generated PrP[Sc]-dimers subsequently aggregate to form larger amyloid plagues. However, these amyloid plagues are not considered essential as they are not associated with the propagation of the disease.[124] There might be some doubts about the template-directed refolding model, as until now there is no clear evidence of stable PrP[Sc] monomers since the misfolded proteins tend to form insoluble aggregates.[126] The seeded nucleation model assumes that there is a reversible thermodynamic equilibrium between the two distinct

monomers. The thermodynamic equilibrium shifts towards the PrP^{Sc} monomer formation, if there are stable oligomeric PrP^{Sc} aggregates, or also called infectious seeds, present. As a result, more infectious seeds are slowly formed. These then rapidly aggregate to form larger amyloid plagues. In this model, it is proposed that these amyloid plague fragments turn again into infectious seeds for further spread of the neurodegenerative disease.[125]

Besides the previously mentioned PMCA technique, it was achieved to develop another method to convert PrP^C to PrP^{SC} in *in vitro* systems by Caughey and coworkers[127]. In their approach, which is called cell-free conversion (CFC) assay, an excess of unlabeled PrP^{Sc} is mixed with PrP^C to obtain protease resistant and radioactive prion proteins (PrPres).[127,128] These experiments were the first to generate PrP^{Sc} from recombinantly expressed prion proteins and since the *in vitro* PrP propagation mimics the species and strain specificity of *in vivo* transmissible prions, conclusions could be drawn about structural properties with respect to the species barrier.[129-131] The disadvantage of the method is that a large amount of infectious prion proteins (PrP^{SC}:PrP^C 50:1) are required to induce *in vitro* prion propagation, making it unfavorable for de-novo generation of infectious particles.[132] However, the CFC assay offers other potential applications, such as screening experiments that may reveal structures that inhibit the PrP^C-PrP^{Sc} interaction.[133,134]

In experiments with PrP and 1-palmitoyl-2oleoyl-sn-glycero-3-phospho-(1'-rac-glycerol) (POPG) lipids performed by Wang *et al*[216], it was shown that under physiological conditions these negatively charged lipids induce a conformational change to PrP^{Sc}-like version. Based on these results, it was important to focus on the proposed primary site for the interaction, the plasma membrane. Naslavsky *et al*[135] demonstrated that both PrP isoforms are connected to Triton X-100-insoluble, low-density complexes or "rafts". Furthermore, they did Triton X-100 extraction at 37°C with a scrapie-infected ScN2a cell clone and brain of a Syrian Hamster with scrapie. They observed two different peaks of different density for PrP^C and PrP^{Sc}, proposing that PrP^C- and PrP^{Sc} associated rafts have distinct characteristics.[135] Campana and coworkers[99] also believe that rafts are important for the PrP^C conversion to PrP^{Sc}, but they suggest that the molecular factors that trigger an interaction of PrP and rafts need to be defined more clearly. Furthermore, the scientists state that although they believe that these specific membrane domains are essential for stabilizing the structure of PrP^C, the interaction with PrP^{Sc} occurs only once PrP^C is separated from the rafts.[99] Further investigations on this topic were made by Baron *et al*[136], as they reported that the conformational change of PrP^C takes place on

membranes that are associated with both PrP isoforms. This would suggest that the two isoforms are inserted in close distance within the membrane, which is in contradiction with the previously mentioned findings[135] in which it was stated that PrP^C and PrP^{Sc} are attached to two distinguishable lipid rafts.

In studies with model lipid membranes, it was shown by tryptophan fluorescence that PrP, which is rich in ß-sheets, is prone to bind to negatively charged lipid membranes, whereas PrP, with an alpha-helical structure, more likely tethers to raft-like membranes.[137] As it is described in several studies, the GPI-anchor is crucially involved in the lipid raft association and therefore it plays an important role in the conformational change of PrP^C.[1,138,139]

1.6 Solid phase peptide synthesis

The method of solid phase peptide synthesis (SPPS) was invented by the American chemist Bruce Merrifield in 1963.[140] Merrifield won the Nobel Prize for his innovative approach 21 years later.[141] The technique of SPPS is utilized to synthesize peptides with a solid material, or also known as resin, as a starting material.[143] A commonly used resin is polystyrol crosslinked with 1% m-divinyl benzene. The first amino acid is connected to the resin via a cleavable linker and is N-terminally protected by a chemical compound called protecting group. The attachment of the first amino acid can be done manually but pre-loaded resins are nowadays commercially available. The synthesis direction of the elongating peptide chain is usually from the C- to the N-terminus, making it mandatory to employ N-terminal protecting groups. Widely used N-terminal protecting groups are fluoren-9-ylmethoxycarbonyl (Fmoc) and tert-butyloxycarbonyl (Boc). Additionally, the amino acids require orthogonal protecting groups for the functional chemical groups of the side chains. The term orthogonal conveys that the specific removing condition of a single protecting group does not affect the remaining ones. During synthesis amino acids are attached step by step to the resin in a repeated cycle stated as "coupling" until the desired sequence is accomplished. Thus, the synthesis of the peptide chain is driven by the addition of constituent amino acids and the selective removal of the respective N-terminal protecting group.[142] The flow of the cycle is listed as follows:

1) Removal of the N-terminal protecting group with suitable deprotecting reagents
2) Washing step *(a commonly used solvent is N,N-dimethylformamide (DMF))*
3) Addition of the next N-terminally protected amino acid *(the C-terminus of the freshly added amino acid has to be activated first via appropriate reagents)*
4) Washing step *(repeat step 1-4 until the synthesis of the desired sequence is accomplished)*
5) After the coupling of the last amino acid, subsequent the cleavage of the peptide chain from the resin and removal of the remaining protecting groups accomplished in a process stated as final cleavage.

1.6.1 N-terminal protecting groups

An essential feature in SPPS is the protective chemistry and as shortly mentioned before, two already well-established protecting groups in the procedure of SPPS are Fmoc and Boc. The Fmoc-strategy is sometimes preferred over the Boc-strategy as the cleavage conditions are milder (base-catalyzed) and it is compatible with the usage of orthogonal protecting groups, since their usual removal requires acidic conditions.[142] However, an advantage of the Boc

protective chemistry is an increased efficiency in longer peptide sequences even included in automated synthesis as it is stated by Schnölzer *et al*.[144]
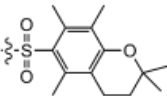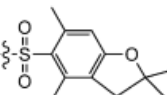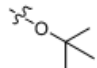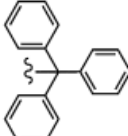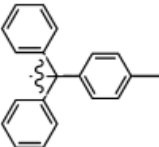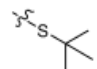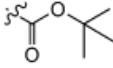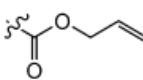
The deprotection of Fmoc is an elimination reaction of the first order and the reaction proceeds with the addition of the base. The addition of piperidine, usually 20% (v/v) piperidine in an organic solvent, removes a proton at the ring structure of the protecting group, thereby producing a reaction intermediate with a negatively charged carbon. Subsequently, cleavage of the Fmoc protecting group occurs and carbon dioxide is released, resulting in the remaining amino acid with the amenable N-terminus.[142]

The deprotection of the N-terminal Boc protecting group is mediated by using an acid. Commonly used acids are concentrated muriatic acid (HCL) in toluol or trifluoroacetic acid in DCM. The underlying deprotection mechanism is categorized as an elimination reaction of the first order. In the first step, the carbonyl oxygen acts as a nucleophile, as the lone pair attacks the proton of the acid. Then two electrons (one bond) of the double bond shift back to the oxygen so that the intermediate positively charged oxygen returns to a neutral charge state. This process is accompanied by two other electron shifts, thereby removing the tert-butyl group. Finally, the volatile products carbon dioxide and isobutylene are released as the deprotected amino acid remains.[142]

1.6.2 Orthogonal protecting groups

It is important to consider which protecting groups will be used for the side chains, before a peptide synthesis is started. Of course, this depends on the selected sequence and the chosen N-terminal protecting group. *Table 1* shows a list of popular side chain protecting groups, including their structure and the respective deprotecting condition.
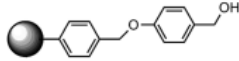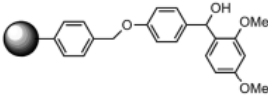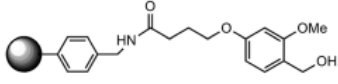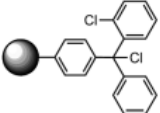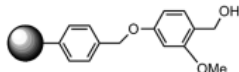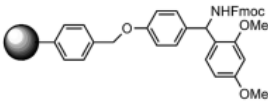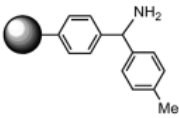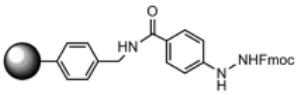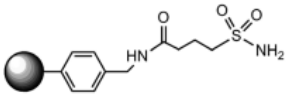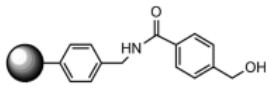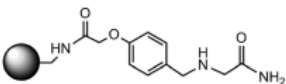
Table 1: Commonly used side chain protecting groups.
The table was taken from Palomo.[142]

Amino acid	Protecting group	Structure	Deprotection conditions
Arg	Pmc		90–95% TFA in CH_2Cl_2, 2–4 h
	Pbf		90% TFA in CH_2Cl_2/TIS, 1 h (longer times in multiple Arg containing peptides)
Asp/Glu	O^{t}Bu		90% TFA in CH_2Cl_2, 30 min
Asn/Gln	Trt		90% TFA in CH_2Cl_2, 30–60 min
Cys	Mtt		1% TFA in CH_2Cl_2, 60 min
	Trt		90% TFA in CH_2Cl_2, 30 min
	S^{t}Bu		TFMSA
His	Mtt		15% TFA in CH_2Cl_2, 1 h
	Trt		90% TFA in CH_2Cl_2, 30 min
	Boc		90% TFA in CH_2Cl_2, 30 min
Lys/Orn	Boc		90% TFA in CH_2Cl_2, 30 min
	Mtt		1% TFA in CH_2Cl_2, 30 min
	Alloc		Pd(PPh$_3$)$_4$ (5 mol%), PhSiH$_3$, THF/CH$_3$OH, 12 h
Ser/Thr	^{t}Bu		90% TFA in CH_2Cl_2, 30 min
Trp	Trt		1% TFA in CH_2Cl_2, 2 h
	Boc		95% TFA in CH_2Cl_2, 1 h
	Alloc		Pd(PPh$_3$)$_4$ (5 mol%), methylanilin, DMSO–THF–0.5 M HCl (1 : 1 : 0.5), 8 h
Tyr	Trt		2% TFA in CH_2Cl_2
	^{t}Bu		35% TFA in CH_2Cl_2
	Alloc		Pd(PPh$_3$)$_4$ (5 mol%), PhSiH$_3$, THF/CH$_3$OH

18

1.6.3 SPPS Linkers

Linkers are chemical compounds that are utilized in SPPS to connect the peptide chain and the resin. Thereby the structure of the linker is crucial in deciding which protecting group chemistry to use for the synthesis. Furthermore, the final cleavage condition of the peptide chain depends on the chemical properties of the used linker. As already mentioned at the beginning of this chapter, a frequently used resin for SPPS is polystyrene. Therefore, a variety of linkers have been designed specifically for polystyrene over the past few years. Most of the widely used resins are cleaved under acidic conditions (e.g. Wang Resin or MBHA resin) favoring Fmoc chemistry. In *Table 2* a list of common resins, including their structure and the respective cleavage condition, can be observed.

Table 2: Popular resins for SPPS.
The table was taken from Palomo.[142]

Resin name	Resin structure	Cleavage conditions	Peptide product
Wang resin		90–95% TFA in CH$_2$Cl$_2$ 1–2 h	Acid
Rink acid resin		1–5% TFA in CH$_2$Cl$_2$ 5–15 min or 10% AcOH in CH$_2$Cl$_2$, 2 h	Acid
HMPB resin		1% TFA in CH$_2$Cl$_2$ 2–5 min	Acid
2-Chlorotrityl chloride resin		1–5% TFA in CH$_2$Cl$_2$ 1 min	Acid
SASRIN resin		1% TFA in CH$_2$Cl$_2$ 5–10 min	Acid
Rink amide resin		50% TFA in CH$_2$Cl$_2$ 1 h	Amide
MBHA resin		HF 0 °C, 1 h	Amide
Hydrazine resin		Cu(OAc)$_2$, pyridine, acetic acid, nucleophile in CH$_2$Cl$_2$ or THF	Acid, ester, amide
Sulfonamide resin		1. ICH$_2$CN/DIPEA/NMP, 24 h 2. Nucleophile, DMAP, 24 h	Acid, ester, thioester, amide, *etc.*
HMBA resin		NaOH, N$_2$H$_4$, NH$_3$ in MeOH 24 h ROH LiBH$_4$	Acid, hydrazide, amide Ester Alcohol
PEGA–BAL resin		TFA–TFMSA (19 : 1)	Acid

19

1.6.4 Activation of amino acids

Before the addition of each amino acid to the reaction vessel, it is essential to activate the α-carboxyl group first to enable a quick and quantitative amide bond formation. This is accomplished by treating the amino acid with a coupling reagent. A substance group that was initially used for peptide synthesis were the carbodiimides.[142] The molecule dicyclohexylcarbodiimide (DCC) was used by Merrifield[141] for solution peptide synthesis back then. However, since the byproduct dicyclohexaurea, formed out of DCC, was insoluble in organic solvents, it could not be utilized for peptide synthesis on resin. An alternative is provided with diisopropylcarbodiimide (DIC) since the respective urea byproduct is soluble and remains in solution. The disadvantage of using DIC as a coupling reagent is that racemization has been observed. The formed byproduct O-acylisourea is quite reactive, thereby affecting the chiral integrity of an amino acid. As the performance with carbodiimides brings along the mentioned problems, it was searched for different alternatives. The development of onium (aminium, uronium and phosphonium) salts introduced another possibility for coupling reagents.[145] Two commonly used salts are N- [(1H-Benzotriazol-1-yl)(dimethylamino)-methylene]-N-methylmethanaminium hexafluorophosphate N-oxide (HBTU) and N-{(Dimethylamino)-1H-1,2,3-triazolo [4,5-b]-pyridino-1-ylmethylene}-N-methylmethan-aminium hexa- fluorophosphate (HATU). In terms of the structure HATU is similar to HBTU, however it reacts faster and during coupling there are less problems with epimerization.[145] The coupling with onium salts is accompanied by the presence of the chemical 1-hydroxybenzotriazole (HOBt) and a base, usually N,N-diisopropylethylamine (DIPEA).[142] DIPEA or also called Hünig's base is a suitable compound as the lone pair of the amine can only attack a single proton due to the steric hindrance.

In the first step of the HATU activation the negatively charged oxygen of the carboxy terminus operates as a nucleophile and attacks the double bond of HATU. Further electron shifts lead to the release of tetramethylurea and the activation of the carboxy terminus. With the addition of the activated amino acid to an amine or the already synthesized peptide chain a reaction intermediate (O-Acyl(tetramethyl)isouronium) arises. In the end an amide bond between the amine (or the N-terminus of the peptide chain) and the carboxy terminus is formed.[142] The structures of the required reagents are shown in *Figure 5*.
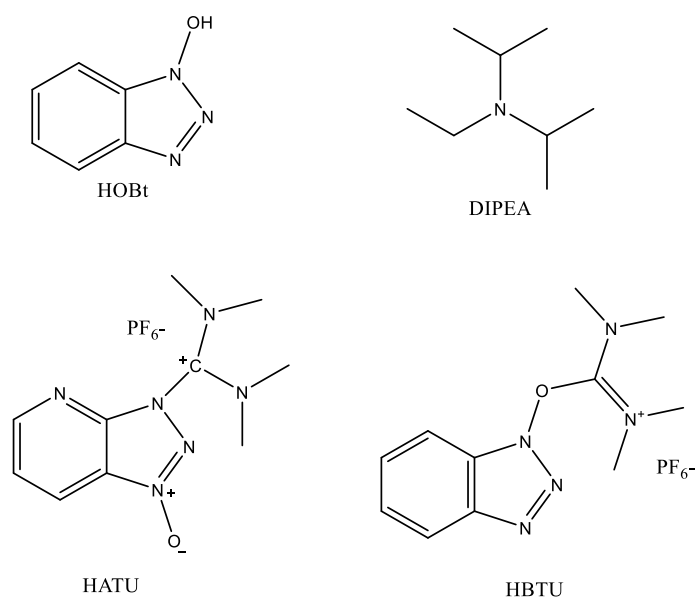
Figure 5: Chemical structures of the compounds required for the carboxy terminus activation of an amino acid.

1.7 Semisynthesis of proteins

Protein semisynthesis is a method in the field of protein engineering in which recombinant and synthesized polypeptides are chemo- and regioselectively combined. It is still difficult to produce membrane proteins and proteins that contain specific posttranslational modifications by utilizing only recombinant expression. This is where the semisynthesis approach shows its remarkable capability, because the access to the primary structure of most proteins can be achieved via the combination of the tools of synthetic organic chemistry and molecular biology. Thereby, it is possible to modify the sequence of the native protein, if required.[146]

The nomenclature protein semisynthesis was first mentioned in the context of an approach in which the proteolytically or chemically cleaved fragments of a natural protein were utilized for a re-synthesis of the protein.[146] It was already reported in 1974 that the chemical cleavage with cyanogen bromide (CNBr) of the pancreatic trypsin inhibitor results in fragments that spontaneously condense to re-form the amide bond of the natural protein.[147] The method of protein semisynthesis also includes site-specific modifications of natural proteins. The incorporation of such modifications was accomplished as well by using other protein labeling methods that are partial or completely selective. For example, there exists the standard site-directed mutagenesis, a technique which introduces a unique cysteine at a precise position in the target protein, thereby enabling selective derivatization of the thiol-group with thiol-reactive compounds.[146] A major part of protein semisynthesis includes the regioselective ligation of the polypeptide fragments. In another biochemical approach, the reverse-proteolysis strategy, the ligation is accomplished by the usage of proteolytic enzymes. Thereby the reaction conditions are adjusted in way that the aminolysis of the arising acyl-enzyme intermediate is favored over hydrolysis. High concentrations of organic solvents such as DMF, acetonitrile or glycerol are preferred to set up appropriate reaction conditions for the reverse-proteolysis approach. The peptidyl-enzyme intermediate and the second polypeptide fragment get linked to each other with the formation of an amide bond during the reaction.[148,149]

As the re-formation of the protein with fragment condensation is often accompanied by insolubility of the protected peptide building blocks, it was looked for different methods. In the chemical ligation approach unprotected fragments are chemoselectively joined together,

thereby the total synthesis of the protein is accomplished.[146] In the 1990s it was shown that it is possible to synthesize a full-length protein via chemoselective ligation in the Kent Laboratories.[150] They managed to assemble the HIV-1 protease by using two unprotected peptide fragments, which were used as a starting material. In the chemical reaction it was accomplished to form a thioester bond between the educts.[150] Over the years there were developed further chemical ligation approaches besides the thioester ligation. These are based on thioether[151], oxime/hydrazone[152-154] and amide[155-158] derivates.

Kent and his collaborators[155] were able to improve their method by introducing the natural peptide bond at the ligation site via a reaction of two unprotected synthesized peptides in aqueous solution (*Scheme 1*). In the first step of the native chemical ligation reaction, the thiol group of the N-terminal cysteine operates as a nucleophile and attacks the second peptide fragment at the α-thioester. This process is stated as reversible transthioesterification and occurs at physiological pH. Then an amide bond is generated at the ligation site due to a spontaneous intramolecular S→N acyl shift. The spontaneous S→N acyl transfer was first discovered by Wieland *et al.*[159] in experiments with amino acid derivates in the 1950s and since then it has been exploited for such ligation approaches.[146,159]
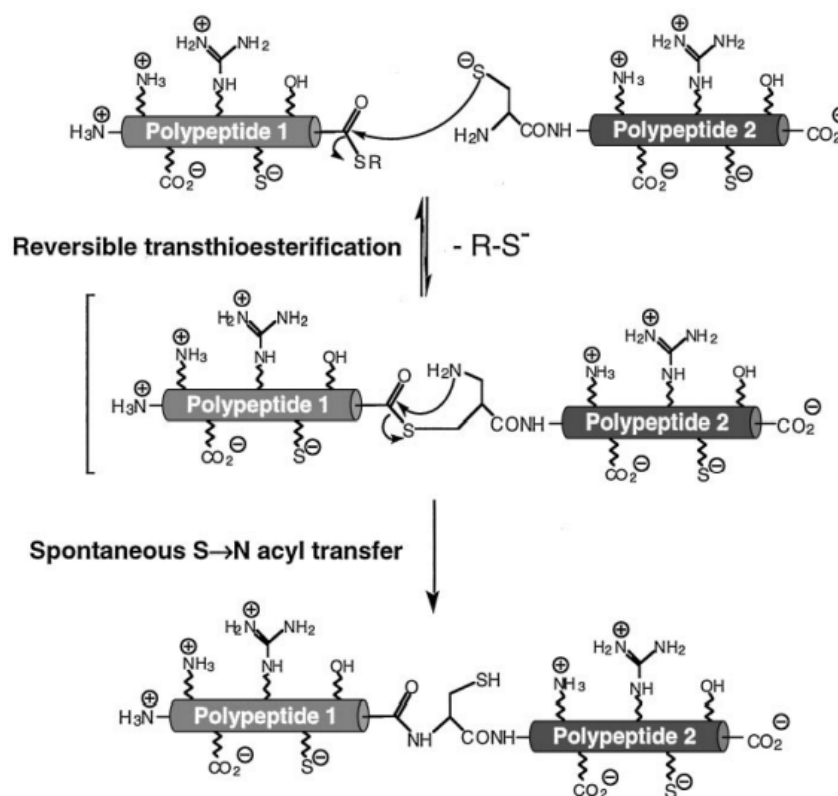
Scheme 1: The reaction mechanism of the Native Chemical Ligation (NCL).
The scheme was taken from Muir *et al.*[146]

So, the only requirement for the NCL includes the appearance of the essential reactive groups, the N-terminal cysteine or the α-thioester.[146] The introduction of an N-terminal cysteine into a recombinant transcription factor (AP-1) via mutagenesis was reported by Verdine and coworkers[160,161], thereby confirming the potential implementation of the native chemical ligation for semisynthesis purposes. Nowadays a simple approach to produce recombinant proteins with a N-terminal cysteine (α-Cys) is to utilize exogenous proteases in *in vitro* experiments. In this procedure a Xa recognition sequence is introduced right in front of the amino-terminal cysteine in the target protein. The recognition sequence is removed by treating the recombinant proteins with the appropriate protease, thereby generating the desired α-Cys proteins.[160]

However, it was still searched for an optimized approach to produce polypeptide α-thioesters. In the context of natural chemical ligation, the naturally occurring process of protein splicing gained importance and through intensive efforts in the field of biotechnology this process could be exploited to generate α-thioesters at the C-terminal end of a polypeptide.[146] In general, protein splicing is a posttranslational process which includes a few intramolecular rearrangements and internal reactions of a precursor protein. The precursor protein consists of a middle segment, stated as intein, which is flanked by two segments termed exteins. The protein splicing of the precursor proteins finally lead to the exclusion of the intein segment, thereby ligating the two exteins. The mechanism can be seen in *Scheme 2*. The first step in protein splicing involves again a N➔S acyl transfer, resulting in a shift of the N-extein to the side chain thiol- or hydroxyl group. The new location of the N-extein is at the N-terminus of the Intein. The reaction is followed by transesterification step, which means that the N-extein segment is transferred to a second conserved Cys/Ser/Thr residue located at the interspace of the intein and C-extein segment. Thereby a branched intermediate is formed, which interacts through a cyclization reaction with a required asparagine residue at the C-terminus of the intein. At this reaction step, the intein is removed and remains as a succinimide derivate. The last steps involve a S➔N acyl shift and the resulting amide bond formation between the two extein segments.[162,163]
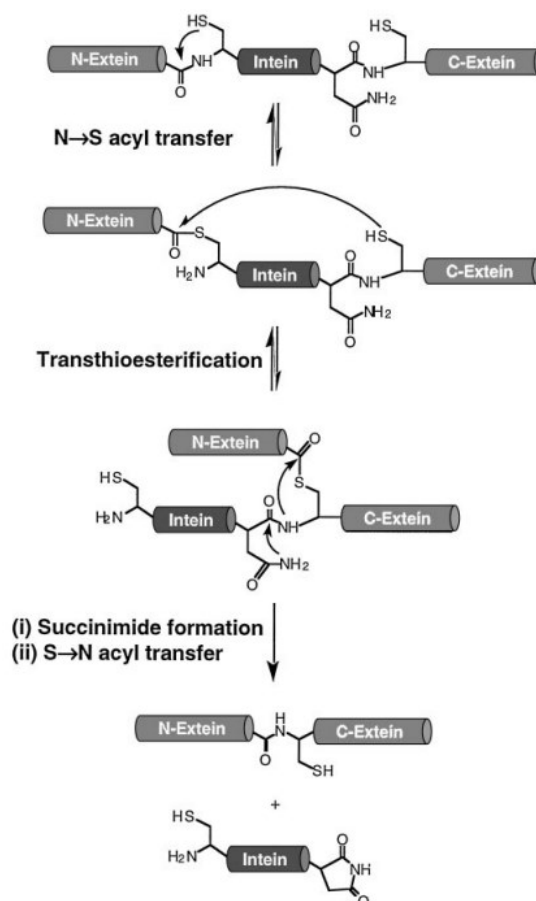
Scheme 2: Natural mechanism of protein splicing.
The scheme was taken from Muir *et al.*[146]

With the knowledge of the protein splicing mechanism, the introduction of the C-terminal α-thioester was accomplished by utilizing inteins that carry beneficial and targeted mutations. To avoid the intein exclusion and the ligation of the two extein segments, it is required to interrupt the splicing process after the N→S acyl transfer. With that in mind, several mutant inteins (many of them involve the crucial C-terminal intein Asn→Ala and the N-terminal C-Extein Cys/Thr/Ser→Ala mutation) have been developed.[164-167] By using these mutant inteins the further reaction process is disrupted, the generated thioester bond at the N-terminal intein side chain residue remains. This is essential, as the intein can now be removed by thiols, such as sodium 2-mercaptoethanesulfonate (MESNa), whereby ultimately the α-thioester is produced.[146]

As described previously, the two fragments that are required for Expressed Protein Ligation (EPL) are obtained either through targeted mutagenesis or the modified version of protein splicing. The usage of a synthetic and a recombinant building block for an altered version of the native chemical ligation was first reported in 1998 by two research groups. These ligation

approaches were named differently (Expressed Protein Ligation[168,169] or Intein-mediated Protein Ligation[170]) even though they referred to the same mechanism. The term EPL is mentioned nowadays, if at least one or both building blocks of the ligation are recombinantly expressed polypeptides. [146]

From the protein engineering point of view, EPL, and of course any semisynthesis approach, offer several possibilities to introduce the modification of interest to a small region in the primary structure of a protein. A frequently used application of EPL is the attachment of a small tag to the N- or the C-terminus of the protein. These chemical compounds involve affinity tags[171,172] or fluorophores[171,173]. Another scope of EPL is the modification of a native residue within the protein. This is often a challenge, since the ligation junction must be determined precisely and it may be that a cysteine has to be introduced via mutation at this position first. With that in mind the usual procedure includes the preparation of the two peptide fragments, one chemically synthesized and one recombinantly expressed. This approach is favorable as only a single ligation reaction is required, once the two segments have been prepared.[146] The synthetic peptide is usually produced via solid phase peptide synthesis.[144]

The EPL reaction itself can be carried out in two different ways. The first approach is a one pot ligation, which means that the thiolysis and the native chemical ligation are executed within the same solution. Even though a one pot ligation sounds favorable in the first place, it brings along a limitation as the intein must maintain its native structure during the reaction. So, it diminishes the usable additives which may be required for the ligation. Though, in the course of time these one-pot ligations have been successfully conducted with detergents[171,174], guanidium chloride[175] and urea[176] mixed in aqueous/organic solvents[175]. The second type of EPL is not performed as one pot ligation as the α-thioester is isolated first. This bears the advantage that a larger variety of additives can be utilized for the ligation reaction. For example, chaotropes or detergents can increase the solubility of the reactant polypeptides, resulting in an enhanced ligation yield.[155]

Summarized, protein semisynthesis is a method that allows the production of rather large proteins, which may possess modifications. It is possible to join at least one recombinant and one synthetic polypeptide together via the ligation reaction, referred as Expressed Protein

Ligation. This is indeed an advantage compared to the traditional total synthesis of proteins, as it is not possible to prepare proteins of this size with the latter method.

1.7.1 Semisynthesis of prion proteins

For a long time there persisted the major challenge of studies concerning structure and function of PrP, that recombinantly produced prion proteins were lacking posttranslational modifications. Consequently, the obtained results had to be taken with a grain of salt.[1] Back then the established approach was to prepare heterogenous proteins out of mammalian cell lines.[177-179] With the knowledge that the cellular prion protein is attached to the membrane via the GPI-anchor, several attempts focused on the preparation of membrane-anchored PrP. Glockshuber *et al*[180] were able to incorporate recombinantly produced full-length PrP into a membrane with thiol-reactive phospholipids. The idea behind their work was to gather information about possible changes in the structure and stability of the recombinant prion proteins once they are linked to a phospholipid bilayer. However, their findings by far UV-dichroism suggested that the covalent attachment of the proteins did not alter the structure substantially.[180] Pinheiro and coworkers pursued a similar approach in *in vitro* experiments.[181] Their strategy focused on the GPI-anchor, as it plays an important role in the attachment to the membrane. A GPI-anchor mimic was synthesized in their laboratories and it was accomplished to couple it to recombinant prion proteins with a C-terminal cysteine. It was reported that these modified prion proteins bind to artificial lipid membranes and that the observable structure of the PrP-GPI-mimic construct indicates a similar composition as a PrP, without the GPI-anchor mimic modification, in solution.[180,181] However, these approaches were *in vitro* experiments and therefore it should be kept in mind that complications may arise in a living organism due to side reactions of the functional thiol group. Baldwin *et al*[182] chemically synthesized variously modified prion protein variants with a length of up 112 amino acids via SPPS. For example, their studies have shown that a "mini-prion", which consists of 106 residues and was produced via native chemical ligation, is prone to undergo a conformational change to the pathogenic isoform PrP^{Sc} in transgenic mice. Based on this result, the research group chemically synthesized PrP106 (sPrP106) and another variant with a histidine-tag (sPrP106HT) via Fmoc chemistry. The chemically synthesized PrP variants tended to aggregate and were not immune to proteinase digestion, but other than that the synthesized proteins were indistinguishable from the recombinant analogs. Their approach to mimic the GPI-anchor included the linkage of lipophilic groups or biotin to the side chain residue of a C-terminal lysine that was orthogonally protected during the synthesis. With the presence of these lipophilic groups the attachment to a cell surface was accomplished.[182]

Another research group focused on click and ligation chemistry to connect lipidated peptides and a PrP segment (aa 214-231).[183]

With the advancing development in protein semisynthesis, Becker *et al*[184-192] managed to utilize such lipidated peptides as GPI-anchor mimetics by attaching them to recombinantly expressed prion proteins via EPL or protein trans splicing (*Scheme 3*). This strategy turned out to be successful and now allows a simpler access to prion proteins with posttranslational modifications. In general, designing an appropriate GPI-anchor peptide mimic and the biophysical characterization of various PrP variants is an ongoing process, that started now over a decade ago in the Becker Lab. The first approaches regarding the GPI-anchor peptide mimic were accomplished by Olschewski *et al*.[184] In that work two approaches based on the EPL were performed, resulting in the production of two different variants: a palmitoylated prion protein and a N-terminally truncated one (aa 90-231). The latter excludes the unfolded N-terminal domain and is modified at the C-terminus with chemically synthesized peptides which are palmitoylated. These fatty acid chains show high affinity to DOPC liposomes, thereby locating the PrP core region to the detergent-resistant domains of cell membranes.[193] Additionally, these semisynthetic PrP variants involve a tobacco etch virus (TEV) protease recognition site that offers the possibility to release the PrP from the membrane in a controlled manner. In the sequence of the chemically synthesized peptides a polyethyleneglycol polyamide oligomer (PPO) linker that operates as a solubilization tag is included. The designed EPL strategy involves the recombinant expression of a PrP variant initially linked to an *Mxe* GyrA intein and two affinity tags (6x histidine, chitin binding domain) in *Escherichia coli*. As previously described in this chapter, the next step includes the cleavage of the fusion tag by treating the PrP-intein-6xHis-CBD with an excess of a thiol compound. This procedure results in the generation of a C-terminal thioester. By mixing the PrP-thioester and GPI-anchor peptide mimic together under EPL reaction conditions, the desired PrP[Palm] is produced. The second approach relies on the protein trans splicing procedure. Here, the PrP is expressed in fusion with the N-terminal part of the DnaE split intein, whereas the C-terminal segment of DnaE is linked to the N-terminus of the chemically synthesized GPI-anchor mimicking peptide via a NCL reaction.[194] If the two split intein segments are brought together in a folded state, the two prepared polypeptide fragments spontaneously associate, thereby triggering the splicing process. As a result, the intein excludes itself and the PrP connected to the GPI-anchor peptide mimic is generated. The PrP[Palm] was used for biochemical studies in

aggregation assays with respect to PK resistance and thioflavin T (ThT) binding, in binding experiments to zwitterionic dioleoylphosphatidylcholine (DOPC) liposomes and in extraction experiments of the cell membrane. The obtained data revealed that the semisynthetically prepared PrP behaved similarly to the native PrP[C].[195]
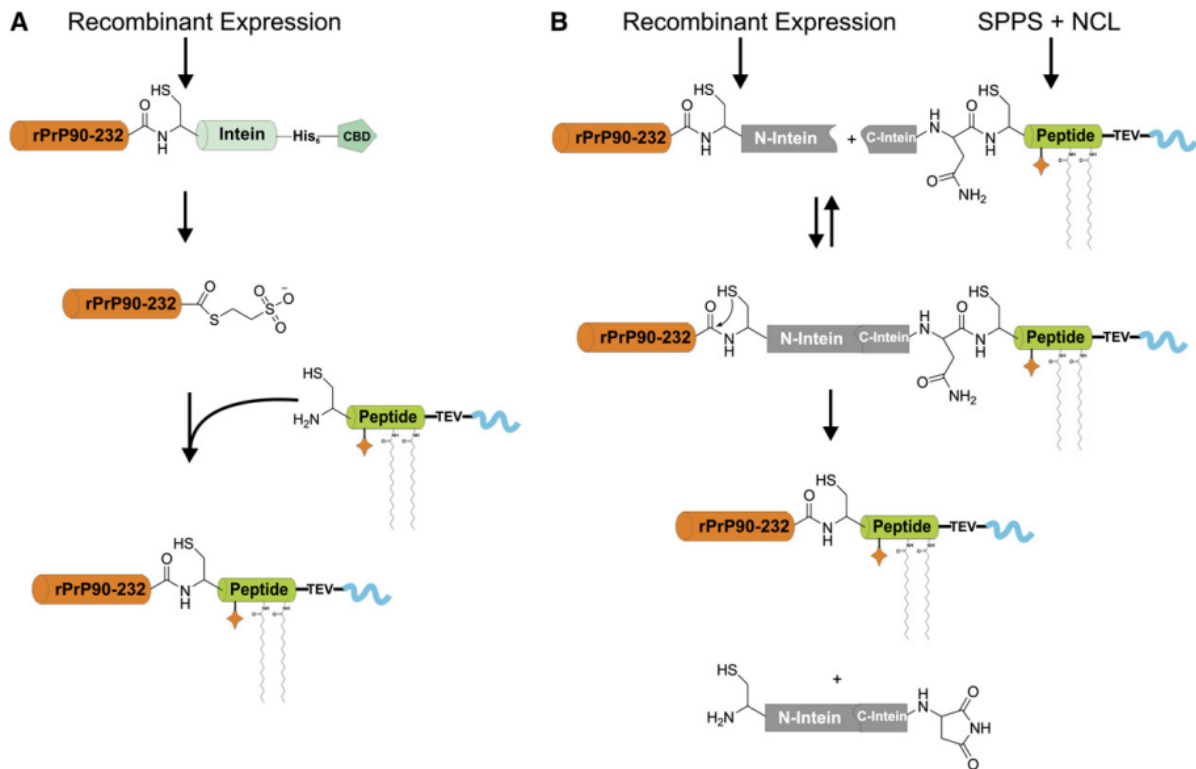
Scheme 3: Two different strategies to produce semisynthetic (prion) proteins developed in the Becker Lab. In A the EPL approach can be observed. Panel B shows the protein trans splicing method. The scheme was inherited from Olschewski *et al.*[184]

Becker and coworkers[188] did improve their strategy even further, as they managed to produce PrP variants with a native homogenous GPI-anchor. The usage of the designed GPI-anchor is not limited to prion proteins as it can be applied to other GPI-anchored proteins too. However, the task of producing a suitable GPI-anchor was not superficial, since it has been reported that there exist different glycoforms of native PrP GPI-anchors. Unfortunately, the exact linkage positions and anomeric configurations of the oligosaccharides have not all been identified yet. With that structural uncertainty in mind, it was rather challenging to design an appropriate GPI-anchor mimic. A core GPI pseudosaccharide with an α-Man-(1→2)-α-Man-(1→6)-α-Man-(1→4)-α-GlcN(1→6)-myo-Ino motif was prepared. Furthermore, the underlying GPI-anchor mimic structure contained a cysteine residue at the 2-aminoethyl phosphate region. The cysteine tag is required for the conduction of NCL. Again, by using the EPL reaction, the PrP-

thioesters could be linked to the synthetic GPI-anchor mimic and after refolding, the structure was determined by CD-spectroscopy. The obtained CD curves were in line with the results of the native PrP^C and PrP^{Palm}.[188]

The disadvantage of the underlying semisynthetic approach involving EPL is that a few denaturation and renaturation steps are required during the purification procedure of the PrP thioesters, because the PrP fusion construct mainly distributes into the inclusion bodies in *Escherichia coli*. Diminished yields are to be expected as the subsequent refolding process of the purified semisynthetic PrP variant is another limiting factor. To overcome these problems regarding the lower total yields of the modified PrP, Chu and Becker[192] developed a different approach that favors soluble expression of the PrP fusion construct in *E. coli*. Further work was done by Chu *et al*[185] by applying their semisynthesis strategy to produce three different PrP variants: a full-length FL_PrP (aa 23-231), a N-terminally truncated T_PrP (aa 90-231) and a variant with the central hydrophobic region deleted ΔCR_PrP (aa 23-231 with 105-125 deleted). All the three protein types were connected to a membrane anchor at the C-terminus. It was demonstrated by binding experiments with phospholipid membranes that the binding behavior from lipidated PrP variants differed to the unmodified PrP. Furthermore, it was observed that the secondary structure elements of the unmodified PrP switch to a high content of ß-sheets upon tethering to POPG vesicles, whereas the modified PrP constructs T_PrP and ΔCR_PrP did maintain an α-helical structure. With fluorescence-based assays the localization of ΔCR_PrP in transfected cells was studied. Regarding the localization there was no difference to the native PrP observed, however distinct binding interactions were recognized as they caused perturbed signaling pathways.[196,197]

A more recent work regarding the impact of membrane composition on the conformation and trafficking of lipidated prion protein variants was done by Hackl in the Becker Lab.[198] In her work she achieved to increase the reaction rate of the EPL by testing several reaction conditions. The usage of the thiols 4-mercaptophenylic acid and thiophenol in the EPL showed the best conversion rate for the PrP-thioesters. She managed to produce fluorescently labeled and folded PrP variants linked with GPI-anchor peptide mimics via the mentioned semisynthetic strategy. With circular dichroism (CD) spectroscopy measurements it was shown that the produced prion proteins exhibit the typical far-UV CD spectrum and the secondary structures were not altered due to the GPI-anchor mimicking peptides or the fluorophores. Based on the results of *in vitro* aggregation assays that were monitored by ThT

fluorescence and PK resistance it was reported that the semisynthetic PrP variants showed usual aggregation behavior. With the folded, homogenous PrP variants in hand, the next step was to obtain more information on the PrP-membrane interaction. Therefore, Hackl performed quartz crystal microbalance-dissipation experiments in real time. As a membrane, artificial supported bilayers were used and by varying pH, lipid and salt compositions the binding behavior of PrP was investigated. It was observed that the semisynthetic PrP variants bind to negatively charged lipid bilayers at physiological pH due to strong hydrophobic interactions. These findings were supported by the results of cell imaging experiments with neuron-like SH-SY5Y cells using super-resolution structured illumination microscopy combined with co-localization analysis. By performing imaging total internal reflection-fluorescence correlation spectroscopy measurements, she found that PrP variants equipped with a GPI-anchor peptide mimic affected the dynamics of a cholesterol-dependent membrane domain, as it becomes more fluid. In contrast, the usage of PrP lacking the C-terminal GPI-anchor mimic in the same experiment did not alter the membrane fluidity. Another experiment regarding the PrP-membrane interaction in presence of methyl-ß-cyclodextrin, a cholesterol-depleting agent, latrunculin A and an actin polymerization inhibitor was conducted by Hackl. Based on these results, they propose that an intact actin cytoskeleton can prevent the PrP^C-PrP^{Sc} conversion on membranes, as the cytoskeleton acts like a barrier and in association with the membrane it immobilizes PrP.[198] Summarized, the results of the dissertation strongly suggested once more that the C-terminal membrane anchor is crucially involved in the localization of PrP and the structural change.

2 Materials & Methods

2.1 Materials

2.1.1 Molecular Biology

For each buffer preparation Milli-Q® water (ddH$_2$O) was used. The pTXB1 vector was purchased from New England Biolabs (Ipswich, USA) and the puc57-bvPrP including the synthesized bvPrP was obtained from BioCat (Heidelberg, Germany). The cutsmart buffer solution and the used restriction enzymes (*NdeI* and *SpeI*) originate from New England Biolabs (Ipswich, USA).

To isolate the bank vole prion protein DNA and the pTXB1 backbone a Gel Extraction Kit from New England Biolabs (Ipswich, USA) was used. The T4 DNA-ligase and the 10x T4 DNA-ligase buffer were purchased from New England Biolabs too. A GeneJET Plasmid Miniprep Kit from Thermo Fisher Scientific (Vienna, Austria) was used to purify the vectors. The plasmids were sequenced by the company Microsynth AG (Balgach, Switzerland). For the transformation three different *E. coli* strains were used. The XL1-, the BL21(DE3)- and the BL21(DE3-ROSETTA2) strain were purchased from Novagen. The required components for the LB Medium originate from Loewe Biochemica GmbH (Sauerlach, Germany). The antibiotic compounds ampicillin and chloramphenicol were acquired from GERBU Biotechnik GmBH (Heidelberg, Germany) and Fisher Scientific GmbH (Schwerte, Germany). The cells were grown in a Infors HT Multitron (Bottmingen, Switzerland) incubator shaker. Centrifugation steps with Eppendorf Tubes were either performed with the Eppendorf Centrifuge S418 from Eppendorf AG (Hamburg, Germany) or the Beckman Coulter$_{TM}$ Microfuge® 22R Centrifuge from Beckman Coulter GmbH (Vienna, Austria). The cells were harvested with Beckman Coulter Avanti J-26 XP Centrifuge from Beckman Coulter GmbH (Vienna, Austria) and disrupted by using the Constant Systems LTD Cell disruptor in combination with the RC-10 Digital Chiller, both from VWR International GmbH (Darmstadt, Germany). The used dialysis membranes with a molecular weight cut off (MWCO) of 6-8 kD were obtained from Spectrum Laboratories, Inc. (California, USA). In the folding experiment Slide-A-Lyzer® dialysis cassettes with a MWCO of 10.000 from Thermo Fisher Scientific (Vienna, Austria) were utilized and in the buffer N-Octyl-ß-D-Glucopyranoside (OG) from GERBU Biotechnik GmbH (Sauerlach, Germany) was included.

The markers used for Agarose gels (1 kb Plus ladder) and SDS-gels (Protein Marker) were purchased from New England Biolabs (Ipswich, USA) and GE Healthcare (Freiburg, Germany). Images of the gels were done with the BioRad ChemiDoc MP Imaging System from Bio-Rad Laboratories GesmbH (Vienna, Austria).

2.1.2 Chemicals & Solid Phase Peptide Synthesis

The Fmoc-Ala-Wang Resin was purchased from NovaBiochem® by Merck KGaA (Darmstadt, Germany) and the various chemicals required for the coupling of the polyethylenglycol-polyamide-oligomer were obtained from ApexBio (Texas, USA), NovaBiochem® (Darmstadt, Germany) and Sigma Aldrich (Vienna, Austria). Most of the used Fmoc-amino acids were purchased from NovaBiochem® (Darmstadt, Germany), except for Fmoc-Lys(Mtt) and Boc-Cys(Trt) which were acquired from GL Biochem Shanghai LTD (Shanghai, China) and Iris Biotech GmbH (Marktredwitz, Germany). Further chemicals used in solid phase peptide synthesis (SPPS), such as DMF, DCM, TFA and TIPS, were either purchased from Sigma Aldrich (Vienna, Austria) or VWR International GmbH (Darmstadt, Germany). The compounds palmitoylchloride and triethylamine which were used in the palmitoylation reaction of the synthesized peptide were purchased from Sigma Aldrich (Vienna, Austria). The reagent sodium 2-mercaptoethane sulfonate was obtained from Acros Organics (Geel, Belgium). In the Expressed Protein Ligation the required ligation buffer included NaH_2PO_4/Na_2HPO_4, Tris(2-carboxyethyl)phosphine hydrochloride (TCEP) and 4-mercaptophenylic acid (MPAA). All these chemicals were purchased from Sigma Aldrich (Vienna, Austria). The frequently used salts guanidine hydrochloride and urea were acquired from Sigma Aldrich (Vienna, Austria) and Carl Roth GmbH (Karlsruhe, Germany). Semi-preparative HPLC purifications of the bank vole prion protein thioester and the chemically synthesized GPI-anchor peptide mimic were performed with different purification systems. The following devices were used: The 2545 Quaternary Gradient module from Waters (Massachusetts, USA), the Varian ProStar Preparative HPLC from Agilent Technologies (Vienna, Austria) and the Shimadzu HPLC from Shimadzu (Kyōto, Japan). The masses of the purified compounds were controlled by using the Auto Purification HPLC/MS system from Waters (Massachusetts, USA) and the MSQ Plus HPLC/MS system from Thermo Fisher Scientific (Vienna, Austria). To prove if the refolding of the semisynthetic prion protein was successful CD spectroscopy was done. Therefore, the Chirascan plus spectrometer from Applied Photophysics (Surrey, United Kingdom) was used.

2.2 Methods

2.2.1 Molecular Cloning

As a starting material two different, purified plasmids with a concentration of 100 ng/ml were used. The puc57-bvPrP vector included the desired bank vole prion protein (bvPrP) DNA. The bvPrP gene was flanked by two distinct restriction enzyme cut sites. The sequence CA/TATG recognized by *NdeI* and A/CTAGT recognized by *SpeI*. The second plasmid was a pTXB1 backbone, containing a hsp27 gene flanked by the same cleavage sites followed by a *Mxe* GyrA intein, 7x histidine tag and a chitin binding domain (CBD) sequence. Furthermore, it included an ampicillin resistance marker. By doing a double digest (*Table 3*), which means that the plasmid was treated with two restriction enzymes simultaneously in the reaction vessel, for each vector, the bvPrP- and the hsp27-DNA were excised.

Table 3: Reagents used for the double digest

Digest 1	Digest 2
10 µL pTXB1-hsp27 vector	16 µL puc57-bvPrP vector
2 µL cutsmart buffer	2 µL cutsmart buffer
1 µL *NdeI*	1 µL *NdeI*
1 µL *SpeI*	1 µL *SpeI*
6 µL H$_2$O	

The digest was done at 37°C for 1 hour. Afterwards, 1 µL of a shrimp alkaline phosphatase (rSAP) was added to digest 1 (*Table 3*) to dephosphorylate the emerging flanks. Then after five minutes the temperature was heated up to 65°C to inhibit rSAP. To isolate the pTXB1 backbone and the bvPrP-DNA the samples were loaded onto a 1%-agarose gel (stained with 0,1% methylene blue). The following steps included cutting out the appropriate DNA bands and purify the DNA by using a Gel Extraction Kit. Once this was accomplished, the isolated bvPrP-DNA insert and the pTXB1 plasmid backbone were connected by using a T4 DNA-ligase. Additionally, a negative control without insert was set up for the ligation to have a proof once the subsequent transformation into *E. coli* cells is done, whether the ligation was successful or not. The ligation was performed for 2 hours at 20°C (*Table 4*).

Afterwards both ligation reactions, so the ligated one and the negative control, were transformed into chemically competent XL1 *E. coli* cells. Then the two samples were plated on a culture medium including ampicillin and they were put into the incubator (37°C) overnight. The transformed ligation reaction resulted in a large number of growing colonies on the plate, whereas the negative control in which the insert was exchanged by water did not show any colonies on the LB plate. This observation indicated that the ligation reaction as well as the transformation of the desired plasmids into *E. coli* were successful. The cells were put in the incubator (37°C, 180 rpm) overnight. It was continued by centrifuging the samples for 30 seconds at 14000 rpm. Then the supernatant was discarded and by using the GeneJET Plasmid Miniprep Kit the plasmids were purified. To have further evidence whether the expressed plasmids contain the correct sequence or not, these plasmids were sequenced.

Table 4: Reagents used for the ligation

Ligation	Ligation – negative control
4 µL pTXB1 backbone	4 µL pTXB1 backbone
13 µL bvPrP	13 µL H_2O
2 µL ligase buffer (10 mM ATP)	2 µL ligase buffer (10 mM ATP)
1 µL T4 DNA-ligase	1 µL T4 DNA-ligase

With the correct bvPrP-pTXB1 plasmids in hands, the next step was to find a suitable *E. coli* strain for the bank vole prion protein expression. The plasmid was incorporated in two distinct *E. coli* expression strains by using the same heat shock transformation protocol. Therefore, the BL21(DE3) and the BL21(DE3-ROSETTA2) strain were used. The culture medium for the BL21(DE3) strain included ampicillin, whereas the culture medium for the BL21(DE3-ROSETTA2) ampicillin + chloramphenicol. The last step was to prepare glycerol stocks for the strains. Under sterile conditions 750 µL cell culture and 750 µL 40% glycerol were transferred into small glass-vials. Afterwards, the glycerol stocks were stored at -80°C.

2.2.2 Protein expression & purification

To start with the expression procedure LB media were prepared. The LB medium consists of tryptone (16 g/L), yeast extract (10 g/L) and sodium chloride (5 g/L). The prepared media were autoclaved by using the Varioklav® from Thermo Fisher Scientific (Vienna, Austria). The appropriate antibiotics were added to the LB medium for each strain, subsequent the BL21(DE3) and the BL21(DE3-ROSETTA2) strain carrying the bvPrP expression plasmid were transferred to the respective 100 ml solution. The cells were grown in the incubator (37°C, 160 rpm) overnight. By measuring the $0D_{600}$ value with the NanoDrop 2000c spectrophotometer from Thermo Fisher Scientific the cell density could be determined. Then the calculated volume was transferred to 1L LB medium to reach the desired cell density (OD_{600} value ~ 0.2) in both cultures. Once an OD_{600}-value of 0.6-0.8 was reached overexpression of the desired bank vole prion protein was induced by adding isopropyl-ß-D-thiogalactoside (IPTG). To determine at which timepoint most of the protein is expressed and which strain was showing a higher expression rate, subsamples were taken at several timepoints. The following timepoints were considered: 0, 1, 2, 4 hours and overnight. These subsamples were loaded onto a sodium dodecylsulfate (SDS)-polyacrylamide gel to acquire information about the expression levels. The analysis of the SDS-gel resulted in a favorable expression for the BL21(DE3-ROSETTA2) strain. With the obtained results, it was decided to use the BL21(DE3-RSOSETTA2) strain for further expression experiments. Four hours after the IPTG addition the cells were harvested via centrifugation (6200 rpm, 10°C, 20 minutes). Then the cells were solubilized in 1x TBS buffer and lysed by using a Constant Systems LTD Cell disruptor. The samples were centrifuged again for 30 min with 15000 rpm, 5°C. SDS page revealed, that the bank vole prion protein *Mxe* GyrA-7xHis-CBD fusion construct is primarily expressed into the insoluble inclusion bodies. Afterwards the proteins were solubilized under denaturing conditions by using 8 M guanidine hydrochloride. To generate a C-terminal thioester and to get rid of the intein fusion tag *Mxe* GyrA-7xHis-CBD, sodium 2-mercaptoethanesulfonate (MESNa)-mediated intein cleavage was performed. Therefore, the 8 M guanidine hydrochloride solution was exchanged with 4 M urea by dialysis. A 1 M MESNa solution was slowly added to the denatured bank vole protein solution resulting in a final concentration of 2 M urea and 500 mM MESNa during the reaction. After an incubation time of 24 hours, the crude reaction solutions were centrifuged (4300 rpm, 20°C, 15 min). The

supernatant was discarded, as SDS-gels revealed that the bvPrP-thioester mainly distributes into the pellet. The pellet was then dissolved in 8-9 ml 6 M guanidine hydrochloride and purified via preparative RP-HPLC. The desired fractions were identified via ESI-MS in positive ion mode by using the Waters Auto Purification System. The collected fractions were pooled, lyophilized, and ultimately stored at -80°C. The purity of the bank vole prion protein thioester was assessed via analytical RP-HPLC.

2.2.3 Agarose gel & SDS-polyacrylamide gel electrophoresis

Agarose gel electrophoresis is a common and efficient method to separate DNA fragments of different sizes ranging from 100 bp to 25 kb. The chemical compound agarose is composed out of repeated L-and D-galactose subunits and is obtained from the seaweed genera *Gelidium*. In the process called gelation, the agarose molecules form a tight network due to non-covalent interactions. This network comprises small pores and therefore it operates as a molecular sieve. Nucleic acids can be loaded into small chambers of the gel, which are prepared during gelation by putting a comb into the gel. If there is voltage applied, the DNA migrates through the pores of the gel into the direction of the anode, because the backbone of DNA is negatively charged. The traveled distance of each DNA fragment is inversely proportional to the logarithm of its molecular weight. This is possible since the mass/charge ratio of DNA is consistent. How far a nucleic acid fragment will migrate depends on the following parameters: Molecular weight of a DNA fragment, DNA conformation, electrophoresis buffer, agarose concentration, the type of agarose, the presence of ethidium bromide and the applied voltage. To make the DNA fragments visible the agarose gel is usually stained with a dye and is observed under UV-light.[199]

In the practical lab work of this master project 1% agarose gels were prepared. As an electrophoresis buffer a 1x TAE-buffer containing 40 mM TRIS, 20 mM acetic acid and 1 mM EDTA was used. 6x loading dye (New England Biolabs) was added to the DNA samples before they were loaded on the gel. 50-80 V was applied for 1-2 hours and afterwards the agarose gels were stained either with 0,1% methylene blue in TAE or ethidium bromide (0.5 μg/ml) for at least half an hour.

The sodium dodecylsulfate gel electrophoresis (SDS-page) is a widely used technique for separating proteins. SDS-page is based on the denaturation of proteins with the denaturing agent sodium dodecylsulfate and the electric current which drives the migration of the proteins through the polyacrylamide gel. The addition of SDS to a protein mixture results in the removal of tertiary and secondary structure of the proteins. SDS coats the exposed polypeptide chain, thereby conferring the same negative electrical charge to the proteins, because the attachment of SDS is proportional to the molecular weight. The biochemical impact of SDS enables the separation of proteins by their size. In this method the gel consists of the polymer polyacrylamide, which is assembled by acrylamide monomers. To form a meshwork of fibers the acrylamide is treated with a crosslinker, usually bis acrylamide, in the presence of a gel buffer. By adding a catalyst (TEMED) and an initiator (APS) the gel polymerizes. The ratio of used acrylamide and its respective crosslinker influences the porosity of the gel. Nowadays the discontinuous electrophoresis is frequently used. In this system the polyacrylamide gel consists of two different types, the stacking and the separation gel. The separation gel is at the bottom and filled up to about ¾ height of the loading chamber. The stacking gel is casted right above the separation gel. Like in the agarose gel, a comb is placed into the stacking gel to create the loading wells. These two distinct gel types differ in the proportion of the chemical reagents, in their function and in the pH value. The stacking gel (pH = 6,8) is utilized to focus the proteins into a sharp band so that a good precondition for the following separation is created. Whereas the separation gel (pH = 8,8), which in our case contained 15% acrylamide is required to separate the proteins. The negatively charged SDS coated proteins start to migrate in the direction of the anode once voltage is applied to gel chamber. The Tris and glycine containing Lämmli buffer system is a widely used buffer system for SDS-page. TRIS maintains the pH of 6,8 in the stacking gel and glycine is needed so that the applied current can flow properly. Commonly used staining methods for SDS-gels are the coomasie blue stain or silver stain.[200]

SDS-page was carried out to analyze the expressed prion protein fusion construct and to follow the timepoints of the EPL during the lab work. The polyacrylamide gels were prepared based on a protocol from Laemmli *et al*[201]. The 10x Laemmli Buffer stock solution included 250 mM TRIS, 2 M glycine and 1% SDS. The prepared SDS-gels were placed in a Mini-PROTEAN® Multi-Casting Chamber from Bio-Rad (Herkules, USA) for the gel electrophoresis. The required reagents for the composition of the polyacrylamide-gels are listed in *Table 5*.

Table 5: Composition of the stacking- and separating gel used for the SDS-page

Gel	30%-acrylamide [mL]	buffer [mL]	10% SDS [µL]	10% APS [µL]	TEMED [µL]	ddH$_2$O [ml]
Stacking	0.9	0.7	53	53	5.3	3.6
Separation	7.5	3.9	157	157	4.7	3.6

For each gel the desired protein samples were mixed 1:1 (v/v%) with a 2x sample loading buffer, which consists of 500 mM TRIS, 6% SDS, 35% glycerine, 3.55% ß-mercaptoethanol and 0.05% bromphenol blue. Furthermore, the samples were heated shortly at 94°C and centrifuged for 30 seconds at 14000 rpm, before they were loaded onto the gel. A voltage of 250 was applied via a PowerSource 300 V from VWR International GmbH (Darmstadt, Germany) and the run time of the gels was set to 37 minutes. The polyacrylamide-gels were stained with a 0.1% coomasie blue dye (Coomasie Serva Blue R).

2.2.4 Refolding of the bank vole prion proteins

Once the semisynthetic prion protein was purified and lyophilized, the biologically active structure was induced by following a protocol from Chu *et al.*[190] All the required steps of the refolding process were carried out at 4°C. The lyophilized protein was solubilized in 400 µL of a 6 M guanidine hydrochloride solution containing 50 mM TRIS (pH = 8). Then the protein concentration of the sample was measured via the NanoDrop 2000c spectrophotometer. Afterwards the denatured bvPrP sample was treated with a sodium acetate refolding buffer, containing a redox system of oxidized and reduced glutathione (20 mM sodium acetate, 0.3 mM glutathione OX, 3 mM glutathione RED, pH =5). The guanidine hydrochloride concentration was diluted to 2.5 M by stepwise addition of the refolding buffer for several hours. The sample was kept on a shaking platform over the weekend. Afterwards the bvPrP sample was transferred into a Slide-A-Lyzer® dialysis cassette (10000 MWCO, 0.5-3 ml capacity). The protein was dialyzed against a 20 mM sodium acetate including 10 mM OG. The dialysis buffer was exchanged two times after three hours and after an overnight incubation the sample was removed from the Slide-A-Lyzer®. Then the refolded bvPrP was centrifuged (13000 rpm, 4°C, 15 min) and the concentration was measured again.

2.2.5 Biophysical characterization

The method of CD spectroscopy is used to analyze the secondary structure and folding properties of proteins. Thereby it is possible to distinguish, whether a protein is folded correctly or specific mutations lead to a flawed phenotype, accompanied by the loss of secondary structure. The biophysical technique is based on the principle that biomolecules (proteins) consist of chiral subunits that can absorb circularly polarizing light in the near and far ultraviolet range. The amide and carbonyl groups absorb the incident, left- and right circularly polarized light resulting in electronic transitions in the wavelength region of 240 to 170 nm. Furthermore, the presence of aromatic amino acids can be determined, since they absorb in the near UV range (300-260 nm). The standard CD spectrometer includes a light source, a monochromator to spectrally isolate a specific wavelength of an incidental beam, a polarizer to produce right- or left-polarized light, a sample chamber and a detector (*Figure 6*).
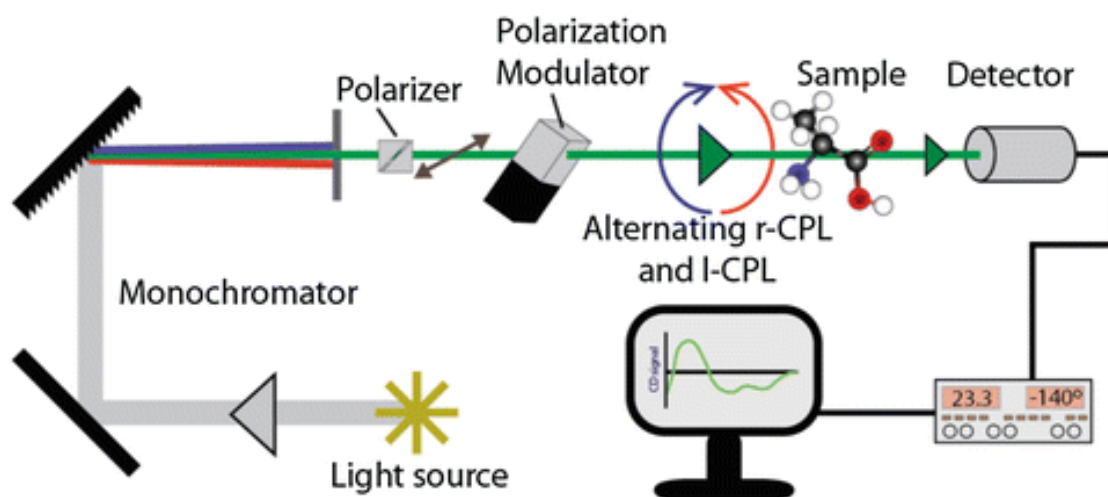
Figure 6: Circular dichroism spectroscopy instrumentation.
The image was taken from Hoffmann *et al.*[217]

The obtained data from CD spectroscopy are often consistent with other biophysical, chemical, or computational methods, such as crystallography, NMR spectroscopy or cryo-electron microscopy. The results of circular dichroism measurements may also include information about protein interactions, dynamic changes in solution or environments such as membranes. To highlight the importance of CD spectroscopy, it offers some advantages compared to the previously mentioned high resolution techniques. One advantage includes that only a small amount of sample is required and after finishing the measurement, the samples can be reused. It is now possible to utilize high light flux due to the ongoing progress

in the development of circular dichroism beamlines. The establishment of these high intensity light sources allows a faster data collection with less amount of the protein needed. A major disadvantage of the CD-spectroscopy is that the resolution is not as high as in other biophysical methods used for the elucidation of secondary structures.[202]

To verify that the semisynthetic bvPrP was folded correctly, circular dichroism (CD) measurements were recorded with the Chirascan Plus CD-spectrometer from Applied Photophysics. A micro cuvette with 1 mm path length was used for the CD-spectroscopy. As a blank the dialysis buffer (20 mM sodium acetate, 10 mM OG) was employed. The bvPrP sample was diluted 1:1 to achieve a suitable concentration of 0.15 mg/ml for the measurement. Each spectrum was measured with the following settings: 200 to 280 nm with 1 nm steps at room temperature (20°C). The acquired spectrum was created out of the average of 10 single measurements and additionally background subtraction was applied. The included data in the chapter results & discussion was processed with OriginPro. Information about the percentual content of secondary structures was acquired by using the curve-fitting software CDNN from Böhm *et al*.[203] The required molar extinction coefficient at 280 nm for the semisynthetic bvPrP was calculated with the help from Expasy-ProtParam (https://web.expasy.org/protparam). Therefore, the combined sequence of the bvPrP and the peptide was used, excluding the palmitoyl chains and the PPO$_3$-tag as it is not possible to insert them in the Expasy-ProtParam inbox. A molar extinction coefficient of 63.495 was calculated for the modified bvPrP with a MW of 26152 Da.

2.2.6 Solid phase peptide synthesis (SPPS)

The GPI-anchor peptide mimic was synthesized by using the method of solid phase peptide synthesis. SPPS was carried out manually in a syringe and the fluorenylmethoxycarbonyl (Fmoc)-strategy was applied with a pre-loaded Fmoc-A-Wang resin as a starting point. The desired peptide with the sequence H-CKGENLYFQSKAAKK-PPO$_3$-A was synthesized according to a protocol from Olschewski *et al*[184] in a scale of 0.2 mmol. It was started with the coupling of the polyethylenglycol-polyamide oligomer (PPO3). Each monomer was attached to the resin within three major reaction steps. First the deprotected resin was treated with 10 eq succinic anhydride in 0.5 M 1-hydroxybenzotriazole (HOBt) in N,N-dimethylformamide (DMF) and 6 eq

N,N-diisopropylethylamine (DIPEA), second with 20 eq 0.5 M 1,1-carbonyldiimidazole (CDI) in DMF, and third with 12 eq of each, 4,7,10-trioxatridecane-1,13-diamine and 0.5 M HOBt. Each reaction step was carried out for 30 minutes and the coupling progress was verified by performing ninhydrin tests in between. The PPO_3-tag should operate as a solubility tag for the peptide. The N-terminal protecting group Fmoc of each amino acid was removed with a solution of 20% (v/v) piperidine in DMF. The deprotection was carried out in two cycles of 3 and 7 minutes. The following orthogonal protecting groups were attached to the side chain residues of the coupled amino acids: 2x Lys(Boc), 2x Lys(Mtt), Ala, Ser(tBu), Gln(Trt), Phe, Tyr(tBu), Leu, Asn(Trt), Glu(OtBu), Gly and Boc-Cys(Trt). Each amino acid was used in amounts of 2.5 eq (0.5 mmol) and activated for coupling with the addition of 2.4 eq 0.5 M (1-[Bis(dimethylamino)methylene]-1H-1,2,3-triazolo[4,5-b]pyridinium 3-oxide hexafluorophosphate (HATU) in DMF and 5 eq DIPEA. The coupling was carried out for 30 minutes under constant shaking. The side chain residues of the lysines at position 11 and 14 were palmitoylated to mimic the lipid properties of the GPI-anchor. Therefore, the 4-methyltrityl (Mtt) protecting groups were selectively deprotected with 2% (v/v) trifluoroacetic acid (TFA), 1% (v/v) triisopropylsilane (TIS) in dichloromethane (DCM). The deprotection was performed in alternate cycles of treating the resin with the deprotection solution for two minutes and washing it with DCM. Once the Mtt deprotection was done, the resin was immediately incubated in a solution of 20 eq palmitoyl chloride, 20 eq HOBt and 22 eq triethylamine in DCM:DMF (3:1) for 16 hours. At this step, the synthesis was finished and the peptide was cleaved off the resin by adding a solution of 92.5% (v/v) TFA, 5% (v/v) TIPS and 2.5% dd H_2O to the syringe. The final cleavage was carried out for three hours, followed by removal of the cleavage solution with argon to obtain the crude peptide. Then the peptide was dissolved in acetonitrile:ddH_2O (1:1), 0.1% (v/v) TFA and lyophilized. Afterwards the dried peptide was solubilized by adding 6 M guanidine hydrochloride (pH = 4,6) and purified via preparative RP-HPLC. The major fractions were collected and the mass of the peptide was verified via ESI-MS (positive ion mode). Then the fractions were pooled, lyophilized and stored at -20°C until further usage. The purity of the GPI-anchor peptide mimic was assessed via analytical RP-HPLC.

2.2.7 Expressed Protein Ligation (EPL)

In this reaction the bvPrP α-thioester and the GPI-anchor peptide mimic were ligated to obtain the semisynthetic bvPrP. For the EPL the synthesized peptide was used in a 2-fold excess to the α-thioester. Concentrations of 3 mM and 1.5 mM were utilized. The reaction was conducted overnight (~20 h) under argon at room temperature (20°C) and constant shaking. The ligation procedure was implemented by dissolving the peptides in a ligation buffer, followed by the addition of the solution to the bvPrP α-thioester. The degassed ligation buffer (pH = 7.2) consisted of 6 M guanidine hydrochloride, 200 mM Na_2HPO_4/NaH_2PO_4, 30 mM 4-mercaptophenylacetic acid (MPAA) and 20 mM TCEP. At several timepoints 1 μL subsamples were taken to analyze the progress of the reaction via LC-MS (Auto Purification System Waters) and SDS-page. For purification the ligation mix, containing the formed lipidated bvPrP, was diluted with 6 M guanidine hydrochloride (pH = 4.6) and isolated via semi-preparative HPLC. The desired fractions were collected and identified via ESI-MS operating in positive-ion mode. The sample was pooled, lyophilized and stored at -80°C. Purity of the semisynthetic bank vole prion proteins was validated via analytical RP-HPLC.

2.2.8 High performance liquid chromatography & mass spectrometry

High performance liquid chromatography (HPLC) is a popular technique to isolate constituent chemical compounds in a mixed solution by passing them through a chromatographic column. The method is based on the principle that molecules, which are dissolved in a liquid, not only interact with the particles of the liquid, but also with the surface molecules of a solid material. Therefore, this technique contains two different phases, the mobile and the stationary phase. If a compound, dissolved in the mobile phase, interacts frequently or less frequently with the stationary phase, depends on the biophysical properties of the molecule. The retention time, which means how long it will take for a molecule to pass through the column, is thereby determined by properties like the solubility in water, the solubility in organic solutions, size and the net electric charge. These conditions enable different applications for HPLC, such as normal-mode, reverse-phase, ion-exchange or size exclusion chromatography. Depending on the used chromatography-mode, the stationary solid-phase differs in its surface environment. The normal-mode requires hydrophilic surface molecules, whereas the reverse-phase

presents an organic surface environment. For the ion-exchange chromatography the surface of the stationary phase is charged and in size exclusion the surface is porous, resulting in restraining smaller molecules. The chromatography instrument consists of four parts: the injector, the pump, the column and the detector (*Figure 7*). Injection can either be manual or automated and is used to load the liquid sample on the column. The pump is important to remain a constant flow rate and to force the mobile phase through the column with a higher velocity compared to gravity-flow columns. The column is essential for a proper chromatographic performance and widely used HPLC column types are packed with silica-particles. Once a molecule elutes from the column, the detector produces a signal proportional to the concentration of the chemical compound. The arising signal is converted to an electrical signal that is amplified, resulting in data points displayed as a peak in the chromatogram. Commonly used detectors are for example the refractive index detector, UV/VIS-detector and the fluorescence detector.
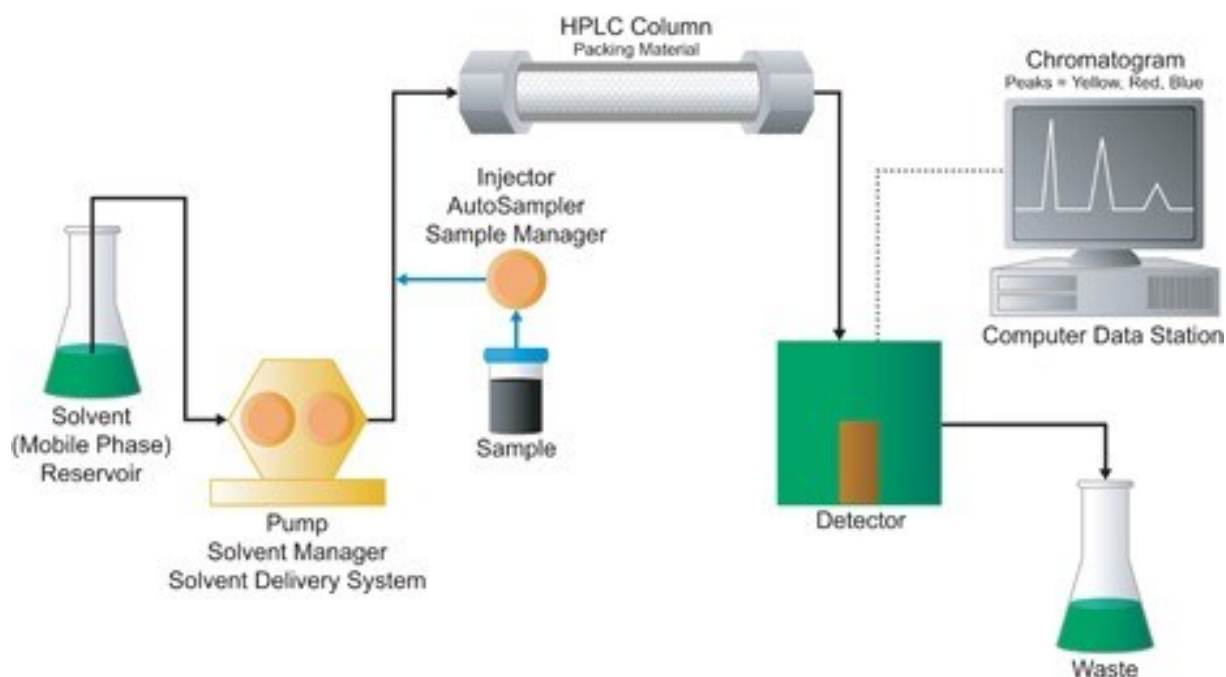
Figure 7: High performance liquid chromatography instrumentation.
The figure was taken from Waters Corporation.[218]

The HPLC technique is used in the area of pharmacy, food technology, forensics, biochemistry, clinical or environment. There it can be either used as a quantification technique via semi- and preparative HPLC or as quality control via analytical HPLC.[204,205]

In the practical work, RP-HPLC was performed on a preparative Shimadzu HPLC system (LC-20 AP pump), a Waters Auto Purification HPLC/MS system (3100 Mass Detector, 2545 Binary

Gradient Module, 2767 Sample Manager, 2489 UV/Visible Detector), a Thermo Scientific MSQ Plus HPLC/MS system (Waters XSelect CSH^{TM} C18 2.5 μm 3 x 75mm XP column) and a preparative Varian ProStar HPLC system. The proteins were separated by semi- and preparative purification using Kromasil C4 columns (300-10-C4, 10 x 250 mm and 21.2 x 250 mm, 10 μm particle size). A linear gradient of 5-75% for the peptide and 5-65% for the bvPrP α-thioesters of buffer B (acetonitrile + 0.08% TFA) in buffer A (ddH$_2$O + 0.1% TFA) was adjusted for the purification and it was carried out at 60°C. The run time of the linear gradient was either set to 40 minutes for the GPI-anchor peptide mimic or to 60 minutes for the α-thioester. The purification of the semisynthetic bvPrP variant was conducted on a semi-preparative scale with a linear gradient of 5-65% buffer B over 60 minutes at 60°C and with a flow rate of 3 ml/min. The purity of the samples was assessed via analytical RP-HPLC by using a Thermo Scientific Vanquish HPLC system. A linear gradient of 5-65% buffer B over 30 minutes was used for the bvPrP α-thioester, whereas for the peptide and the modified bvPrP the same gradient at 60°C was adjusted. For analytical RP-HPLC a flow rate of 1 ml/min and a Kromasil C4 column (300-5-C4, 150 x 4.6 mm, 5 μm particle diameter) were used. UV absorption of 214 and emission of 650 nm respectively were monitored with a charged aerosol detector (CAD).

Mass spectrometry:

The method of mass spectrometry (MS) is used to monitor the mass to charge ratio of ions. The technique is employed for quantitative and qualitative analysis in natural sciences, especially in the fields of biochemistry or biology for the identification of biomolecules, sugars proteins and peptides. Nowadays MS instruments are preferably coupled to chromatographic techniques because it provides a robust and simple interface and allows a high throughput of many compounds in a single analytical run. It is possible to monitor proteins up to mass of over 300.000 Da. Furthermore, mass spectrometry offers the opportunity to analyze samples from the gas, liquid or solid state. A MS instrument consists of four major constituents, the ion source, a mass analyzer, the ion collector and the detector. Depending on the ion source type the samples molecules become ionized in various ways. Popular ion sources are electro-spray ionization (ESI), chemical ionization, electron impact ionization, thermal ionization and matrix assisted laser desorption ionization (MALDI). The choice of a specific ion source takes different characteristics into account, such as the degree of ionization, sample properties and

if fragmentation should be desired or not. The sample molecules are injected in a liquid state if a ESI source is used. The ESI source includes a needle to which a voltage is applied and once the inlet stream passes through the capillary the sample is ionized. Thereby, a spray of multiply charged droplets is generated. Then these droplets migrate through a heated capillary to induce solvation. Each droplet gets smaller in size but keeps the number of electrical charges until the Rayleigh limit is reached. The Rayleigh limit is a physical principle implying that a droplet can only carry a limited number of electrical charges depending on the size of the droplet and the surface tension. Once the Rayleigh limit is reached, the droplet divides in a process called coulomb explosion. This cycle is repeated until the solvent is fully dissolved. An advantage of the ESI ion source is that the ions can carry multiple charges, resulting in an increased range of detected masses, since the m/z ratio is monitored. As the ionized samples leave the ion source, the ion beam is focused and forced into the direction of the mass analyzer. In the mass analyzer the ions are separated by filtering specific m/z at consecutive times. There exist three major properties which influence the performance of a mass analyzer: the resolution, the transmission and the upper mass limit. The underlying formula for the resolution is $\delta m/m$. The term resolution describes the ability of the mass analyzer to display two different but close masses in a delimited manner. δm is the smallest possible mass difference of two peaks that can be monitored. The transmission describes the number of ions that are generated in the ion source and actually arrive at the detector. In order to measure as sensitive as possible a high transmission would be desirable. The upper mass limit estimates the highest measurable m/z. Widely used mass analyzers are the quadrupole, the time of flight (TOF) analyzer, the orbitrap, the ion trap and the Fourier transform-ion cyclotron resonance analyzer. The ion collection and detection are coherent in MS instruments. For example, in the Q Exactive Orbitrap Mass Spectrometer, a modern instrument from Thermo Fisher Scientific, a C-Trap connected to a collision cell is prefixed to the orbitrap. The C-trap is filled with ions and if required, they can be directed into the multipole collision cell to undergo fragmentation. Afterwards the sample molecules head back to the C-trap, followed by injection into the Orbitrap for detection. Frequently used detectors are the electron multiplier and the microchannel plate. The detection in both is carried out by dashing of the ionized samples against metal plates, resulting in a cascade of electron emissions. These emissions lead to a measurable current.[206]

Mass spectroscopy was conducted on the Waters Auto Purification HPLC/MS system and on the Thermo Scientific MSQ Plus HPLC/MS system. The samples were either injected directly or into the pre-coupled HPLC system. Mass spectra were obtained by ESI operating in positive ion mode. To identify the masses, spectra were deconvoluted by using the softwares MagTran and MassLynx. The acquired raw data was exported and processed with OriginPro.

3 Results & Discussion

3.1 Cloning of bvPrP

As the purchased synthetic bvPrP gene was cloned into a puc57 vector, the first step was to transfer the gene into a pTBX1 plasmid to obtain a bvPrP *Mxe* GyrA-7xHis-CBD fusion construct. Therefore, a double digest of the flanking restriction sites *NdeI* and *SpeI* was conducted. To see if the digest was successful, the samples were loaded on a 1%-agarose gel. As a size standard a mixture of 12 µL H_2O, 3 µL 1 kb plus ladder and 3 µL 6x loading dye (New England Biolabs) was used. 4 µL of the 6x loading dye was added to each sample, before they were loaded into the wells. The runtime of the agarose gel was set to 1h with 80V. Afterwards the gel was stained with 0.1% methylene blue for 1-2 hours.
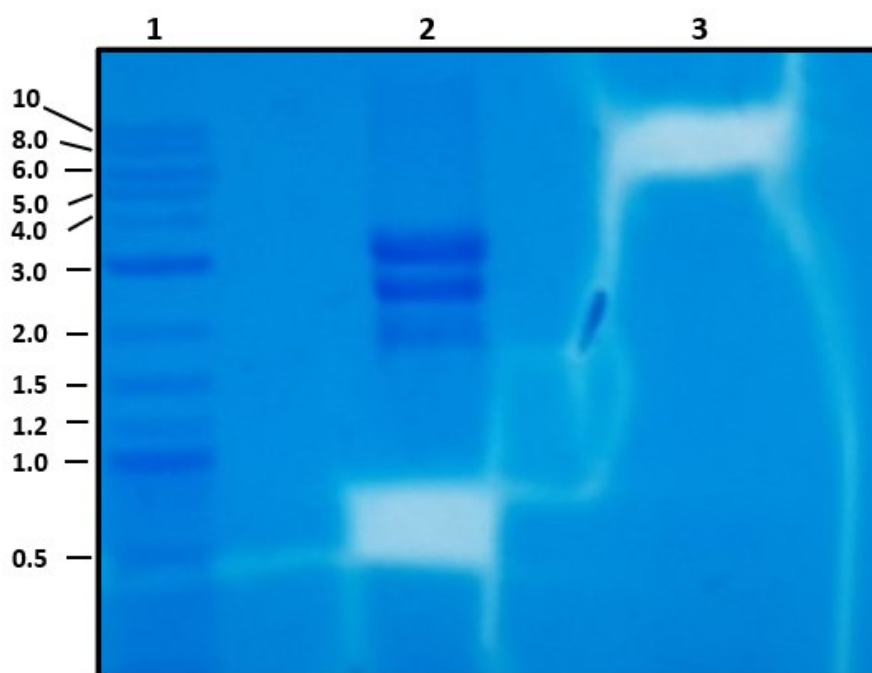
Figure 8: Agarose gel electrophoresis of NdeI / SpeI digested plasmids puc57-bvPrP (lane 2) and pTXB1-hsp27 (lane 3). The light blue spots indicate the positions where the desired DNA fragments were excised from the gel. Lane 1 shows the bands of the 1 kb plus ladder marker.

The agarose gel image was taken, after the DNA bands of the bvPrP gene in lane 2 and the pTXB1 vector backbone in lane 3 were excised for a better visualization as the respective for the bvPrP-DNA was observed with a weak intensity. The double digest of the puc57-bvPrP plasmid with *NdeI* and *SpeI* was successful, as the bvPrP DNA (630 bp long) is located between the two marker bands 0.6 kb and 0.7 kb in lane 2. The band with a high intensity, observable

at approximately 3 kb, in lane 2 indicates the puc57 backbone. However, as the band is accompanied by two further bands directly below, it could be possible that the digest of the vector was not fully completed. Normally, three DNA bands in a narrow distance on the agarose gel indicate an uncut plasmid in three different conformations: supercoiled, relaxed and nicked. The backbone of the pTXB1 vector is 6706 bp long. In lane 3 the appearance of a single band at around 6 kbp indicates that the double digest was conducted properly. The intensity of the hsp27 insert was very low and is therefore not observable on the gel image in *Figure 8*.

Next, the bvPrP-DNA was ligated with the pTXB1 backbone. Then chemically competent XL1 *E. coli* cells were transformed with the ligated plasmid construct (pTXB1-bvPrP) and plated on LB medium including the antibiotic ampicillin. On the next day, the culture plates were examined. The ones including several colonies did indicate a successful transformation and ligation, as with the replication of a functional pTXB1 plasmid the bacteria gain ampicillin resistance. Four clones were inoculated in LB-medium + ampicillin. After the overnight incubation at 37°C under constant shaking, the plasmids were isolated with GeneJET Plasmid Miniprep Kit.

The concentrations of the purified pTXB1-bvPrP plasmids were measured with a NanoDrop 2000c spectrophotometer. The obtained concentration of each sample can be observed in *Table 6*.

Table 6: Concentrations of the purified pTXB1-bvPrP plasmids measured by a NanoDrop 2000c spectrophotometer

Clone	Concentration [ng/µL]
1	76.4
2	60.4
3	76.0
4	74.8

To verify, if the exact DNA sequence of bvPrP was successfully inserted, sample 1 and 3 were sequenced. Additionally, all clones were analyzed by restriction digest with the enzymes *NdeI* and *SpeI*. Therefore another 1% agarose-gel was prepared. 5 µL of each sample were mixed with 2 µL cutsmart buffer, 1 µL *NdeI*, 1 µL *SpeI* and 11 µL H$_2$O. Two control samples with the

same composition, except one including 5 µL puc57-bvPrP and the other 5 µL pTXB1-hsp27 instead of 5 µL pTXB1-bvPrP, were loaded onto the gel too. Again, each sample was mixed with a 6x loading dye purple before loading and as a marker the 1 kb plus ladder was used. This time the agarose gel was stained with ethidium bromide (0.5 µg/ml) and the run time was set to 1 hour with 100 V.
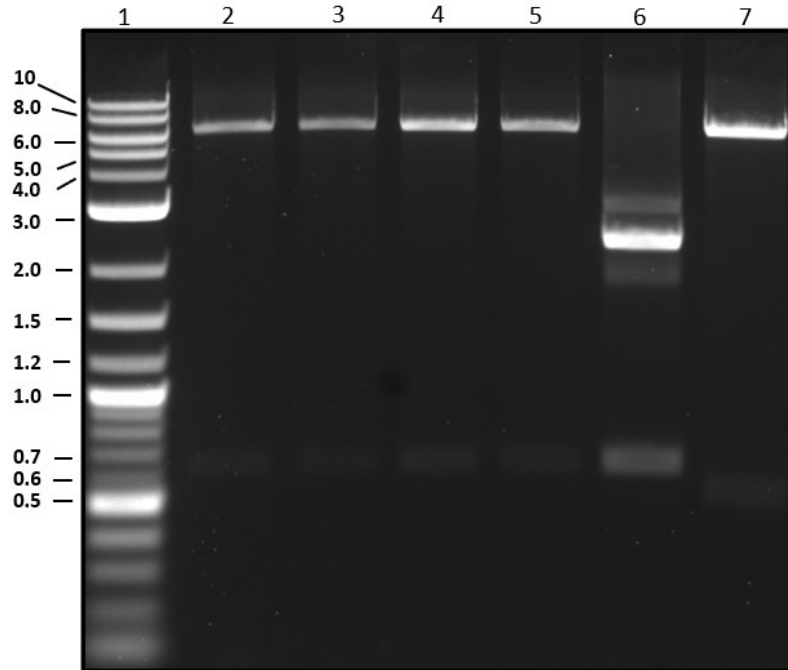
Figure 9: Double digest of the pTXB1-bvPrP subsamples followed by agarose gel electrophoresis. Lanes 2, 3, 4 and 5 show the double digest with *NdeI* and *SpeI* with the clones 1-4 of the pTXB1-bvPrP. Lane 6 shows the double digest of the puc57-bvPrP control and lane 7 the pTXB1-hsp27 control. In Lane 1 the bands of the 1 kb plus ladder marker can be observed.

In the taken image of the agarose gel in *Figure 9* it can be observed that all the 4 clones (lane 2, 3, 4 and 5) contain the desired DNA fragments. The upper high intensity bands indicate the pTXB1 backbone (6706 bp long), whereas the weak intensity bands on the bottom show the bvPrP DNA (630 bp). As the bvPrP DNA band in the control sample in lane 6 is at the same height, the assumption that the ligation was conducted properly in all four samples is approved. A stronger intensity is observed for the bvPrP DNA band in the control, because the plasmids were more concentrated in this sample. The three bands between 2 kb and 3 kb region indicates again the uncut puc57 plasmid in the supercoil, relaxed and nicked state. Further confirmation is gained by the pTXB1 backbone DNA band in lane 7, as it is equal to the height of the ones in the target samples. The low intensity band between the 0.5 kb and 0.6 kb region of the marker indicates the hsp27 DNA. The sequencing results from Microsynth AG confirmed that sample 1 showed a 100% match with the target sequence. The information

obtained by the agarose gel and the sequencing data was evidence enough to continue with the test expressions of the bvPrP fusion construct in three different *E. coli* strains.

3.2 Semisynthesis of bvPrP

The semisynthetic strategy utilized in this project was developed by Becker *et al*[184-192]. The underlying working procedure involving EPL can be observed in *Scheme 4*.
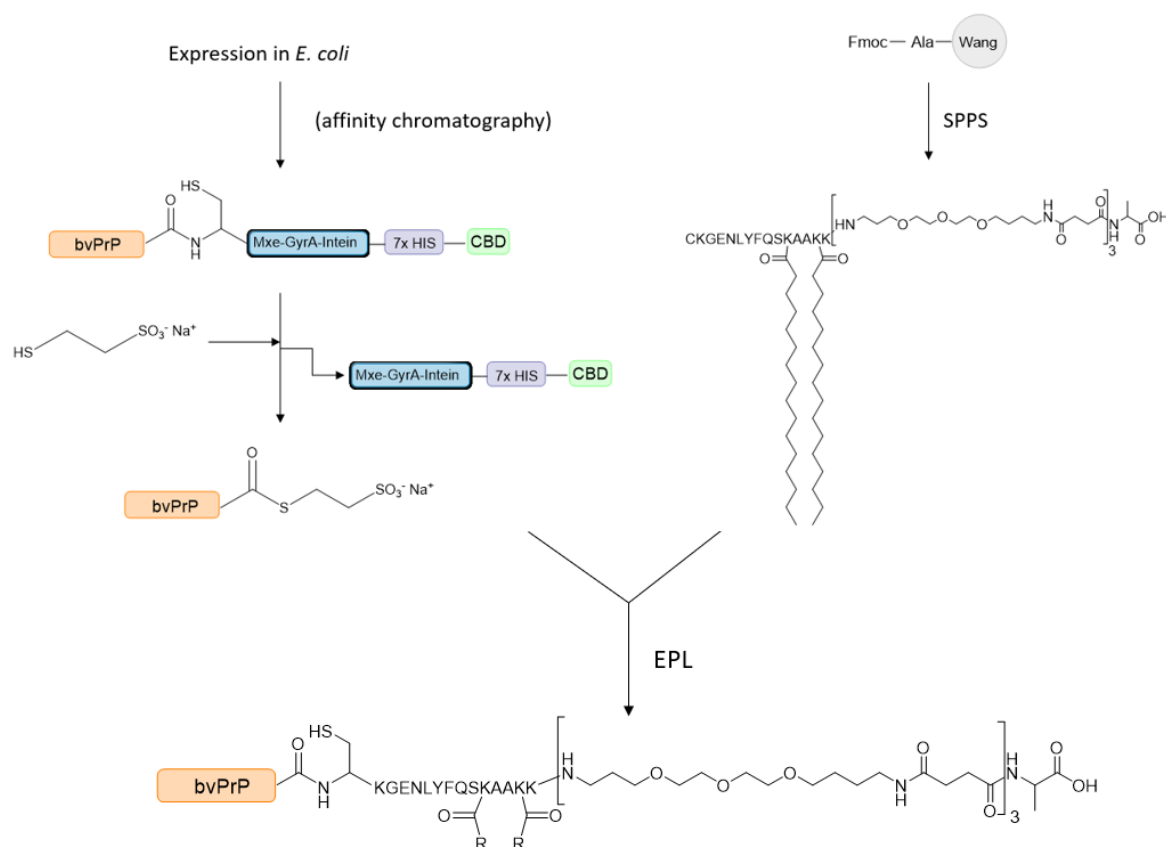
Scheme 4: Semisyntethic strategy for the lipidated bvPrP. In the EPL reaction the recombinantly expressed bvPrP with the C-terminal thioester is linked to the GPI-anchor peptide mimic, which was prepared via SPPS.

The bvPrP, indicated in orange (*Scheme 4*), comprises the amino acids 23-231 and is recombinantly expressed in *E. coli*. The N-terminal signal sequence (aa 1-22) is excluded. The bvPrP is expressed as a fusion construct with a C-terminal *Mxe* GyrA-intein-His-CBD sequence. The intein is essential for the intermolecular rearrangement and by adding MESNa the bvPrP α-thioester is produced. The GPI-anchor peptide mimic is obtained via SPPS with Fmoc protective chemistry. The synthesized peptide contains a N-terminal cysteine, which is required for the ligation. The EPL reaction affords the generation of lipidated bvPrP by linking the two prepared polypeptides.

3.2.1 Expression and purification of the bvPrP-thioester

The prepared pTXB1-bvPrP plasmid was introduced into two different *E. coli* expression strains BL21(DE3) and BL21(DE3-ROSETTA2) via transformation. To identify the strain with the strongest expression of the bvPrP fusion construct, for both strains one liter cell culture in LB-medium, including the respective antibiotics, was prepared. At a measured cell density (OD_{600} value) between 0.6 and 0.8 IPTG was added to the cell cultures to induce over-expression. Then at several timepoints (0 h, 2 h, 4 h and overnight) subsamples were taken for SDS-gel analysis.
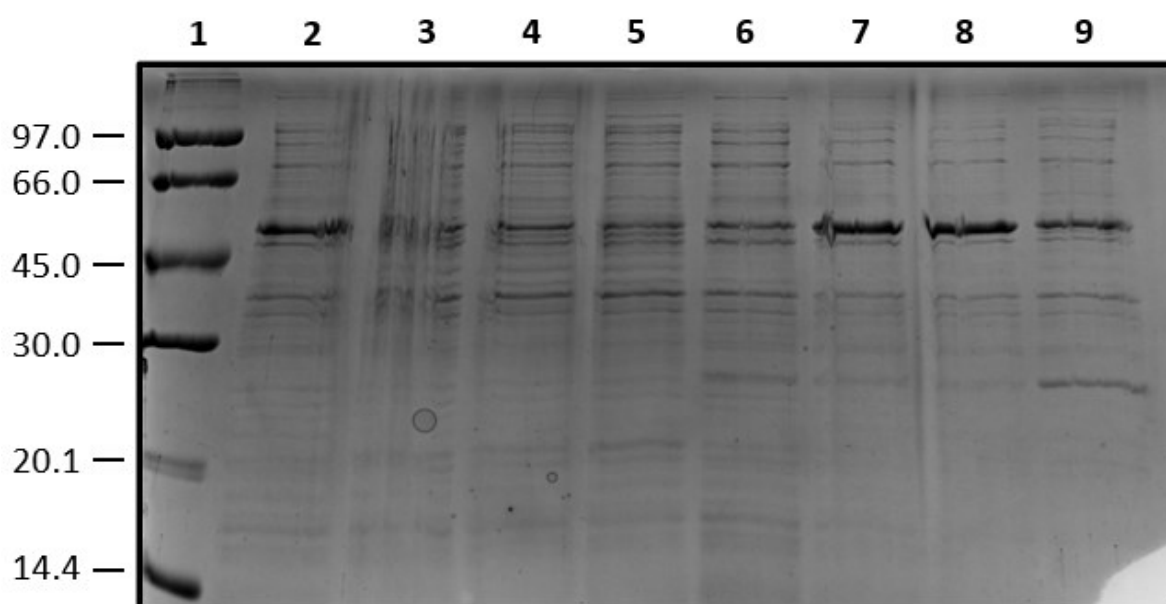
Figure 10: Comparison of the bvPrP fusion protein expression in two different E. coli strains. The lanes 2, 3, 4 and 5 show the expression pattern of the BL21(DE3) strain at the timepoints 0, 2 h, 4 h and overnight. Lanes 6, 7, 8 and 9 show the produced proteins of the BL21(DE3-ROSETTA2) strain at the timepoints 0, 2 h, 4 h and overnight respectively. The protein bands in lane 1 belong to the Amersham Low Molecular Weight (LMW) marker.

As shown in *Figure 10*, SDS gel analysis of the bvPrP *Mxe* GyrA-7xHis-CBD expression revealed that the *E. coli* strain BL21(DE3-ROSETTA2) showed a higher expression rate of the bvPrP fusion construct. The significant protein band in each sample between the 45 kDa and 66 kDa region of the marker is representative for the bvPrP fusion protein as the expected MW is 52059 Da. The observed high intensity bands in lanes 7 and 8 show the expression of the bvPrP fusion protein in the BL21(DE3-ROSETTA2) after 2 and 4 hours, whereas at the other timepoints in both strands the respective bands shows a weaker intensity. In lane 9 the characteristic band is visible with reduced intensity. This may indicate that overnight some of

the overexpressed bvPrP fusion protein gets already degraded within the bacteria cells or that the fusion tag was removed, since the increased intensity of the band below 30 kDa would fit the intein fusion tag (28934 Da). However, it was surprising that the target band in lane 2 showed a high intensity, as the expression pattern indicates the BL21(DE3) expression at the starting point. Usually, one would expect to observe a band with a weak intensity at timepoint zero, since the expression of the bvPrP gene is not induced without the addition of IPTG. Once IPTG is added to the cells, the expression of the bvPrP fusion protein is started and overtime the band should increase in its intensity. Therefore, an explanation for the unexpected appearance of the band could be that the promoter was leaky. The term leaky promoter ascribes the condition of a promoter, in which the mRNA production is still driven even when not stimulated by an inducer. Another explanation would be that the samples 0h and 2h were exchanged unintendedly. However, as the results of the expression in the BL21(DE3-ROSETTA2) strain for two and four hours looked promising, it was decided to use the BL21(DE3-ROSETTA2) cells as host system for the expression of the bvPrP fusion construct. The purified bvPrP fusion protein is required for further experiments including the thiolysis to remove the fusion tag and the expressed protein ligation. Based on the results, it was decided that the *E. coli* cells would be harvested four hours after IPTG addition.

Now, with the obtained information about the expression conditions, two 2 L cultures of the BL21(DE3-ROSETTA2) cells were prepared. After the cells were harvested, a treatment with the cell disruptor and subsequent centrifugation of the sample provided access soluble and insoluble (inclusion bodies) fractions of the lysed culture. To check, if the bvPrP fusion protein is mainly expressed in the inclusion bodies or in the soluble supernatant, another SDS-Page was conducted. Therefore, a small subsample of the inclusion body pellet was transferred with a spatula in a 1.5 ml tube. It was mixed with 25 μL H_2O and 25 μL 2x sample loading buffer, whereas 20 μL of the supernatant sample were added to 20 μL 2x sample loading buffer. Two further samples were included on the gel, a cell pellet originating from a subsample taken directly after and four hours after the IPTG addition.
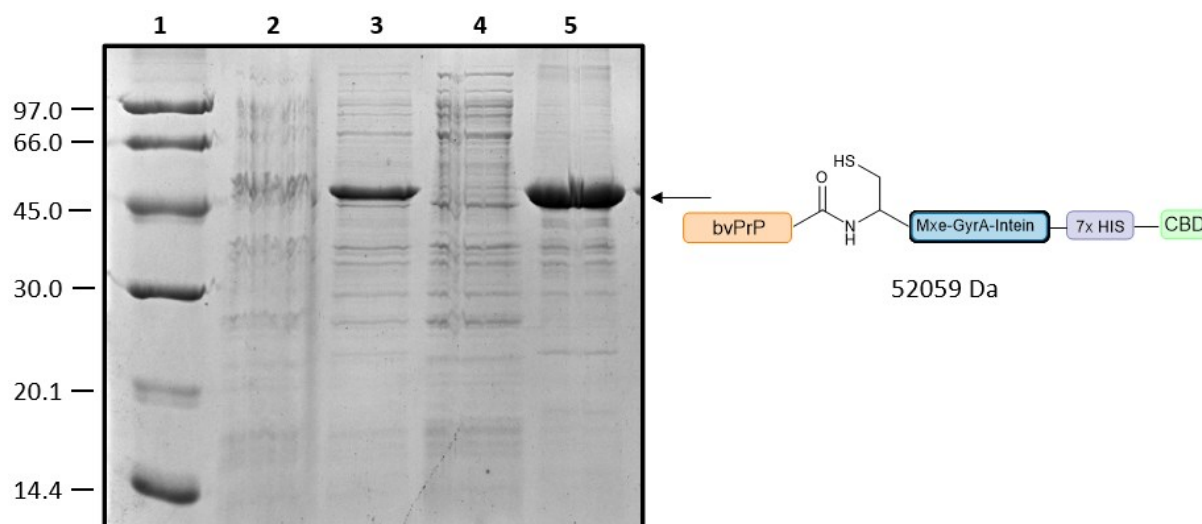
Figure 11: Determination if the bvPrP fusion construct is mainly expressed in the supernatant or the inclusion bodies in BL21(DE3-ROSETTA2) cells followed by SDS-page. Lane 2 shows the expression pattern of the intact cell pellet that originates from a subsample taken directly after the treatment with IPTG, whereas lane 3 shows the same sample taken four hours after the IPTG addition. Lane 4 depicts the protein bands of the supernatant (collected after the cells were disrupted) and lane 5 shows the expression pattern of the inclusion bodies. Lane 1 shows the protein bands of the LMW Marker.

The comparison between the supernatant and the inclusion bodies revealed that the bvPrP fusion protein is exclusively expressed in the inclusion bodies. As it can be observed in *Figure 11*, the inclusion body sample shows a thick and high intensity band, whereas a significant band for the bvPrP fusion protein is not observable in the supernatant sample. The high intensity band in lane 5 is located between 45 kDa and 66 kDa region of the LMW Marker, which would fit the expected MW of 52059 Da for bvPrP *Mxe* GyrA-7xHis-CBD. The efficacy of IPTG regarding the activation of the bvPrP fusion construct expression can be observed in *Figure 11* (lane 2 and 3). At the timepoint zero the intensity of the bvPrP fusion protein band is weak compared to the respective band of the sample taken four hours after the IPTG addition. This is as expected, because IPTG is a chemical compound that mimics allolactose, thereby removing the repressor from the lac operon. As the lac operon is included in the designed pTXB1 vector, the exclusion of the repressor leads to an enhanced expression of the target gene. Unfortunately, the protein bands in lane 2 of the prepared SDS-page (*Figure 11*) are not very well structured, which may affect the validity for the sample that indicates the starting point of the IPTG induced expression. Usually, if the expression pattern of the inclusion body sample is cluttered with various protein bands of a higher intensity, the next step would include affinity chromatography to isolate the bvPrP fusion protein from the other remaining proteins. For the bvPrP *Mxe* GyrA-7xHis-CBD, this would be accomplished by passing the

sample through a column with a nickel-nitrilotriacetic acid (Ni-NTA) matrix. The fusion protein includes the 7xHis tag, which shows affinity to the nickel ions. Isolation of the His-tagged protein can be achieved by performing a bind-wash-elute procedure under native or denaturing conditions. Undesired proteins are removed during the flow-through, as they miss the respective His-tag. The desired protein is immobilized on the nickel matrix and can be eluted by adding a suitable concentration of a competitor such as imidazole.[207] However, as the inclusion body sample looked rather pure in lane 5 (*Figure 11*), it was decided to skip affinity chromatography and move on with the MESNa-mediated intein cleavage.

The inclusion body pellets were solubilized in 50 ml 8 M guanidine hydrochloride (pH = 7.8), thereby denaturing the bvPrP fusion construct. At this point the mass of the bvPrP fusion construct (MW = 52059 Da) was confirmed via LC-MS on the Waters Auto Purification LC/MS system. The analysis with the software MagTran revealed a mass of 52051 Da, which is in an acceptable range for a high molecular weight protein. Next, the 8 M guanidine hydrochloride buffer was exchanged for urea via stepwise dialysis. The starting urea concentration of 6 M was gradually reduced until a final concentration of 4 M was reached. A concentration of 0.8 mg/ml for the bvPrP fusion protein was measured with the NanoDrop 2000c spectrophotometer. Therefore, approximately 80 mg of the protein was present in the sample, as each of the two inclusion body pellets was initially solubilized in 50 ml 8 M guanidine hydrochloride.

To remove the *Mxe* GyrA-intein-7xHis-CBD tag, MESNa mediated intein cleavage was performed. First, the reaction was conducted in a small scale, to check which concentrations of MESNa and urea are suitable for a high output of the bvPrP-thioester. The test cleavage reaction was started by adding 1 M MESNa slowly to 4 M urea bvPrP at room temperature. The solutions were diluted 1:1, resulting in final concentrations of 500 mM MESNa and 2 M urea. The reaction was conducted overnight (~20 hours) under constant shaking. These conditions turned out to be the best for bvPrP-thioester generation. Then, the samples were centrifuged for 5 minutes at 14000 rpm, followed by discarding the supernatant. In previously performed SDS gel analysis it was observed that the supernatant mainly contains the cleaved inteins, whereas the cleaved bvPrP-thioester precipitates and can be found in the pellet. The remaining pellets were re-solubilized in 6 M Gdn·HCl and gel samples were prepared by ethanol precipitation.
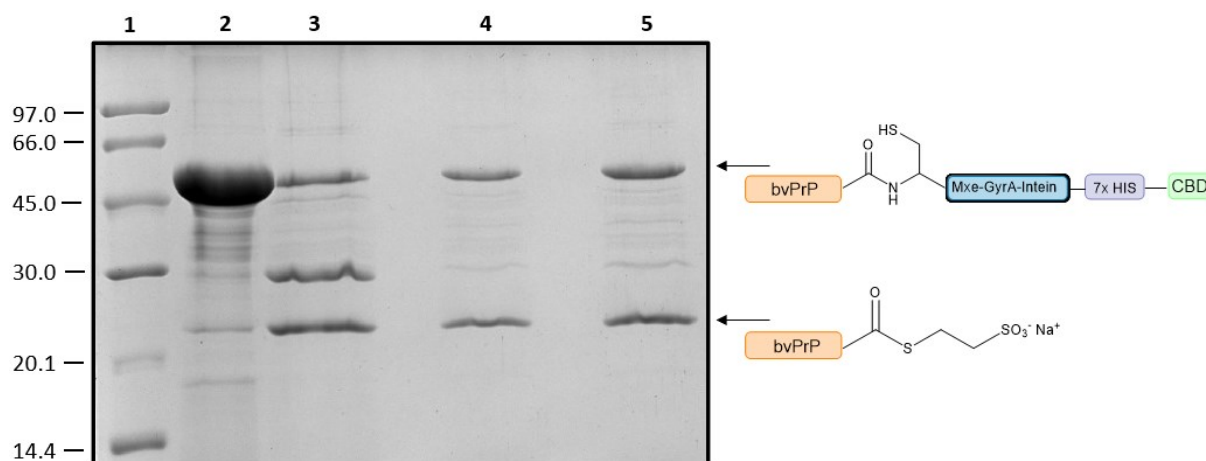
Figure 12: MESNa-mediated intein cleavage test reaction followed by SDS-Page (small scale).
Lane 2 shows the protein band of the untreated bvPrP fusion protein, in lane 3 subjected to 500 mM MESNa for
~20 hours. Lanes 4 and 5 show the pellet samples obtained after centrifugation of the MESNa-mediated intein
cleavage solution and subsequent ethanol precipitation. For the pellet sample in lane 5 twice as much was loaded
on the gel. The protein bands in lane 1 belong to the LMW marker.

The MESNa-mediated intein cleavage was successfully accomplished, as it can be observed in *Figure 12*. The intensity of the bvPrP fusion protein band is drastically reduced in the sample that is subjected overnight to an excess of MESNa (lane 2 and 3). Furthermore, the respective bands for the intein (MW = 28934 Da) and the bvPrP-thioester (MW = 23125 Da) are now visible with a high intensity in lane 3. The chemical reagent MESNa operates as a nucleophile in the reaction and attacks the carbonyl group adjacent to the intein segment, thereby removing the intein-7xHis-CBD tag. It is important to carefully monitor the pH value, since at a pH of 8 or higher hydrolysis occurs, thereby eliminating the C-terminal thioester of the protein. This should be avoided at all costs, as the α-thioester is required for the subsequent expressed protein ligation. Therefore, it is advisable to keep the reaction time as short as possible, as with longer reaction times the probability of pH fluctuations is increased. Based on the gel analysis we could conclude that the thioester is present in the supernatant as well as in the pellet and at this point it was unclear where the majority of the thioester was located. Further analysis and purifications revealed that with the applied conditions during MESNa cleavage, the majority of the thioester precipitates and needs to be isolated from the obtained pellet. Additionally, it can be observed that in the pellet samples (lane 4 and 5), some of the bvPrP fusion construct remains. Longer reaction times would maybe yield a higher cleavage rate, but as previously mentioned this could be accompanied by other arising problems such as hydrolysis. However, the remaining bank vole prion fusion protein is going to be separated via preparative HPLC and could be recycled in following cleavage reactions.

Further MESNA-mediated intein cleavages were conducted in a larger scale. 20 ml 1 M MESNA was added to the 20 ml 4 M urea bvPrP fusion construct solution (pH = 7.3). The pellets were dissolved in 8-9 ml 6 M Gdn·HCl (pH = 4.7) and filtered before the samples were loaded on a preparative HPLC column. The thioester containing fractions were identified by LC-MS analysis, pooled and lyophilized. The analytical HPLC-trace based on the detection of 214 nm absorption can be seen in *Figure 13*. The mass of the bvPrP-thioester was determined by MS direct injection. The obtained mass of 23123.4 Da was in agreement with the calculated value of 23125 Da.
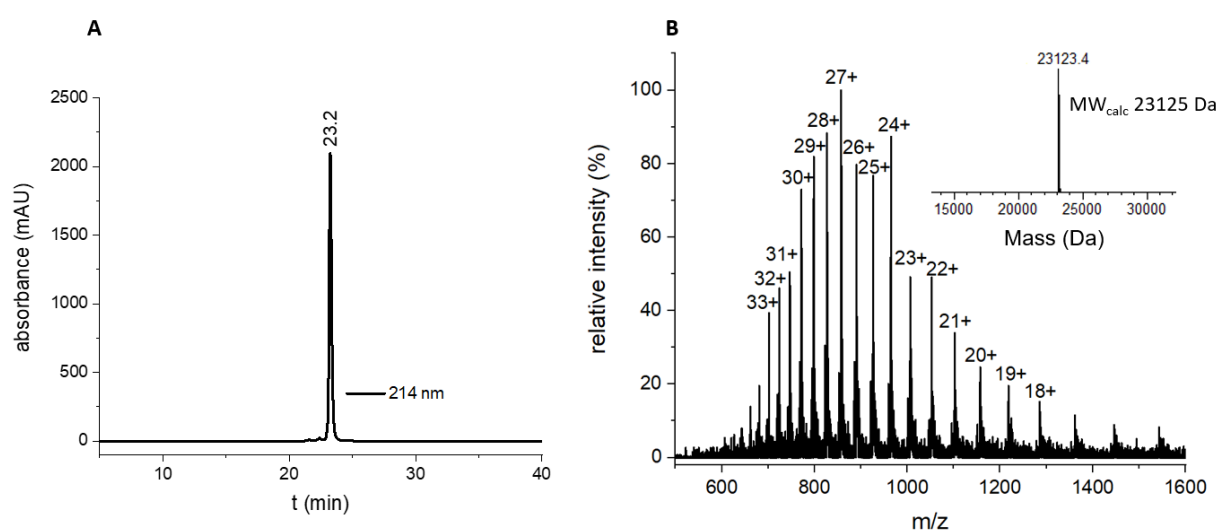
Figure 13: Characterization of bvPrP α-thioester.
Panel A shows the analytical HPLC trace ($\lambda_{abs} = 214$ nm, baseline corrected) and panel B features the ESI-MS spectrum of the purified α-thioester.

As it can be observed in panel A (*Figure 13*), the analytical HPLC revealed a single sharp peak and a yield of 9.5 mg/L for the bvPrP α-thioester was obtained.

3.2.2 SPPS of the GPI-anchor peptide mimic

Even though it has been managed to chemically synthesize the GPI-anchor, it remains still a challenge to obtain sufficient amounts. This is due to the complex structure of the GPI-anchor, which consists of a phosphoethanolamine linker, a glycan core and a phospholipid tail. The native structure of the GPI-anchor is shown in *Scheme 5*. The glycan core includes three mannose residues, a glucosamine and a phosphatidylinositol monomer. The phospholipid tail comprises a glycerol backbone with two fatty acid tails and the inositol. The phospholipid structure is essential for the attachment of the protein-GPI-anchor complex to the cell membrane. As it is already stated in section 1 of this work, the GPI-anchor is a biologically appreciable posttranslational modification of the prion protein, because it has a major impact on the PrP^C into PrP^{SC} conversion and on the development of the disease. Therefore, it is inevitable to introduce a modification on the C-terminus that is at least similar in its structure to the native GPI-anchor regarding the studies on PrP and its membrane attachment.

An appropriate peptide mimic structure was developed by Olschewski *et al.*[184] The structure can be seen in *Scheme 5*.
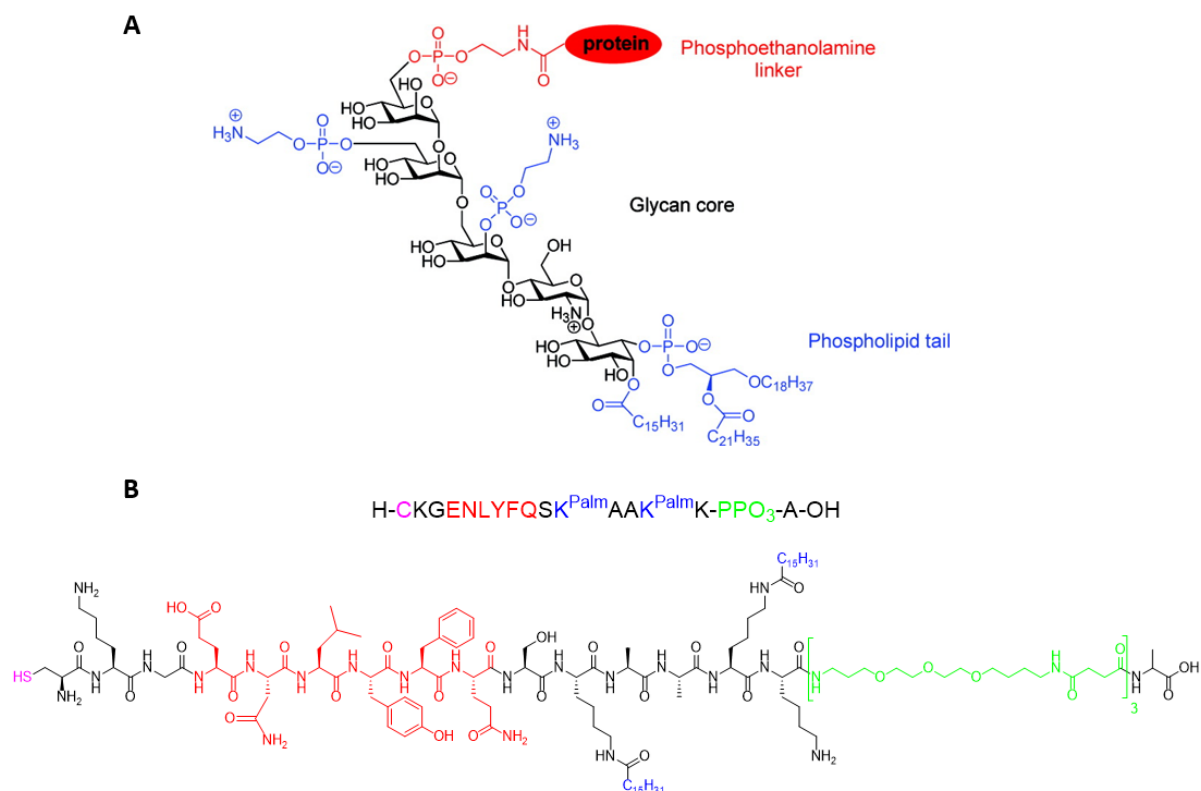
Scheme 5: Chemical structures of the native GPI anchor and the GPI-anchor peptide mimic. In panel A the typical structure of a native GPI-anchor from human erythrocyte acetylincholinesterase is shown.[213] The major components are color coded. Panel B shows the sequence and the structure of the GPI-anchor peptide mimic, designed by Olschweski *et al*. It was used for the semisynthesis with the recombinantly expressed bvPrP.

The palmitoylated lysine residues (blue in *Scheme 5*) are important for the semisynthetic protein to be located correctly, as the palmitoic acid tails mimic the phospholipid tail dependent cell membrane anchoring. This has already been shown by Olschewski *et al.*[184] However, as the structure of palmitoic acid involves hydrophobic properties, the solubility of the bvPrP is decreased once the GPI-anchor peptide mimic is linked to the protein via Expressed Protein Ligation. The insolubility is countered by the addition of the PPO$_3$-tag (green in *Scheme 5*) to the structure. The tobacco etch virus cleavage sequence, indicated in red (*Scheme 5*), offers a tool to remove the lipid anchor and release the bvPrP from any membrane respectively. As the modified and semisynthetic bvPrP is going to be used in bank vole model organisms, the release from the cell membrane in a controlled fashion is favorable.

The solid phase peptide synthesis of the GPI-anchor peptide mimic was done manually in a syringe. At the start a synthesis scale of 0.2 mmol was used, however as the resin was separated in halves after the coupling of the 14th amino acid, the final synthesis scale was 0.1 mmol. The analytical HPLC trace of the lipidated peptide based on the detection of 214 nm absorption is shown in *Figure 14*. The mass spectrum of the GPI-anchor peptide mimic could be deconvoluted to molecular weights with the software MagTran or MassLynx.
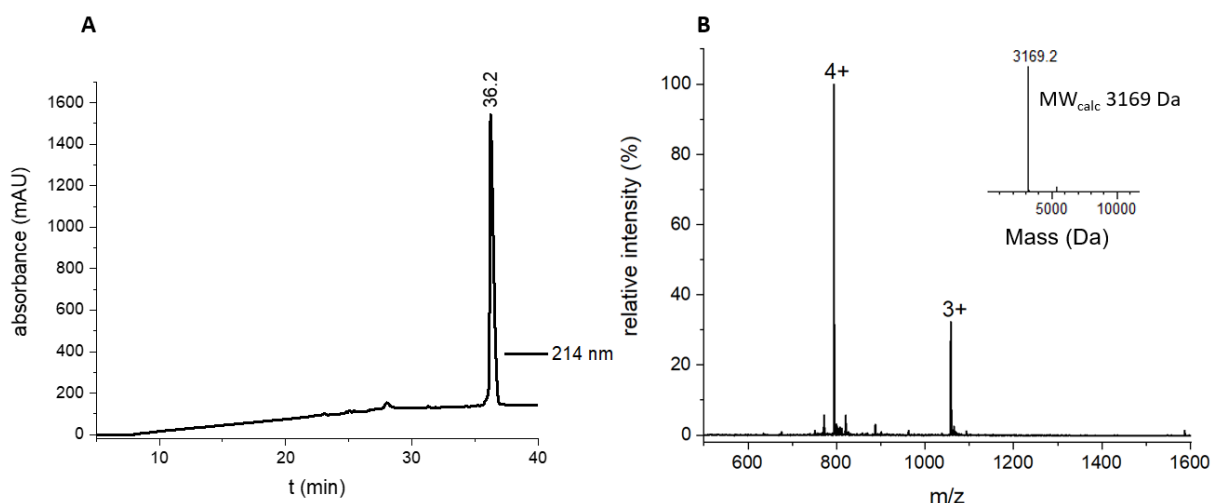
Figure 14: *Characterization of the GPI-anchor peptide mimic.*
Panel A shows the analytical HPLC trace ($\lambda_{abs} = 214$ nm). In B the ESI-MS spectrum of the lipidated peptide can be observed.

The deconvolution of the mass spectrum revealed a molecular weight of 3169.2 Da for the GPI-anchor peptide mimic. This result was in agreement with the calculated mass of 3169 Da. As it is seen in *Figure 14* panel A, a sharp peak at the retention time 36.2 min for the lipidated peptide was received. At a retention time of 28 minutes, there can be seen a tiny fluctuation

in the baseline. However, as the baseline did not proceed smoothly at that day, the tiny peak could be ascribed to that problem.

Table 7: Achieved yield of the GPI-anchor peptide mimic synthesized via SPPS and purified via preparative HPLC

type of peptide	synthesis scale (mmol)	crude peptide		purified peptide		
		Yield of				
		(mg)	(%)	(mg)	Based on scale (%)	Based on crude peptide (%)
lipidated peptide	0.1	220	69.4	16.7	5.3	7.6

Usually, it is often unavoidable that the yield shrinks during the processing from the crude peptide to the purified peptide. However, the loss of the yield to that extent was rather unusual. A possible reason for the yield shrinkage could be identified. After the palmitoylation of the peptide, a test cleavage was performed. During the analysis of the HPLC UV trace recorded by the Thermo Scientific MSQ Plus HPLC/MS system, it was found that another peak with a mass of 3407 Da was present. The mass difference of +238 fits to the peptide with three palmitoic acids instead of two. The mass of the unwanted product is of course, but unfortunately included in the obtained yield of the crude peptide. Since the time allotted for the practical part of the master thesis was already well planned, there was unfortunately no time to possibly test another method for the palmitoylation of lysine. However, a main pool yield of 16.7 mg was obtained, as it can be observed in *Table 7*. The unwanted triple lipidated peptide was removed via preparative HPLC.

3.2.3 Expressed protein ligation with the GPI-anchor peptide mimic

It was proceeded with the expressed protein ligation, since both, the bvPrP α-thioester and the GPI-anchor peptide mimic were obtained in high purity and in sufficient amounts for the imminent reaction. The applied strategy (*Scheme 6*) was developed in the Becker Lab. The

underlying reaction includes a nucleophilic attack of the N-terminal thiol group of the GPI-anchor peptide mimic towards the C-terminal thioester of bvPrP, followed by the irreversible S→N shift. As a result, the native amide bond is formed. To accomplish the assembly of the semisynthetic bvPrP, the two polypeptides are dissolved in a ligation buffer, that contains an excess of an appropriate thiol. The thiol is required to remove MESNa first and then it acts as a leaving group during the nucleophilic attack of the lipidated peptide. The reaction rate can be enhanced depending on the nucleophilic property, the performance as a leaving group, the pKa value and water solubility of the thiol. Commonly used ligation mediators are thiophenol or 4-mercaptophenylacetic acid (MPAA). The latter was employed in the EPL (*Scheme 6*).
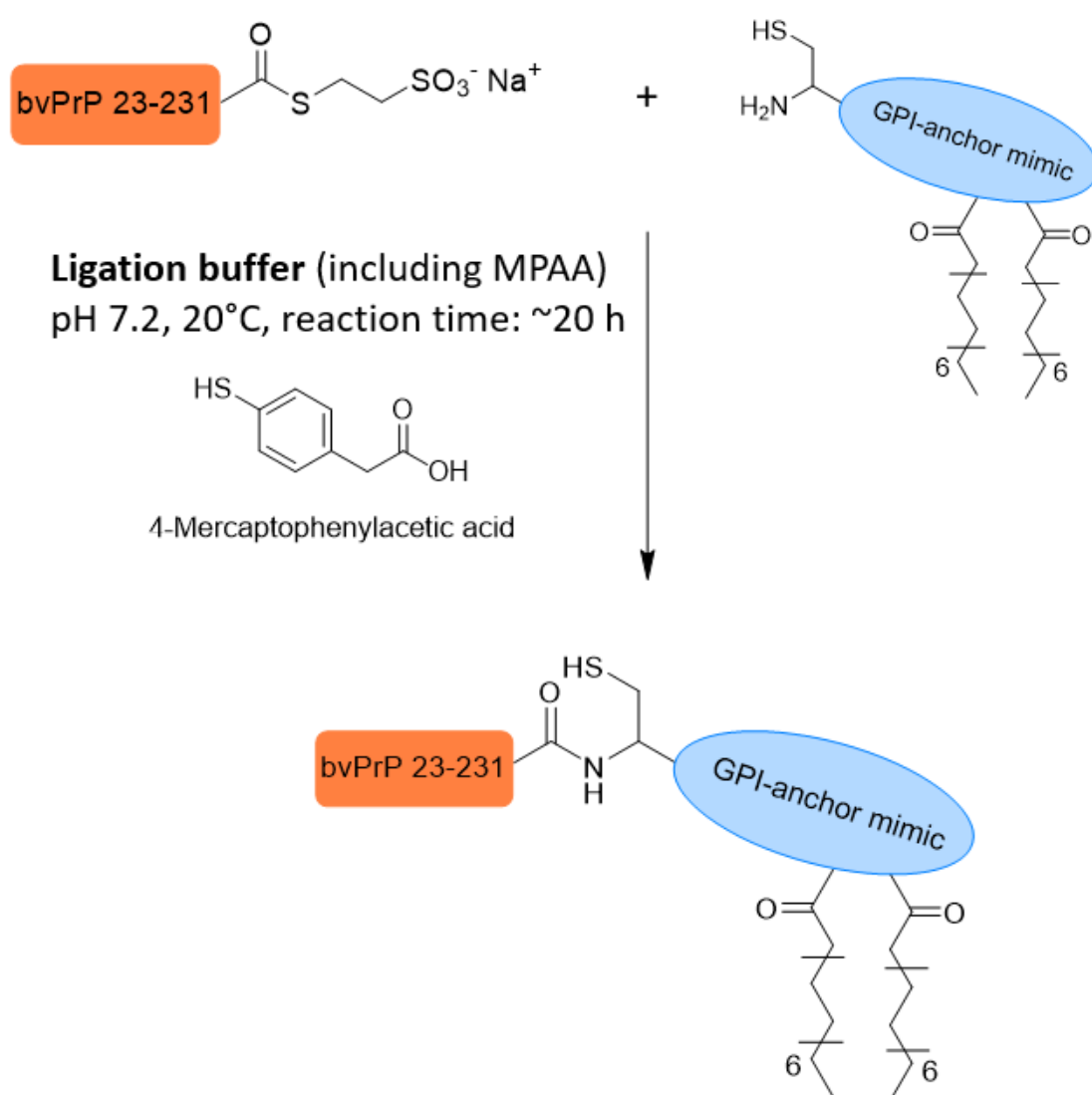
Scheme 6: Reaction scheme of the EPL including the used ligation buffer.

Test ligations in a small scale were performed to identify when the majority of the α-thioester has been converted and thus the EPL was complete. Therefore, EPL was followed by LC-MS and SDS-page, as at several timepoints subsamples were taken.
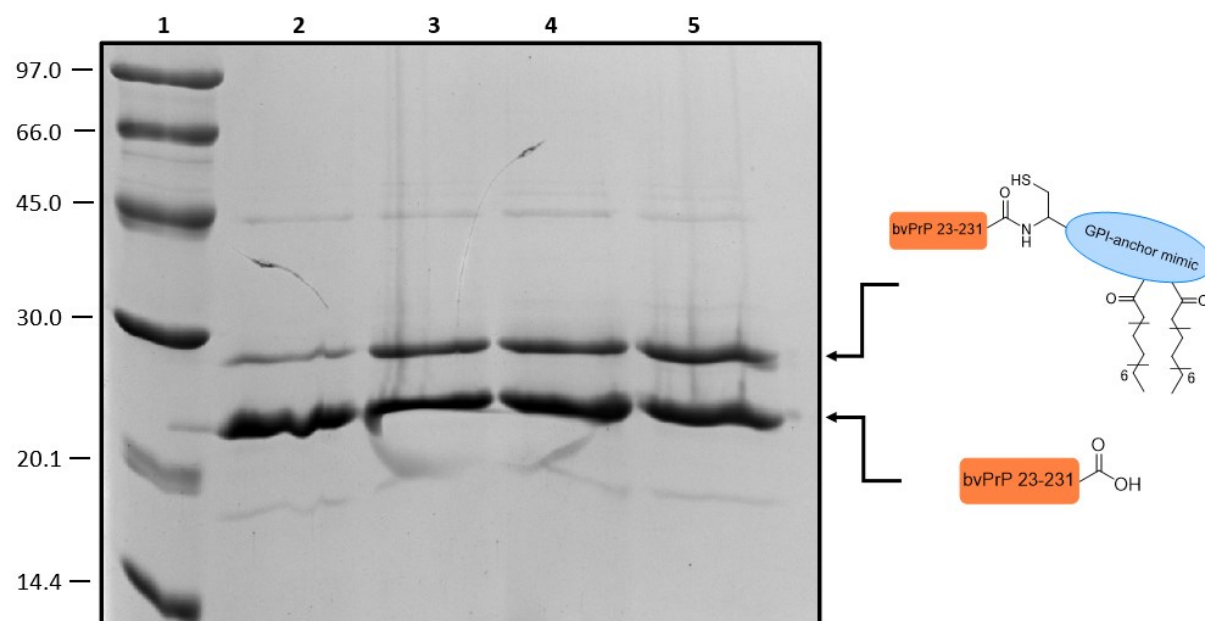
Figure 15: Test EPL of the bvPrP-thioester and the GPI-anchor peptide mimic followed by SDS-page. Lanes 2, 3, 4 and 5 show the subsamples of the proceeding reaction taken at the timepoints 0 h, 2 h, 4 h and overnight. Lane 1 shows the protein bands of the LMW marker.

Following the SDS-page in *Figure 15*, it can be observed that the desired semisynthetic bvPrP (MW = 26152) is formed. However, already after 4 hours the EPL was completed, as the intensity of the semisynthetic bvPrP band in the overnight sample did not increase compared to the respective 4 hours band. The reaction rate of the underlying EPL is fast, as there is already the lipidated bvPrP band visible at the starting point. The high intensity bands of the subsamples 3, 4 and 5 located at a region around 23 kDa indicate the hydrolyzed α-thioester (MW = 23001), as it was verified by the analysis of the time-dependent HPLC traces. However, against the observation made on the SDS-page, the HPLC traces (*Figure 16*) revealed that there is still a little bit of product formation happening overnight. So, the respective bands in lane 2 and 3 located at the 23 kDa region, contain primarily the hydrolyzed faction and remaining unconverted α-thioester. Based on these results, it was decided to conduct the EPL overnight, to produce as much of the lipidated bvPrP as possible. It was tested to use ligation buffers with different concentrations and pH, but nevertheless the partial hydrolysis of the bvPrP-thioesters was inevitable. The hydrolyzed α-thioester faction was removed from the desired product via semi-preparative HPLC.
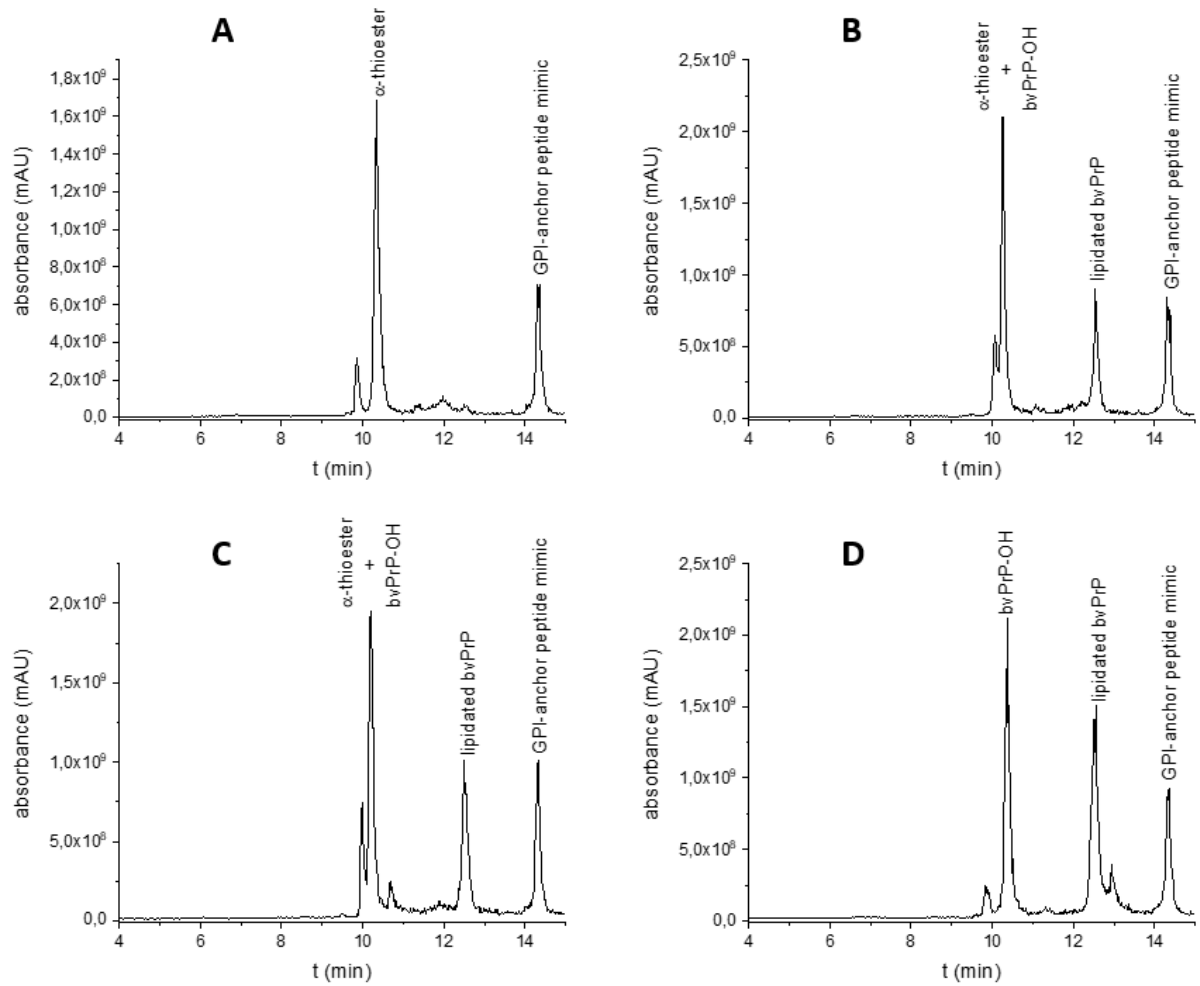
Figure 16: Time dependent HPLC traces ($\lambda_{abs} = 214$ nm) of the EPL.
A shows the timepoint zero 0 of the conducted ligation reaction. The large peak with a retention time of 10.5 minutes indicates the bvPrP-thioester, whereas the peak with a retention time of 14.5 minutes features the GPI-anchor peptide mimic. In Panel B the reaction at the timepoint 2 hours can be observed. The novel peak with a retention time of 12.5 minutes indicates the lipidated bvPrP. Panel C and D show the timepoints 4 hours and overnight.

65

The analytical HPLC trace based on the detection of 214 nm absorption of the isolated semisynthetic bvPrP revealed a single peak (*Figure 17*). The respective mass spectrum could be deconvoluted to a molecular weight of 26154 Da. The obtained mass did match with the calculated mass of 26152 Da.
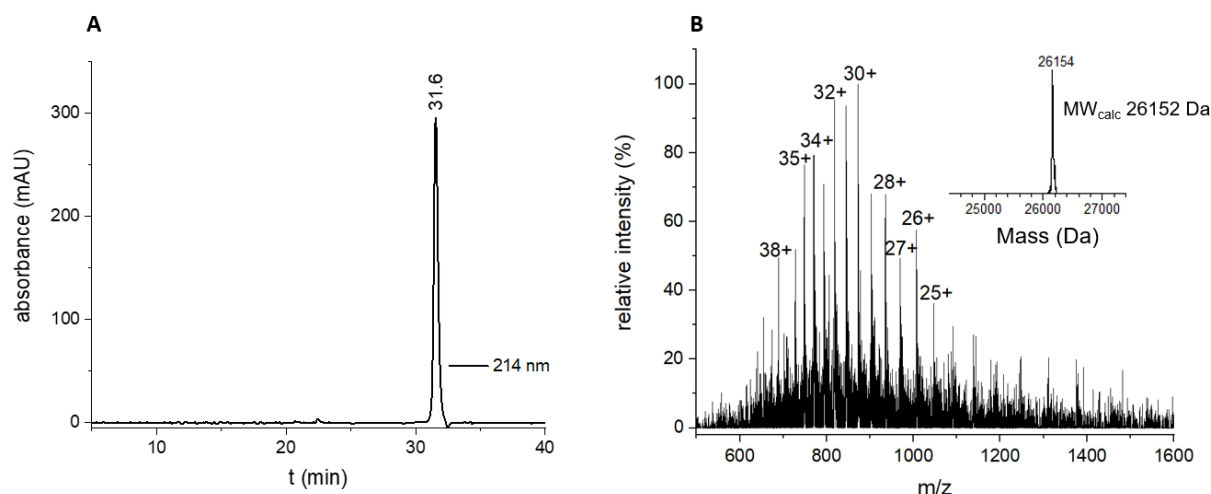
Figure 17: Characterization of the semisynthetic bvPrP.
Panel A shows the analytical HPLC trace ($\lambda_{abs} = 214$ nm). In panel B the ESI-MS spectrum of the lipidated bvPrP can be seen.

The semisynthetic bvPrP could be isolated via HPLC purification and a yield of 26% was attained. Next, the modified bvPrP was prepared to be refolded, as it was present in a denatured state for the purification procedure.

3.3 Biophysical characterization – CD spectroscopy

The purified and lyophilized lipidated bvPrP were treated with a refolding buffer to induce the native folding state. The conducted lab work is explained in more detail in section 2.2.4. The secondary structure of the prepared semisynthetic bvPrP was assessed via CD-spectroscopy. The dialysis buffer (20 mM sodium acetate + 10 mM OG) was used as a blank for the measurement.
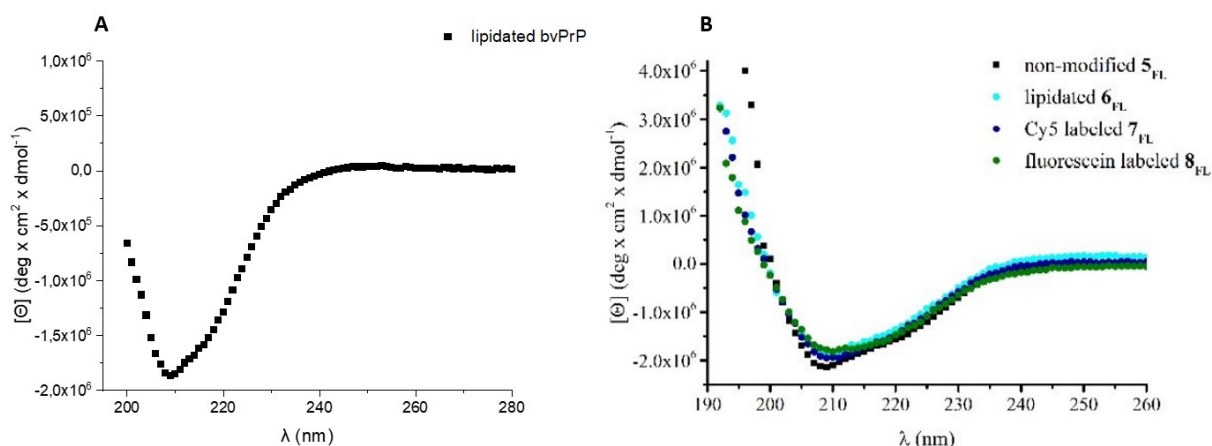
Figure 18: Far-UV CD-spectra of semisynthetic bvPrP and PrP variants.
In A the recorded CD-spectrum of the lipidated bvPrP is observed. Panel B shows the CD-spectra of the non-modified full length PrP and different modified PrP variants extracted from the work of Hackl, S.[198]

For comparison, recorded CD-spectra obtained by Hackl, S[198]. were included in *Figure 18*. As a different nm range (190-260 nm) was adjusted for the spectra in B, the obtained diagram of the semisynthetic bvPrP in panel A differs in the appearance. As stated by Corrêa and Ramos[208], a characteristic CD-spectrum of an α-helix protein includes two negative bands of a similar magnitude at 222 and 208 nm. The significant minimum at 208 nm can be observed in the CD-spectra in *Figure 18*. The second minimum at 220 nm is barely visible in the recorded CD-spectrum of the lipidated bvPrP. However, as it is hardly observable in the CD-spectra for the full length PrP and the respective variants too, it might correlate with the glutathione-based redox system of the folding buffer, as similar refolding conditions were applied by Hackl[198]. According to the work of Safar *et al*.[209], PrP^C exhibits an α-helical content of 36%. By using the CDNN software an α-helix content of 28.5% for the lipidated bvPrP was revealed (*Table 8*). The small deviation may arise from differences in the concentrations of (bv)PrP and the used glutathione redox system, as it was described by Chu *et al*[210]. Additionally, the organism diversity of the expressed prion protein should be taken into account, when the folding characteristics are compared to the literature.

Table 8: Percentage of the secondary structure contents based on the recorded far-UV CD-spectrum of the lipidated bvPrP, calculated by using the CDNN software.

	α-helix	β-sheet	β-turn	random coil
lipidated bvPrP	28.5 %	20.1 %	18.3 %	32.3 %

To make sure that the sample did not include any misfolded proteins, a centrifugation step was performed before the CD-measurement. The observed precipitate stuck on the tube was removed from the dissolved lipidated bvPrP. Based on the received CD-spectrum and the comparison to the results published by Hackl[198], it is suggested that the correct disulfide linkage for the semisynthetic bvPrP was attained. The findings of Maiti and collaborators[211] did support the assertion that a correct folding was achieved. They prepared PrP variants with two cysteine residues replaced by alanine (C179A/C214A) and reported that the refolding of the respective PrP variant was accomplished. Spectroscopic measurements were done as well, and it was argued against an allegation that a stable monomeric PrP is rich in ß-sheet structure.

4 Conclusion & Outlook

4.1 Conclusion

It remains a major goal to elucidate the pathogenesis of prion diseases, which involve the conformational change of the cellular prion protein (PrP^C) into the scrapie prion protein (PrP^{Sc}) at the cellular membrane. It is believed that PrP^{Sc} drives the conversion of cellular prion proteins by inducing a misfolded state. In the late years of the 20th century a major limitation of the research included the production of modified PrP variants, since at that time there were no appropriate methods available to obtain such proteins in sufficient amounts. This changed with the semisynthesis strategy developed by Becker *et al.*, as it was now possible to generate modified PrP variants in acceptable quantities by conducting a reaction stated as Expressed Protein Ligation (EPL). These PrP variants also include PTM's that mimic the GPI-anchor, which is known to be essential for the PrP^C conversion, since it tethers the protein to the cellular membrane. Semisynthetic human prion proteins have already been successfully produced in the Becker Lab and been used to perform binding experiments with artificial membranes. It was demonstrated that the produced PrP variants interacted with negatively charged lipid bilayers at a physiological pH. Furthermore, it was reported that the connection between the modified PrP and the lipid bilayer was non-reversible due to strong hydrophobic interactions.

In this work, the semisynthetic route was transferred to bvPrP, which led to folded bank vole prion protein carrying a GPI-anchor peptide mimic at the C-terminus. For the EPL reaction a ligation buffer with the thiol MPAA was used, as previously developed by Hackl *et al.*[198] The secondary structure of the lipidated bvPrP was assessed via circular dichroism (CD) spectroscopy. The CD-spectrum showed the characteristic minima of a predominantly α-helical protein. With production of the site-specific modified bank vole prion protein, a foundation was created to generate further bvPrP variants in the future. Since our partner from the United States, Surachai Supattapone (Dartmouth College) works with bank vole as a model organism, it was necessary to establish this semisynthesis as no bank vole prion proteins had been previously produced in the Becker Lab.

4.2 Outlook

The data generated in this project provides a suitable basis to produce bank vole PrP variants. For further *in vivo* experiments the lipidated bvPrP constructs were shipped to the Dartmouth Geisel School of Medicine in the United States. There, Supattapone *et al.*[214,215] investigate the conversion of PrP^C into PrP^{Sc}. They were able to produce prion proteins with infectivity levels similar to brain-derived prions in the presence of chemically synthesized cofactors. It was identified that the cofactor phosphatidylethanolamine (PE) has a major impact on the propagation of PrP^{Sc} molecules derived from several mammalian prion strains. Additionally, it was reported that such cofactors may influence prion strain properties. However, these results still leave open the question whether the infectivity is only due to the presence of the cofactors or whether it is exclusively due to the prion protein itself. This could be elucidated by comparing the detailed structures of the produced infectious PrP^{Sc} (cofactor + PrP^{Sc}) and non-infectious prion proteins without a cofactor. Future studies would include the determination of further "cofactors" (e.g. PTMs) that are essential for the propagation of a prion strain. By monitoring the selective susceptibility of neuronal populations *in vivo*, it could be possible to identify strain specific factors and their respective expression pattern in different cell types.[215] For this purpose, the lipidated bank vole prion protein generated here may be implemented in such experiments.

Even though the production of the semisynthetic bvPrP was successfully accomplished, there is still room for improvement concerning the yields. One approach would include the synthesis of a GPI-anchor peptide mimic equipped with a N-terminal selenocysteine instead of a cysteine. The reaction rate of the underlying EPL reaction could be increased by using a selenocysteine-containing peptide. However, the purification of such peptides is rather challenging.

In general, the produced modified bvPrP can be used for several biophysical experiments such as membrane binding studies or aggregation assays.

5 References

1. Hackl, S., & Becker, C. F. W. (2019). Prion protein—Semisynthetic prion protein (PrP) variants with posttranslational modifications. *Journal of Peptide Science*, *25*(10), e3216.

2. Weissmann, C. (1999). Molecular Genetics of Transmissible Spongiform Encephalopathies *. *Journal of Biological Chemistry*, *274*(1), 3–6.

3. Prusiner, S. B. (2009). 3. History of Prion Research. In *Prions in Humans and Animals* (pp. 44–58). De Gruyter.

4. National Institute of Neurological Disorders and Stroke. (2021, November 15). *Creutzfeldt-Jakob Disease Fact Sheet | National Institute of Neurological Disorders and Stroke*. https://www.ninds.nih.gov/Disorders/Patient-Caregiver-Education/Fact-Sheets/Creutzfeldt-Jakob-Disease-Fact-Sheet

5. Mead, S., Stumpf, M. P. H., Whitfield, J., Beck, J. A., Poulter, M., Campbell, T., Uphill, J. B., Goldstein, D., Alpers, M., Fisher, E. M. C., & Collinge, J. (2003). Balancing Selection at the Prion Protein Gene Consistent with Prehistoric Kurulike Epidemics. *Science*, *300*(5619), 640–643.

6. Gajdusek, D. C., Gibbs, C. J., & Alpers, M. (1966). Experimental transmission of a Kuru-like syndrome to chimpanzees. *Nature*, *209*(5025), 794–796.

7. Prusiner, S. B. (1998). Prions. *Proceedings of the National Academy of Sciences of the United States of America*, *95*(23), 13363–13383.

8. Prusiner, S. B. (1982). Novel proteinaceous infectious particles cause scrapie. *Science (New York, N.Y.)*, *216*(4542), 136–144.

9. Oesch, B., Westaway, D., Wälchli, M., McKinley, M. P., Kent, S. B. H., Aebersold, R., Barry, R. A., Tempst, P., Teplow, D. B., Hood, L. E., Prusiner, S. B., & Weissmann, C. (1985). A cellular gene encodes scrapie PrP 27-30 protein. *Cell*, *40*(4), 735–746.

10. Prusiner, S. B. (1987). Prions and neurodegenerative diseases. *The New England Journal of Medicine*, *317*(25), 1571–1581.

11. Verma, A. (2016). Prions, prion-like prionoids, and neurodegenerative disordersVacancy. *Annals of Indian Academy of Neurology*, *19*(2), 169.

12. Leighton, P. L. A., & Allison, W. T. (2016). Protein Misfolding in Prion and Prion-Like Diseases: Reconsidering a Required Role for Protein Loss-of-Function. *Journal of Alzheimer's Disease*, *54*(1), 3–29.

13. Kocisko, D. A., Come, J. H., Priola, S. A., Chesebro, B., Raymond, G. J., Lansbury, P. T., & Caughey, B. (1994). Cell-free formation of protease-resistant prion protein. *Nature*, *370*(6489), 471–474.

14. Herms, J., Tings, T., Gall, S., Madlung, A., Giese, A., Siebert, H., Schürmann, P., Windl, O., Brose, N., & Kretzschmar, H. (1999). Evidence of presynaptic location and function of the prion protein. *The Journal of Neuroscience: The Official Journal of the Society for Neuroscience*, *19*(20), 8866–8875.

15. Aguzzi, A., & Calella, A. M. (2009). Prions: Protein aggregation and infectious diseases. *Physiological Reviews*, *89*(4), 1105–1152.

16. Manson, J., West, J. D., Thomson, V., McBride, P., Kaufman, M. H., & Hope, J. (1992). The prion protein gene: A role in mouse embryogenesis? *Development (Cambridge, England)*, *115*(1), 117–122.

17. Bagyinszky, E., Giau, V. V., Youn, Y. C., An, S. S. A., & Kim, S. (2018). Characterization of mutations in PRNP (prion) gene and their possible roles in neurodegenerative diseases. *Neuropsychiatric Disease and Treatment*, *14*, 2067–2085.

18. Puckett, C., Concannon, P., Casey, C., & Hood, L. (1991). Genomic structure of the human prion protein gene. *American Journal of Human Genetics*, *49*(2), 320–329.

19. Westaway, D., Cooper, C., Turner, S., Costa, M. D., Carlson, G. A., & Prusiner, S. B. (1994). Structure and polymorphism of the mouse prion protein gene. *Proceedings of the National Academy of Sciences*, *91*(14), 6418–6422.

20. Kretzschmar, H. A., Stowring, L. E., Westaway, D., Stubblebine, W. H., Prusiner, S. B., & Dearmond, S. J. (1986). Molecular cloning of a human prion protein cDNA. *DNA (Mary Ann Liebert, Inc.)*, *5*(4), 315–324.

21. Pan, K. M., Baldwin, M., Nguyen, J., Gasset, M., Serban, A., Groth, D., Mehlhorn, I., Huang, Z., Fletterick, R. J., & Cohen, F. E. (1993). Conversion of alpha-helices into beta-sheets features in the formation of the scrapie prion proteins. *Proceedings of the National Academy of Sciences of the United States of America*, *90*(23), 10962–10966.

22. Timmes, A. G., Moore, R. A., Fischer, E. R., & Priola, S. A. (2013). Recombinant Prion Protein Refolded with Lipid and RNA Has the Biochemical Hallmarks of a Prion but Lacks In Vivo Infectivity. *PLOS ONE*, *8*(7), e71081.

23. Wang, F., Wang, X., Orrú, C. D., Groveman, B. R., Surewicz, K., Abskharon, R., Imamura, M., Yokoyama, T., Kim, Y.-S., Vander Stel, K. J., Sinniah, K., Priola, S. A., Surewicz, W. K., Caughey, B., & Ma, J. (2017). Self-propagating, protease-resistant, recombinant prion protein conformers with or without in vivo pathogenicity. *PLoS Pathogens*, *13*(7), e1006491.

24. Castilla, J., Saá, P., Hetz, C., & Soto, C. (2005). In vitro generation of infectious scrapie prions. *Cell*, *121*(2), 195–206.

25. Wang, F., Wang, X., Yuan, C.-G., & Ma, J. (2010). Generating a prion with bacterially expressed recombinant prion protein. *Science (New York, N.Y.)*, *327*(5969), 1132–1135.

26. Hornemann, S., Korth, C., Oesch, B., Riek, R., Wider, G., Wüthrich, K., & Glockshuber, R. (1997). Recombinant full-length murine prion protein, mPrP(23-231): Purification and spectroscopic characterization. *FEBS Letters*, *413*(2), 277–281.

27. Riek, R., Hornemann, S., Wider, G., Billeter, M., Glockshuber, R., & Wüthrich, K. (1996). NMR structure of the mouse prion protein domain PrP(121-231). *Nature*, *382*(6587), 180–182.

28. Riek, R., Hornemann, S., Wider, G., Glockshuber, R., & Wüthrich, K. (2020). NMR characterization of the full-length recombinant murine prion protein, mPrP(23-231). In *NMR with Biological Macromolecules in Solution* (pp. 120–126). WORLD SCIENTIFIC.

29. Zahn, R., Liu, A., Lührs, T., Riek, R., Schroetter, C. von, García, F. L., Billeter, M., Calzolai, L., Wider, G., & Wüthrich, K. (2000). NMR solution structure of the human prion protein. *Proceedings of the National Academy of Sciences*, *97*(1), 145–150.

30. Wulf, M.-A., Senatore, A., & Aguzzi, A. (2017). The biological function of the cellular prion protein: An update. *BMC Biology*, *15*(1), 34.

31. Castle, A. R., & Gill, A. C. (2017). Physiological Functions of the Cellular Prion Protein. *Frontiers in Molecular Biosciences*, *4*, 19.

32. Mentler, M., Weiss, A., Grantner, K., del Pino, P., Deluca, D., Fiori, S., Renner, C., Klaucke, W. M., Moroder, L., Bertsch, U., Kretzschmar, H. A., Tavan, P., & Parak, F. G. (2005). A new method to determine the structure of the metal environment in metalloproteins: Investigation of the prion protein octapeptide repeat Cu(2+) complex. *European Biophysics Journal: EBJ*, *34*(2), 97–112.

33. Burns, C. S., Aronoff-Spencer, E., Legname, G., Prusiner, S. B., Antholine, W. E., Gerfen, G. J., Peisach, J., & Millhauser, G. L. (2003). Copper Coordination in the Full-Length, Recombinant Prion Protein. *Biochemistry*, *42*(22), 6794–6803.

34. del Pino, P., Weiss, A., Bertsch, U., Renner, C., Mentler, M., Grantner, K., Fiorino, F., Meyer-Klaucke, W., Moroder, L., Kretzschmar, H. A., & Parak, F. G. (2007). The configuration of the Cu2+ binding region in full-length human prion protein. *European Biophysics Journal*, *36*(3), 239–252.

35. Haraguchi, T., Fisher, S., Olofsson, S., Endo, T., Groth, D., Tarentino, A., Borchelt, D. R., Teplow, D., Hood, L., & Burlingame, A. (1989). Asparagine-linked glycosylation of the scrapie and cellular prion proteins. *Archives of Biochemistry and Biophysics*, *274*(1), 1–13.

36. Zuegg, J., & Gready, J. E. (2000). Molecular dynamics simulation of human prion protein including both N-linked oligosaccharides and the GPI anchor. *Glycobiology*, *10*(10), 959–974.

37. Yi, C.-W., Wang, L.-Q., Huang, J.-J., Pan, K., Chen, J., & Liang, Y. (2018). Glycosylation Significantly Inhibits the Aggregation of Human Prion Protein and Decreases Its Cytotoxicity. *Scientific Reports*, *8*(1), 12603.

38. Stahl, N., Borchelt, D. R., Hsiao, K., & Prusiner, S. B. (1987). Scrapie prion protein contains a phosphatidylinositol glycolipid. *Cell*, *51*(2), 229–240.

39. Brown, K., & Mastrianni, J. A. (2010). The prion diseases. *Journal of Geriatric Psychiatry and Neurology*, *23*(4), 277–298.

40. Collinge, J. (2001). Prion diseases of humans and animals: Their causes and molecular basis. *Annual Review of Neuroscience*, *24*, 519–550.

41. Beck, J., Collinge, J., & Mead, S. (2012). Prion protein gene M232R variation is probably an uncommon polymorphism rather than a pathogenic mutation. *Brain*, *135*(2), e209.

42. Basler, K., Oesch, B., Scott, M., Westaway, D., Wälchli, M., Groth, D. F., McKinley, M. P., Prusiner, S. B., & Weissmann, C. (1986). Scrapie and cellular PrP isoforms are encoded by the same chromosomal gene. *Cell*, *46*(3), 417–428.

43. Vázquez-Fernández, E., Young, H. S., Requena, J. R., & Wille, H. (2017). The Structure of Mammalian Prions and Their Aggregates. *International Review of Cell and Molecular Biology*, *329*, 277–301.

44. Wille, H., & Requena, J. R. (2018). The Structure of PrPSc Prions. *Pathogens*, *7*(1), 20.

45. Vázquez-Fernández, E., Vos, M. R., Afanasyev, P., Cebey, L., Sevillano, A. M., Vidal, E., Rosa, I., Renault, L., Ramos, A., Peters, P. J., Fernández, J. J., van Heel, M., Young, H. S., Requena, J. R., & Wille, H. (2016). The Structural Architecture of an Infectious Mammalian Prion Using Electron Cryomicroscopy. *PLoS Pathogens*, *12*(9), e1005835.

46. Wille, H., Bian, W., McDonald, M., Kendall, A., Colby, D. W., Bloch, L., Ollesch, J., Borovinskiy, A. L., Cohen, F. E., Prusiner, S. B., & Stubbs, G. (2009). Natural and synthetic prion structure from X-ray fiber diffraction. *Proceedings of the National Academy of Sciences of the United States of America*, *106*(40), 16990–16995.

47. Caughey, B. W., Dong, A., Bhat, K. S., Ernst, D., Hayes, S. F., & Caughey, W. S. (1991). Secondary structure analysis of the scrapie-associated protein PrP 27-30 in water by infrared spectroscopy. *Biochemistry*, *30*(31), 7672–7680.

48. Caughey, B., Raymond, G. J., & Bessen, R. A. (1998). Strain-dependent differences in beta-sheet conformations of abnormal prion protein. *The Journal of Biological Chemistry*, *273*(48), 32230–32235.

49. Pan, K. M., Baldwin, M., Nguyen, J., Gasset, M., Serban, A., Groth, D., Mehlhorn, I., Huang, Z., Fletterick, R. J., & Cohen, F. E. (1993). Conversion of alpha-helices into beta-sheets features in the formation of the scrapie prion proteins. *Proceedings of the National Academy of Sciences of the United States of America*, *90*(23), 10962–10966.

50. Schmitz, M., Dittmar, K., Llorens, F., Gelpi, E., Ferrer, I., Schulz-Schaeffer, W. J., & Zerr, I. (2017). Hereditary Human Prion Diseases: An Update. *Molecular Neurobiology*, *54*(6), 4138–4149.

51. Vázquez-Fernández, E., Alonso, J., Pastrana, M. A., Ramos, A., Stitz, L., Vidal, E., Dynin, I., Petsch, B., Silva, C. J., & Requena, J. R. (2012). Structural organization of mammalian prions as probed by limited proteolysis. *PloS One*, *7*(11), e50111.

52. Hubbard, S. J. (1998). The structural aspects of limited proteolysis of native proteins. *Biochimica Et Biophysica Acta*, *1382*(2), 191–206.

53. Silva, C. J., Vázquez-Fernández, E., Onisko, B., & Requena, J. R. (2015). Proteinase K and the structure of PrPSc: The good, the bad and the ugly. *Virus Research*, *207*, 120–126.

54. Bolton, D. C., McKinley, M. P., & Prusiner, S. B. (1982). Identification of a Protein That Purifies with the Scrapie Prion. *Science*, *218*(4579), 1309–1311.

55. Zou, W.-Q., Capellari, S., Parchi, P., Sy, M.-S., Gambetti, P., & Chen, S. G. (2003). Identification of novel proteinase K-resistant C-terminal fragments of PrP in Creutzfeldt-Jakob disease. *The Journal of Biological Chemistry*, *278*(42), 40429–40436.

56. Zanusso, G., Farinazzo, A., Prelli, F., Fiorini, M., Gelati, M., Ferrari, S., Righetti, P. G., Rizzuto, N., Frangione, B., & Monaco, S. (2004). Identification of distinct N-terminal truncated forms of prion protein in different Creutzfeldt-Jakob disease subtypes. *The Journal of Biological Chemistry*, *279*(37), 38936–38942.

57. Sajnani, G., Pastrana, M. A., Dynin, I., Onisko, B., & Requena, J. R. (2008). Scrapie prion protein structural constraints obtained by limited proteolysis and mass spectrometry. *Journal of Molecular Biology*, *382*(1), 88–98.

58. Watts, J. C., Giles, K., Stöhr, J., Oehler, A., Bhardwaj, S., Grillo, S. K., Patel, S., DeArmond, S. J., & Prusiner, S. B. (2012). Spontaneous generation of rapidly transmissible prions in transgenic mice expressing wild-type bank vole prion protein. *Proceedings of the National Academy of Sciences of the United States of America*, *109*(9), 3498–3503.

59. Watts, J. C., Giles, K., Bourkas, M. E. C., Patel, S., Oehler, A., Gavidia, M., Bhardwaj, S., Lee, J., & Prusiner, S. B. (2016). Towards authentic transgenic mouse models of heritable PrP prion diseases. *Acta Neuropathologica*, *132*(4), 593–610.

60. Colby, D. W., & Prusiner, S. B. (2011). De novo generation of prion strains. *Nature Reviews Microbiology*, *9*(11), 771–777.

61. Groveman, B. R., Dolan, M. A., Taubner, L. M., Kraus, A., Wickner, R. B., & Caughey, B. (2014). Parallel in-register intermolecular β-sheet architectures for prion-seeded prion protein (PrP) amyloids. *The Journal of Biological Chemistry*, *289*(35), 24129–24142.

62. Richardson, J. S., & Richardson, D. C. (2002). Natural beta-sheet proteins use negative design to avoid edge-to-edge aggregation. *Proceedings of the National Academy of Sciences of the United States of America*, *99*(5), 2754–2759.

63. Bryan, A. W., Starner-Kreinbrink, J. L., Hosur, R., Clark, P. L., & Berger, B. (2011). Structure-based prediction reveals capping motifs that inhibit β-helix aggregation. *Proceedings of the National Academy of Sciences of the United States of America*, *108*(27), 11099–11104.

64. Bendheim, P. E., Brown, H. R., Rudelli, R. D., Scala, L. J., Goller, N. L., Wen, G. Y., Kascsak, R. J., Cashman, N. R., & Bolton, D. C. (1992). Nearly ubiquitous tissue distribution of the scrapie agent precursor protein. *Neurology*, *42*(1), 149–156.

65. Salès, N., Rodolfo, K., Hässig, R., Faucheux, B., Di Giamberardino, L., & Moya, K. L. (1998). Cellular prion protein localization in rodent and primate brain. *The European Journal of Neuroscience*, *10*(7), 2464–2471.

66. Salès, N., Hässig, R., Rodolfo, K., Di Giamberardino, L., Traiffort, E., Ruat, M., Frétier, P., & Moya, K. L. (2002). Developmental expression of the cellular prion protein in elongating axons. *The European Journal of Neuroscience*, *15*(7), 1163–1177.

67. Herms, J., Tings, T., Gall, S., Madlung, A., Giese, A., Siebert, H., Schürmann, P., Windl, O., Brose, N., & Kretzschmar, H. (1999). Evidence of presynaptic location and function of the prion protein. *The Journal of Neuroscience: The Official Journal of the Society for Neuroscience*, *19*(20), 8866–8875.

68. Mironov, A., Latawiec, D., Wille, H., Bouzamondo-Bernstein, E., Legname, G., Williamson, R. A., Burton, D., DeArmond, S. J., Prusiner, S. B., & Peters, P. J. (2003). Cytosolic Prion Protein in Neurons. *Journal of Neuroscience*, *23*(18), 7183–7193.

69. Haeberlé, A., Ribaut-Barassin, C., Bombarde, G., Mariani, J., Hunsmann, G., Grassi, J., & Bailly, Y. (2000). Synaptic prion protein immuno-reactivity in the rodent cerebellum. *Microscopy Research and Technique*, *50*, 66–75.

70. Um, J. W., Nygaard, H. B., Heiss, J. K., Kostylev, M. A., Stagi, M., Vortmeyer, A., Wisniewski, T., Gunther, E. C., & Strittmatter, S. M. (2012). Alzheimer amyloid-β oligomer bound to postsynaptic prion protein activates Fyn to impair neurons. *Nature Neuroscience*, *15*(9), 1227–1235.

71. Bate, C., Nolan, W., McHale-Owen, H., & Williams, A. (2016). Sialic Acid within the Glycosylphosphatidylinositol Anchor Targets the Cellular Prion Protein to Synapses. *The Journal of Biological Chemistry*, *291*(33), 17093–17101.

72. Jeffrey, M., Halliday, W. G., Bell, J., Johnston, A. R., MacLeod, N. K., Ingham, C., Sayers, A. R., Brown, D. A., & Fraser, J. R. (2000). Synapse loss associated with abnormal PrP precedes neuronal degeneration in the scrapie-infected murine hippocampus. *Neuropathology and Applied Neurobiology*, *26*(1), 41–54.

73. Šišková, Z., Reynolds, R. A., O'Connor, V., & Perry, V. H. (2013). Brain Region Specific Pre-Synaptic and Post-Synaptic Degeneration Are Early Components of Neuropathology in Prion Disease. *PLOS ONE*, *8*(1), e55004.

74. Collinge, J., Whittington, M. A., Sidle, K. C. L., Smith, C. J., Palmer, M. S., Clarke, A. R., & Jefferys, J. G. R. (1994). Prion protein is necessary for normal synaptic function. *Nature*, *370*(6487), 295–297.

75. Manson, J. C., Hope, J., Clarke, A. R., Johnston, A., Black, C., & MacLeod, N. (1995). PrP gene dosage and long term potentiation. *Neurodegeneration: A Journal for Neurodegenerative Disorders, Neuroprotection, and Neuroregeneration*, *4*(1), 113–114.

76. Bliss, T. V. P., & Collingridge, G. L. (1993). A synaptic model of memory: Long-term potentiation in the hippocampus. *Nature*, *361*(6407), 31–39.

77. Büeler, H., Fischer, M., Lang, Y., Bluethmann, H., Lipp, H. P., DeArmond, S. J., Prusiner, S. B., Aguet, M., & Weissmann, C. (1992). Normal development and behaviour of mice lacking the neuronal cell-surface PrP protein. *Nature*, *356*(6370), 577–582.

78. Lugaresi, E., Medori, R., Montagna, P., Baruzzi, A., Cortelli, P., Lugaresi, A., Tinuper, P., Zucconi, M., & Gambetti, P. (1986). Fatal Familial Insomnia and Dysautonomia with Selective Degeneration of Thalamic Nuclei. *New England Journal of Medicine*, *315*(16), 997–1003.

79. Mastrianni, J. A., Nixon, R., Layzer, R., Telling, G. C., Han, D., DeArmond, S. J., & Prusiner, S. B. (1999). Prion protein conformation in a patient with sporadic fatal insomnia. *The New England Journal of Medicine*, *340*(21), 1630–1638.

80. Tobler, I., Gaus, S. E., Deboer, T., Achermann, P., Fischer, M., Rülicke, T., Moser, M., Oesch, B., McBride, P. A., & Manson, J. C. (1996). Altered circadian activity rhythms and sleep in mice devoid of prion protein. *Nature*, *380*(6575), 639–642.

81. Mercer, R. C. C., Ma, L., Watts, J. C., Strome, R., Wohlgemuth, S., Yang, J., Cashman, N. R., Coulthart, M. B., Schmitt-Ulms, G., Jhamandas, J. H., & Westaway, D. (2013). The prion protein modulates A-type K+ currents mediated by Kv4.2 complexes through dipeptidyl aminopeptidase-like protein 6. *The Journal of Biological Chemistry*, *288*(52), 37241–37255.

82. Senatore, A., Colleoni, S., Verderio, C., Restelli, E., Morini, R., Condliffe, S. B., Bertani, I., Mantovani, S., Canovi, M., Micotti, E., Forloni, G., Dolphin, A. C., Matteoli, M., Gobbi, M., & Chiesa, R. (2012). Mutant PrP Suppresses Glutamatergic Neurotransmission in Cerebellar Granule Neurons by Impairing Membrane Delivery of VGCC α2δ-1 Subunit. *Neuron*, *74*(2), 300–313.

83. Herms, J. W., Korte, S., Gall, S., Schneider, I., Dunker, S., & Kretzschmar, H. A. (2000). Altered Intracellular Calcium Homeostasis in Cerebellar Granule Cells of Prion Protein-Deficient Mice. *Journal of Neurochemistry*, *75*(4), 1487–1492.

84. Fuhrmann, M., Bittner, T., Mitteregger, G., Haider, N., Moosmang, S., Kretzschmar, H., & Herms, J. (2006). Loss of the cellular prion protein affects the Ca2+ homeostasis in hippocampal CA1 neurons. *Journal of Neurochemistry*, *98*(6), 1876–1885.

85. Carulla, P., Bribián, A., Rangel, A., Gavín, R., Ferrer, I., Caelles, C., del Río, J. A., & Llorens, F. (2011). Neuroprotective role of PrPC against kainate-induced epileptic seizures and cell death depends on the modulation of JNK3 activation by GluR6/7–PSD-95 binding. *Molecular Biology of the Cell*, *22*(17), 3041–3054.

86. Maglio, L. E., Perez, M. F., Martins, V. R., Brentani, R. R., & Ramirez, O. A. (2004). Hippocampal synaptic plasticity in mice devoid of cellular prion protein. *Molecular Brain Research*, *131*(1), 58–64.

87. Rangel, A., Burgaya, F., Gavín, R., Soriano, E., Aguzzi, A., & Río, J. A. del. (2007). Enhanced susceptibility of Prnp-deficient mice to kainate-induced seizures, neuronal apoptosis, and death: Role of AMPA/kainate receptors. *Journal of Neuroscience Research*, *85*(12), 2741–2755.

88. Mitteregger, G., Vosko, M., Krebs, B., Xiang, W., Kohlmannsperger, V., Nölting, S., Hamann, G. F., & Kretzschmar, H. A. (2007). The Role of the Octarepeat Region in Neuroprotective Function of the Cellular Prion Protein. *Brain Pathology*, *17*(2), 174–183.

89. Guillot-Sestier, M.-V., Sunyach, C., Druon, C., Scarzello, S., & Checler, F. (2009). The alpha-secretase-derived N-terminal product of cellular prion, N1, displays neuroprotective function in vitro and in vivo. *The Journal of Biological Chemistry*, *284*(51), 35973–35986.

90. Chiarini, L. B., Freitas, A. R. O., Zanata, S. M., Brentani, R. R., Martins, V. R., & Linden, R. (2002). Cellular prion protein transduces neuroprotective signals. *The EMBO Journal*, *21*(13), 3317–3326.

91. Lopes, M. H., Hajj, G. N. M., Muras, A. G., Mancini, G. L., Castro, R. M. P. S., Ribeiro, K. C. B., Brentani, R. R., Linden, R., & Martins, V. R. (2005). Interaction of Cellular Prion and Stress-Inducible Protein 1 Promotes Neuritogenesis and Neuroprotection by Distinct Signaling Pathways. *Journal of Neuroscience*, *25*(49), 11330–11339.

92. Manson, J., West, J. D., Thomson, V., McBride, P., Kaufman, M. H., & Hope, J. (1992). The prion protein gene: A role in mouse embryogenesis? *Development (Cambridge, England)*, *115*(1), 117–122.

93. Tremblay, P., Bouzamondo-Bernstein, E., Heinrich, C., Prusiner, S. B., & DeArmond, S. J. (2007). Developmental expression of PrP in the post-implantation embryo. *Brain Research*, *1139*, 60–67.

94. Nuvolone, M., Hermann, M., Sorce, S., Russo, G., Tiberi, C., Schwarz, P., Minikel, E., Sanoudou, D., Pelczar, P., & Aguzzi, A. (2016). Strictly co-isogenic C57BL/6J-Prnp−/− mice: A rigorous resource for prion science. *Journal of Experimental Medicine*, *213*(3), 313–327.

95. Benvegnù, S., Roncaglia, P., Agostini, F., Casalone, C., Corona, C., Gustincich, S., & Legname, G. (2011). Developmental influence of the cellular prion protein on the gene expression profile in mouse hippocampus. *Physiological Genomics*, *43*(12), 711–725.

96. Chadi, S., Young, R., Le Guillou, S., Tilly, G., Bitton, F., Martin-Magniette, M.-L., Soubigou-Taconnat, L., Balzergue, S., Vilotte, M., Peyre, C., Passet, B., Béringue, V., Renou, J.-P., Le Provost, F., Laude, H., & Vilotte, J.-L. (2010). Brain transcriptional stability upon prion protein-encoding gene invalidation in zygotic or adult mouse. *BMC Genomics*, *11*(1), 448.

97. Bremer, J., Baumann, F., Tiberi, C., Wessig, C., Fischer, H., Schwarz, P., Steele, A. D., Toyka, K. V., Nave, K.-A., Weis, J., & Aguzzi, A. (2010). Axonal prion protein is required for peripheral myelin maintenance. *Nature Neuroscience*, *13*(3), 310–318.

98. Nishida, N., Tremblay, P., Sugimoto, T., Shigematsu, K., Shirabe, S., Petromilli, C., Erpel, S. P., Nakaoke, R., Atarashi, R., Houtani, T., Torchia, M., Sakaguchi, S., DeArmond, S. J., Prusiner, S. B., & Katamine, S. (1999). A mouse prion protein transgene rescues mice deficient for the prion protein gene from purkinje cell degeneration and demyelination. *Laboratory Investigation; a Journal of Technical Methods and Pathology*, *79*(6), 689–697.

99. Campana, V., Sarnataro, D., & Zurzolo, C. (2005). The highways and byways of prion protein trafficking. *Trends in Cell Biology*, *15*(2), 102–111.

100. Alves, R. N., Iglesia, R. P., Prado, M. B., Melo Escobar, M. I., Boccacino, J. M., Fernandes, C. F. de L., Coelho, B. P., Fortes, A. C., & Lopes, M. H. (2020). A New Take on Prion Protein Dynamics in Cellular Trafficking. *International Journal of Molecular Sciences*, *21*(20), 7763.

101. Heller, U., Winklhofer, K. F., Heske, J., Reintjes, A., & Tatzelt, J. (2003). Post-translational Import of the Prion Protein into the Endoplasmic Reticulum Interferes with Cell Viability: A CRITICAL ROLE FOR THE PUTATIVE TRANSMEMBRANE DOMAIN *. *Journal of Biological Chemistry*, *278*(38), 36139–36147.

102. Taylor, D. R., & Hooper, N. M. (2006). The prion protein and lipid rafts. *Molecular Membrane Biology*, *23*(1), 89–99.

103. Linsenmeier, L., Altmeppen, H. C., Wetzel, S., Mohammadi, B., Saftig, P., & Glatzel, M. (2017). Diverse functions of the prion protein – Does proteolytic processing hold the key? *Biochimica et Biophysica Acta (BBA) - Molecular Cell Research*, *1864*(11, Part B), 2128–2137.

104. Sarnataro, D., Pepe, A., & Zurzolo, C. (2017). Cell Biology of Prion Protein. *Progress in Molecular Biology and Translational Science*, *150*, 57–82.

105. Sarnataro, D., Caputo, A., Casanova, P., Puri, C., Paladino, S., Tivodar, S. S., Campana, V., Tacchetti, C., & Zurzolo, C. (2009). Lipid Rafts and Clathrin Cooperate in the Internalization of PrPC in Epithelial FRT Cells. *PLOS ONE*, *4*(6), e5829.

106. Taraboulos, A., Raeber, A. J., Borchelt, D. R., Serban, D., & Prusiner, S. B. (1992). Synthesis and trafficking of prion proteins in cultured cells. *Molecular Biology of the Cell*, *3*(8), 851–863.

107. Prado, M. A. M., Alves-Silva, J., Magalhães, A. C., Prado, V. F., Linden, R., Martins, V. R., & Brentani, R. R. (2004). PrPc on the road: Trafficking of the cellular prion protein. *Journal of Neurochemistry*, *88*(4), 769–781.

108. Caetano, F. A., Lopes, M. H., Hajj, G. N. M., Machado, C. F., Arantes, C. P., Magalhães, A. C., Vieira, M. D. P. B., Américo, T. A., Massensini, A. R., Priola, S. A., Vorberg, I., Gomez, M. V., Linden, R., Prado, V. F., Martins, V. R., & Prado, M. A. M. (2008). Endocytosis of Prion Protein Is Required for ERK1/2 Signaling Induced by Stress-Inducible Protein 1. *Journal of Neuroscience*, *28*(26), 6691–6702.

109. Peters, P. J., Mironov, A., Jr., Peretz, D., van Donselaar, E., Leclerc, E., Erpel, S., DeArmond, S. J., Burton, D. R., Williamson, R. A., Vey, M., & Prusiner, S. B. (2003). Trafficking of prion proteins through a caveolae-mediated endosomal pathway. *Journal of Cell Biology*, *162*(4), 703–717.

110. Schmid, S. L. (1997). CLATHRIN-COATED VESICLE FORMATION AND PROTEIN SORTING: An Integrated Process. *Annual Review of Biochemistry*, *66*(1), 511–548.

111. Taylor, D. R., & Hooper, N. M. (2007). The low-density lipoprotein receptor-related protein 1 (LRP1) mediates the endocytosis of the cellular prion protein. *Biochemical Journal*, *402*(1), 17–23.

112. Parkyn, C. J., Vermeulen, E. G. M., Mootoosamy, R. C., Sunyach, C., Jacobsen, C., Oxvig, C., Moestrup, S., Liu, Q., Bu, G., Jen, A., & Morris, R. J. (2008). LRP1 controls biosynthetic and endocytic trafficking of neuronal prion protein. *Journal of Cell Science*, *121*(6), 773–783.

113. Gauczynski, S., Nikles, D., El-Gogo, S., Papy-Garcia, D., Rey, C., Alban, S., Barritault, D., Lasmézas, C. I., & Weiss, S. (2006). The 37-kDa/67-kDa Laminin Receptor Acts as a Receptor for Infectious Prions and Is Inhibited by Polysulfated Glycanes. *The Journal of Infectious Diseases*, *194*(5), 702–709.

114. Kang, Y.-S., Zhao, X., Lovaas, J., Eisenberg, E., & Greene, L. E. (2009). Clathrin-independent internalization of normal cellular prion protein in neuroblastoma cells is associated with the Arf6 pathway. *Journal of Cell Science*, *122*(Pt 22), 4062–4069.

115. Caetano, F. A., Lopes, M. H., Hajj, G. N. M., Machado, C. F., Arantes, C. P., Magalhães, A. C., Vieira, M. D. P. B., Américo, T. A., Massensini, A. R., Priola, S. A., Vorberg, I., Gomez, M. V., Linden, R., Prado, V. F., Martins, V. R., & Prado, M. A. M. (2008). Endocytosis of Prion Protein Is Required for ERK1/2 Signaling Induced by Stress-Inducible Protein 1. *Journal of Neuroscience*, *28*(26), 6691–6702.

116. Pantera, B., Bini, C., Cirri, P., Paoli, P., Camici, G., Manao, G., & Caselli, A. (2009). PrPc activation induces neurite outgrowth and differentiation in PC12 cells: Role for caveolin-1 in the signal transduction pathway. *Journal of Neurochemistry*, *110*(1), 194–207.

117. Toni, M., Spisni, E., Griffoni, C., Santi, S., Riccio, M., Lenaz, P., & Tomasi, V. (2006). Cellular Prion Protein and Caveolin-1 Interaction in a Neuronal Cell Line Precedes Fyn/Erk 1/2 Signal Transduction. *Journal of Biomedicine and Biotechnology*, *2006*, e69469.

118. Santuccione, A., Sytnyk, V., Leshchyns'ka, I., & Schachner, M. (2005). Prion protein recruits its neuronal receptor NCAM to lipid rafts to activate p59fyn and to enhance neurite outgrowth. *Journal of Cell Biology*, *169*(2), 341–354.

119. Chesebro, B., Trifilo, M., Race, R., Meade-White, K., Teng, C., LaCasse, R., Raymond, L., Favara, C., Baron, G., Priola, S., Caughey, B., Masliah, E., & Oldstone, M. (2005). Anchorless prion protein results in infectious amyloid disease without clinical scrapie. *Science (New York, N.Y.)*, *308*(5727), 1435–1439.

120. Prusiner, S. B., Scott, M., Foster, D., Pan, K. M., Groth, D., Mirenda, C., Torchia, M., Yang, S. L., Serban, D., & Carlson, G. A. (1990). Transgenetic studies implicate interactions between homologous PrP isoforms in scrapie prion replication. *Cell*, *63*(4), 673–686.

121. Sailer, A., Büeler, H., Fischer, M., Aguzzi, A., & Weissmann, C. (1994). No propagation of prions in mice devoid of PrP. *Cell*, *77*(7), 967–968.

122. Büeler, H., Raeber, A., Sailer, A., Fischer, M., Aguzzi, A., & Weissmann, C. (1994). High Prion and PrPSc Levels but Delayed Onset of Disease in Scrapie-Inoculated Mice Heterozygous for a Disrupted PrP Gene. *Molecular Medicine*, *1*(1), 19–30.

123. Manson, J. C., Clarke, A. R., McBride, P. A., McConnell, I., & Hope, J. (1994). PrP gene dosage determines the timing but not the final intensity or distribution of lesions in scrapie pathology. *Neurodegeneration: A Journal for Neurodegenerative Disorders, Neuroprotection, and Neuroregeneration*, *3*(4), 331–340.

124. Prusiner, S. B. (1991). Molecular Biology of Prion Diseases. *Science*, *252*(5012), 1515–1522.

125. Jarrett, J. T., & Lansbury, P. T. (1993). Seeding "one-dimensional crystallization" of amyloid: A pathogenic mechanism in Alzheimer's disease and scrapie? *Cell*, *73*(6), 1055–1058.

126. Zhou, Z., & Xiao, G. (2013). Conformational conversion of prion protein in prion diseases. *Acta Biochimica et Biophysica Sinica*, *45*(6), 465–476.

127. Kocisko, D. A., Come, J. H., Priola, S. A., Chesebro, B., Raymond, G. J., Lansbury, P. T., & Caughey, B. (1994). Cell-free formation of protease-resistant prion protein. *Nature*, *370*(6489), 471–474.

128. Bessen, R. A., Kocisko, D. A., Raymond, G. J., Nandan, S., Lansbury, P. T., & Caughey, B. (1995). Non-genetic propagation of strain-specific properties of scrapie prion protein. *Nature*, *375*(6533), 698–700.

129. Priola, S. A., Chabry, J., & Chan, K. (2001). Efficient Conversion of Normal Prion Protein (PrP) by Abnormal Hamster PrP Is Determined by Homology at Amino Acid Residue 155. *Journal of Virology*, *75*(10), 4673–4680.

130. Glycosylation influences cross-species formation of protease-resistant prion protein. (2001). *The EMBO Journal*, *20*(23), 6692–6699.

131. Specific binding of normal prion protein to the scrapie form via a localized domain initiates its conversion to the protease-resistant state. (1999). *The EMBO Journal*, *18*(12), 3193–3203.

132. Graner, E., Mercadante, A. F., Zanata, S. M., Forlenza, O. V., Cabral, A. L., Veiga, S. S., Juliano, M. A., Roesler, R., Walz, R., Minetti, A., Izquierdo, I., Martins, V. R., & Brentani, R. R. (2000). Cellular prion protein binds laminin and mediates neuritogenesis. *Brain Research. Molecular Brain Research*, *76*(1), 85–92.

133. Caughey, W. S., Raymond, L. D., Horiuchi, M., & Caughey, B. (1998). Inhibition of protease-resistant prion protein formation by porphyrins and phthalocyanines. *Proceedings of the National Academy of Sciences*, *95*(21), 12117–12122.

134. Maxson, L., Wong, C., Herrmann, L. M., Caughey, B., & Baron, G. S. (2003). A solid-phase assay for identification of modulators of prion protein interactions. *Analytical Biochemistry*, *323*(1), 54–64.

135. Naslavsky, N., Stein, R., Yanai, A., Friedlander, G., & Taraboulos, A. (1997). Characterization of detergent-insoluble complexes containing the cellular prion protein and its scrapie isoform. *The Journal of Biological Chemistry*, *272*(10), 6324–6331.

136. Baron, G. S., Wehrly, K., Dorward, D. W., Chesebro, B., & Caughey, B. (2002). Conversion of raft associated prion protein to the protease-resistant state requires insertion of PrP-res (PrPSc) into contiguous membranes. *The EMBO Journal*, *21*(5), 1031–1040.

137. Sanghera, N., & Pinheiro, T. J. T. (2002). Binding of prion protein to lipid membranes and implications for prion conversion11Edited by F. Cohen. *Journal of Molecular Biology*, *315*(5), 1241–1256.

138. Taraboulos, A., Scott, M., Semenov, A., Avrahami, D., Laszlo, L., Prusiner, S. B., & Avraham, D. (1995). Cholesterol depletion and modification of COOH-terminal targeting sequence of the prion protein inhibit formation of the scrapie isoform. *Journal of Cell Biology*, *129*(1), 121–132.

139. Kaneko, K., Vey, M., Scott, M., Pilkuhn, S., Cohen, F. E., & Prusiner, S. B. (1997). COOH-terminal sequence of the cellular prion protein directs subcellular trafficking and controls conversion into the scrapie isoform. *Proceedings of the National Academy of Sciences*, *94*(6), 2333–2338.

140. Merrifield, R. B. (1963). Solid Phase Peptide Synthesis. I. The Synthesis of a Tetrapeptide. *Journal of the American Chemical Society*, *85*(14), 2149–2154.

141. Merrifield, R. B. (1985). Solid Phase Synthesis (Nobel Lecture). *Angewandte Chemie International Edition in English*, *24*(10), 799–810.

142. Palomo, J. M. (2014). Solid-phase peptide synthesis: An overview focused on the preparation of biologically relevant peptides. *RSC Adv.*, *4*(62), 32658–32672.

143. Merrifield, B. (1986). Solid Phase Synthesis. *Science*, *232*(4748), 341–347.

144. Schnölzer, M., Alewood, P., Jones, A., Alewood, D., & Kent, S. B. (1992). In situ neutralization in Boc-chemistry solid phase peptide synthesis. Rapid, high yield assembly of difficult sequences. *International Journal of Peptide and Protein Research*, *40*(3–4), 180–193.

145. Pedersen, S. L., Tofteng, A. P., Malik, L., & Jensen, K. J. (2012). Microwave heating in solid-phase peptide synthesis. *Chemical Society Reviews*, *41*(5), 1826–1844.

146. Muir, T. W. (2003). Semisynthesis of Proteins by Expressed Protein Ligation. *Annual Review of Biochemistry*, *72*(1), 249–289.

147. Dyckes, D. F., Creighton, T., & Sheppard, R. C. (1974). Spontaneous Re-formation of a Broken Peptide Chain. *Nature*, *247*(5438), 202–204.

148. Homandberg, G. A., & Laskowski, M. (1979). Enzymic resynthesis of the hydrolyzed peptide bond(s) in ribonuclease S. *Biochemistry*, *18*(4), 586–592.

149. Vogel, K., & Chmielewski, J. (1994). Rapid and Efficient Resynthesis of Proteolyzed Triose Phosphate Isomerase. *Journal of the American Chemical Society*, *116*(24), 11163–11164.

150. Schnölzer, M., & Kent, S. B. H. (1992). Constructing Proteins by Dovetailing Unprotected Synthetic Peptides: Backbone-Engineered HIV Protease. *Science*, *256*(5054), 221–225.

151. Muir, T. W., Williams, M. J., Ginsberg, M. H., & Kent, S. B. H. (1994). Design and Chemical Synthesis of a Neoprotein Structural Model for the Cytoplasmic Domain of a Multisubunit Cell-Surface Receptor: Integrin .alpha.IIb.beta.3 (Platelet GPIIb-IIIa). *Biochemistry*, *33*(24), 7701–7708.

152. Gaertner, H. F., Rose, K., Cotton, R., Timms, D., Camble, R., & Offord, R. E. (1992). Construction of protein analogs by site-specific condensation of unprotected fragments. *Bioconjugate Chemistry*, *3*(3), 262–268.

153. Gaertner, H. F., Offord, R. E., Cotton, R., Timms, D., Camble, R., & Rose, K. (1994). Chemo-enzymic backbone engineering of proteins. Site-specific incorporation of synthetic peptides that mimic the 64-74 disulfide loop of granulocyte colony-stimulating factor. *The Journal of Biological Chemistry*, *269*(10), 7224–7230.

154. Rose, K. (1994). Facile synthesis of homogeneous artificial proteins. *Journal of the American Chemical Society*, *116*(1), 30–33.

155. Dawson, P. E., Muir, T. W., Clark-Lewis, I., & Kent, S. B. H. (1994). Synthesis of Proteins by Native Chemical Ligation. *Science*, *266*(5186), 776–779.

156. Tam, J. P., Lu, Y. A., Liu, C. F., & Shao, J. (1995). Peptide synthesis using unprotected peptides through orthogonal coupling methods. *Proceedings of the National Academy of Sciences*, *92*(26), 12485–12489.

157. Nilsson, B. L., Kiessling, L. L., & Raines, R. T. (2000). Staudinger Ligation: A Peptide from a Thioester and Azide. *Organic Letters*, *2*(13), 1939–1941.

158. Saxon, E., Armstrong, J. I., & Bertozzi, C. R. (2000). A "Traceless" Staudinger Ligation for the Chemoselective Synthesis of Amide Bonds. *Organic Letters*, *2*(14), 2141–2143.

159. Wieland, T., Bokelmann, E., Bauer, L., Lang, H. U., & Lau, H. (1953). Über Peptidsynthesen. 8. Mitteilung Bildung von S-haltigen Peptiden durch intramolekulare Wanderung von Aminoacylresten. *Justus Liebigs Annalen Der Chemie*, *583*(1), 129–149.

160. Erlanson, D. A., Chytil, M., & Verdine, G. L. (1996). The leucine zipper domain controls the orientation of AP-1 in the NFAT·AP-1·DNA complex. *Chemistry & Biology*, *3*(12), 981–991.

161. Chytil, M., Peterson, B. R., Erlanson, D. A., & Verdine, G. L. (1998). The orientation of the AP-1 heterodimer on DNA strongly affects transcriptional potency. *Proceedings of the National Academy of Sciences*, *95*(24), 14076–14081.

162. Noren, C. J., Wang, J., & Perler, F. B. (2000). Dissecting the Chemistry of Protein Splicing and Its Applications. *Angewandte Chemie International Edition*, *39*(3), 450–466.

163. Paulus, H. (2000). Protein Splicing and Related Forms of Protein Autoprocessing. *Annual Review of Biochemistry*, *69*(1), 447–496.

164. Xu, M. Q., & Perler, F. B. (1996). The mechanism of protein splicing and its modulation by mutation. *The EMBO Journal*, *15*(19), 5146–5153.

165. Chong, S., Mersha, F. B., Comb, D. G., Scott, M. E., Landry, D., Vence, L. M., Perler, F. B., Benner, J., Kucera, R. B., Hirvonen, C. A., Pelletier, J. J., Paulus, H., & Xu, M.-Q. (1997). Single-column purification of free recombinant proteins using a self-cleavable affinity tag derived from a protein splicing element. *Gene*, *192*(2), 271–281.

166. Evans, T. C., Benner, J., & Xu, M.-Q. (1999). The in Vitro Ligation of Bacterially Expressed Proteins Using an Intein from Methanobacterium thermoautotrophicum *. *Journal of Biological Chemistry*, *274*(7), 3923–3926.

167. Mathys, S., Evans, T. C., Chute, I. C., Wu, H., Chong, S., Benner, J., Liu, X.-Q., & Xu, M.-Q. (1999). Characterization of a self-splicing mini-intein and its conversion into autocatalytic N- and C-terminal cleavage elements: Facile production of protein building blocks for protein ligation. *Gene*, *231*(1), 1–13.

168. Muir, T. W., Sondhi, D., & Cole, P. A. (1998). Expressed protein ligation: A general method for protein engineering. *Proceedings of the National Academy of Sciences*, *95*(12), 6705–6710.

169. Severinov, K., & Muir, T. W. (1998). Expressed Protein Ligation, a Novel Method for Studying Protein-Protein Interactions in Transcription*. *Journal of Biological Chemistry*, *273*(26), 16205–16209.

170. Evans Jr., T. C., Benner, J., & Xu, M.-Q. (1998). Semisynthesis of cytotoxic proteins using a modified protein splicing element. *Protein Science*, *7*(11), 2256–2264.

171. Cotton, G. J., & Muir, T. W. (2000). Generation of a dual-labeled fluorescence biosensor for Crk-II phosphorylation using solid-phase expressed protein ligation. *Chemistry & Biology*, *7*(4), 253–261.

References

172. Tolbert, T. J., & Wong, C.-H. (2000). Intein-Mediated Synthesis of Proteins Containing Carbohydrates and Other Molecular Probes. *Journal of the American Chemical Society*, *122*(23), 5421–5428.

173. Mukhopadhyay, J., Kapanidis, A. N., Mekler, V., Kortkhonjia, E., Ebright, Y. W., & Ebright, R. H. (2001). Translocation of σ70 with RNA Polymerase during Transcription: Fluorescence Resonance Energy Transfer Assay for Movement Relative to DNA. *Cell*, *106*(4), 453–463.

174. Camarero, J. A., Shekhtman, A., Campbell, E. A., Chlenov, M., Gruber, T. M., Bryant, D. A., Darst, S. A., Cowburn, D., & Muir, T. W. (2002). Autoregulation of a bacterial σ factor explored by using segmental isotopic labeling and NMR. *Proceedings of the National Academy of Sciences*, *99*(13), 8536–8541.

175. Ayers, B., Blaschke, U. K., Camarero, J. A., Cotton, G. J., Holford, M., & Muir, T. W. (1999). Introduction of unnatural amino acids into proteins using expressed protein ligation. *Peptide Science*, *51*(5), 343–354.

176. Sydor, J. R., Mariano, M., Sideris, S., & Nock, S. (2002). Establishment of Intein-Mediated Protein Ligation under Denaturing Conditions: C-Terminal Labeling of a Single-Chain Antibody for Biochip Screening. *Bioconjugate Chemistry*, *13*(4), 707–712.

177. Gorodinsky, A., & Harris, D. A. (1995). Glycolipid-anchored proteins in neuroblastoma cells form detergent-resistant complexes without caveolin. *The Journal of Cell Biology*, *129*(3), 619–627.

178. Aguzzi, A., & Heppner, F. L. (2000). Pathogenesis of prion diseases: A progress report. *Cell Death and Differentiation*, *7*(10), 889–902.

179. Weissmann, C. (1994). Molecular biology of prion diseases. *Trends in Cell Biology*, *4*(1), 10–14.

180. Eberl, H., Tittmann, P., & Glockshuber, R. (2004). Characterization of recombinant, membrane-attached full-length prion protein. *The Journal of Biological Chemistry*, *279*(24), 25058–25065.

181. Hicks, M. R., Gill, A. C., Bath, I. K., Rullay, A. K., Sylvester, I. D., Crout, D. H., & Pinheiro, T. J. T. (2006). Synthesis and structural characterization of a mimetic membrane-anchored prion protein. *The FEBS Journal*, *273*(6), 1285–1299.

182. Ball, H. L., King, D. S., Cohen, F. E., Prusiner, S. B., & Baldwin, M. A. (2001). Engineering the prion protein using chemical synthesis. *The Journal of Peptide Research: Official Journal of the American Peptide Society*, *58*(5), 357–374.

183. Musiol, H.-J., Dong, S., Kaiser, M., Bausinger, R., Zumbusch, A., Bertsch, U., & Moroder, L. (2005). Toward semisynthetic lipoproteins by convergent strategies based on click and ligation chemistry. *Chembiochem: A European Journal of Chemical Biology*, *6*(4), 625–628.

184. Olschewski, D., Seidel, R., Miesbauer, M., Rambold, A. S., Oesterhelt, D., Winklhofer, K. F., Tatzelt, J., Engelhard, M., & Becker, C. F. W. (2007). Semisynthetic Murine Prion Protein Equipped with a GPI Anchor Mimic Incorporates into Cellular Membranes. *Chemistry & Biology*, *14*(9), 994–1006.

185. Chu, N. K., Shabbir, W., Bove-Fenderson, E., Araman, C., Lemmens-Gruber, R., Harris, D. A., & Becker, C. F. W. (2014). A C-terminal Membrane Anchor Affects the Interactions of Prion Proteins with Lipid Membranes. *The Journal of Biological Chemistry*, *289*(43), 30144–30160.

186. Araman, C., Thompson, R. E., Wang, S., Hackl, S., Payne, R. J., & Becker, C. F. W. (2017). Semisynthetic prion protein (PrP) variants carrying glycan mimics at position 181 and 197 do not form fibrils. *Chemical Science*, *8*(9), 6626–6632.

187. Matveenko, M., Hackl, S., & Becker, C. F. W. (2018). Utility of the Phenacyl Protecting Group in Traceless Protein Semisynthesis through Ligation–Desulfurization Chemistry. *ChemistryOpen*, *7*(1), 106–110.

188. Becker, C. F. W., Liu, X., Olschewski, D., Castelli, R., Seidel, R., & Seeberger, P. H. (2008). Semisynthesis of a Glycosylphosphatidylinositol-Anchored Prion Protein. *Angewandte Chemie International Edition*, *47*(43), 8215–8219.

189. Olschewski, D., & Becker, C. F. W. (2008). Chemical synthesis and semisynthesis of membrane proteins. *Molecular BioSystems*, *4*(7), 733–740.

190. Chu, N. K., & Becker, C. F. W. (2009). Semisynthesis of membrane-attached prion proteins. *Methods in Enzymology*, *462*, 177–193.

191. Chu, N. K., Olschewski, D., Seidel, R., Winklhofer, K. F., Tatzelt, J., Engelhard, M., & Becker, C. F. W. (2010). Protein immobilization on liposomes and lipid-coated nanoparticles by protein trans-splicing. *Journal of Peptide Science: An Official Publication of the European Peptide Society*, *16*(10), 582–588.

192. Chu, N. K., & Becker, C. F. W. (2013). Recombinant expression of soluble murine prion protein for C-terminal modification. *FEBS Letters*, *587*(5), 430–435.

193. Zacharias, D. A., Violin, J. D., Newton, A. C., & Tsien, R. Y. (2002). Partitioning of lipid-modified monomeric GFPs into membrane microdomains of live cells. *Science (New York, N.Y.)*, *296*(5569), 913–916.

194. Martin, D. D., Xu, M. Q., & Evans, T. C. (2001). Characterization of a naturally occurring trans-splicing intein from Synechocystis sp. PCC6803. *Biochemistry*, *40*(5), 1393–1402.

195. Kaneko, K., Wille, H., Mehlhorn, I., Zhang, H., Ball, H., Cohen, F. E., Baldwin, M. A., & Prusiner, S. B. (1997). Molecular properties of complexes formed between the prion protein and synthetic peptides. *Journal of Molecular Biology*, *270*(4), 574–586.

196. Li, A., Christensen, H. M., Stewart, L. R., Roth, K. A., Chiesa, R., & Harris, D. A. (2007). Neonatal lethality in transgenic mice expressing prion protein with a deletion of residues 105-125. *The EMBO Journal*, *26*(2), 548–558.

197. Christensen, H. M., & Harris, D. A. (2009). A deleted prion protein that is neurotoxic in vivo is localized normally in cultured cells. *Journal of Neurochemistry*, *108*(1), 44–56.

198. Hackl, S. (2019). *The impact of membrane composition on conformation and trafficking of lipidated prion protein (PrP) variants*.

References

199. Lee, P. Y., Costumbrado, J., Hsu, C.-Y., & Kim, Y. H. (2012). Agarose Gel Electrophoresis for the Separation of DNA Fragments. *Journal of Visualized Experiments : JoVE*, *62*, 3923.

200. Roy, S., & Kumar, V. (2012). *A Practical Approach on SDS PAGE for Separation of Protein*. *3*(8), 6.

201. Laemmli, U. K. (1970). Cleavage of Structural Proteins during the Assembly of the Head of Bacteriophage T4. *Nature*, *227*(5259), 680–685.

202. Miles, A. J., Janes, R. W., & Wallace, B. A. (2021). Tools and methods for circular dichroism spectroscopy of proteins: A tutorial review. *Chemical Society Reviews*, *50*(15), 8400–8413.

203. Böhm, G., Muhr, R., & Jaenicke, R. (1992). Quantitative analysis of protein far UV circular dichroism spectra by neural networks. *Protein Engineering*, *5*(3), 191–195.

204. Bird, I. M. (1989). High performance liquid chromatography: Principles and clinical applications. *British Medical Journal*, *299*(6702), 783–787.

205. Baloch, S. (n.d.). *Review on Methods and Applications of High-Performance Liquid Chromatography*. *858*, 3.

206. Finehout, E. J., & Lee, K. H. (2004). An introduction to mass spectrometry applications in biological research. *Biochemistry and Molecular Biology Education*, *32*(2), 93–100.

207. Spriestersbach, A., Kubicek, J., Schäfer, F., Block, H., & Maertens, B. (2015). Purification of His-Tagged Proteins. *Methods in Enzymology*, *559*, 1–15.

208. Corrêa, D., & Ramos, C. (2009). The use of circular dichroism spectroscopy to study protein folding, form and function. *African Journal of Biochemistry Research*, *3*, 164–173.

209. Safar, J., Roller, P. P., Gajdusek, D. C., & Gibbs, C. J. (1993). Conformational transitions, dissociation, and unfolding of scrapie amyloid (prion) protein. *The Journal of Biological Chemistry*, *268*(27), 20276–20284.

210. N. K. Chu, Dissertation, 2013.

211. Maiti, N. R., & Surewicz, W. K. (2001). The role of disulfide bridge in the folding and stability of the recombinant human prion protein. *The Journal of Biological Chemistry*, *276*(4), 2427–2431.

212. New England Biolabs Inc. (2021). *Restriction Maps pTXB1*. https://international.neb.com/-/media/nebus/page-images/tools-and-resources/interactive-tools/dna-sequences-and-maps/ptxb1_map.pdf?rev=1e4526af0318415f9a9466b8d05b6e90&hash=E376C536A8FC8A1B4EBCA9D3C3D3129D

213. Paulick, M. G., & Bertozzi, C. R. (2008). The Glycosylphosphatidylinositol Anchor: A Complex Membrane-Anchoring Structure for Proteins. *Biochemistry*, *47*(27), 6991–7000.

214. Deleault, N. R., Walsh, D. J., Piro, J. R., Wang, F., Wang, X., Ma, J., Rees, J. R., & Supattapone, S. (2012). Cofactor molecules maintain infectious conformation and restrict strain properties in purified prions. *Proceedings of the National Academy of Sciences of the United States of America*, *109*(28), E1938-1946.

215. Supattapone, S. (2014). Synthesis of High Titer Infectious Prions with Cofactor Molecules. *Journal of Biological Chemistry*, *289*(29), 19850–19854.

216. Wang, F., Yang, F., Hu, Y., Wang, X., Wang, X., Jin, C., & Ma, J. (2007). Lipid interaction converts prion protein to a PrPSc-like proteinase K-resistant conformation under physiological conditions. *Biochemistry*, *46*(23), 7045–7053.

217. Hoffmann, S. V., Fano, M., & van de Weert, M. (2016). Circular Dichroism Spectroscopy for Structural Characterization of Proteins. In A. Müllertz, Y. Perrie, & T. Rades (Eds.), *Analytical Techniques in the Pharmaceutical Sciences* (pp. 223–251). Springer.

218. Waters Corporation. (2022, January 2). *How Does High Performance Liquid Chromatography Work? | Waters*. https://www.waters.com/waters/en_US/How-Does-High-Performance-Liquid-Chromatography-Work%3F/nav.htm?cid=10049055&locale=en_US

6 Appendix

6.1 Nucleotide and amino acid sequences

6.1.1 pTXB1-*Mxe* GyrA intein-His-CBD bvPrP (aa 23-231) via *Nde*I/*Spe*I

```
  1  TATGAAAAAACGTCCGAAACCGGGTGGTTG
 31  GAACACCGGTGGTTCTCGTTACCCGGGTCA
 61  GGGTTCTCCGGGTGGTAACCGTTACCCGCC
 91  GCAGGGTGGTGGTACCTGGGGTCAGCCGCA
121  CGGTGGTGGTTGGGGTCAGCCGCACGGTGG
151  TGGTTGGGGTCAGCCGCACGGTGGTGGTTG
181  GGGTCAGCCGCACGGTGGTGGTTGGGGTCA
211  GGGTGGTGGTACCCACAACCAGTGGAACAA
241  ACCGTCTAAACCGAAAACCAACATGAAACA
271  CGTTGCTGGTGCTGCTGCTGCTGGTGCTGT
301  TGTTGGTGGTCTGGGTGGTTACATGCTGGG
331  TTCTGCTATGTCTCGTCCGATGATCCACTT
361  CGGTAACGACTGGGAAGACCGTTACTACCG
391  TGAAAACATGAACCGTTACCCGAACCAGGT
421  TTACTACCGTCCGGTTGACCAGTACAACAA
451  ACCAGAACAACTTCGTTCACGACTGCGTTA
481  ACATCACCATCAAACAGCACACCGTTACCA
511  CCACCACCAAAGGTGAAAACTTCACCGAAA
541  CCGACGTTAAAATGATGGAACGTGTTGTTG
571  AACAGATGTGCGTTACCCAGTACCAGAAAG
601  AATCTCAGGCTTACTACGAAGGTCGTTCTT
631  CT
```

```
  1  MKKRPKPGGWNTGGSRYPGQGSPGGNRYPP
 31  QGGGTWGQPHGGGWGQPHGGGWGQPHGGGW
 61  GQPHGGGWGQGGGTHNQWNKPSKPKTNMKH
 91  VAGAAAAGAVVGGLGGYMLGSAMSRPMIHF
121  GNDWEDRYYRENMNRYPNQVYYRPVDQYNN
151  QNNFVHDCVNITIKQHTVTTTTKGENFTET
181  DVKMMERVVEQMCVTQYQKESQAYYEGRSS
```

6.1.2 Amino acid sequence *Mxe* GyrA intein-His-CBD

```
  1  CITGDALVALPEGESVRIADIVPGARPNSD
 31  NAIDLKVLDRHGNPVLADRLFHSGEHPVYT
 61  VRTVEGLRVTGTANHPLLCLVDVAGVPTLL
 91  WKLIDEIKPGDYAVIQRSAFSVDCAGFARG
121  KPEFAPTTYTVGVPGLVRFLEAHHRDPDAQ
151  AIADELTDGRFYYAKVASVTDAGVQPVYSL
181  RVDTADHAFITNGFVSHATGLTGIHHHHHH
211  HSGLNSGLTTNPGVSAWQVNTAYTAGQLVT
241  YNGKTYKCLQPHTSLAGWEPSNVPALWQLQ
```

6.2 pTXB1 vector map
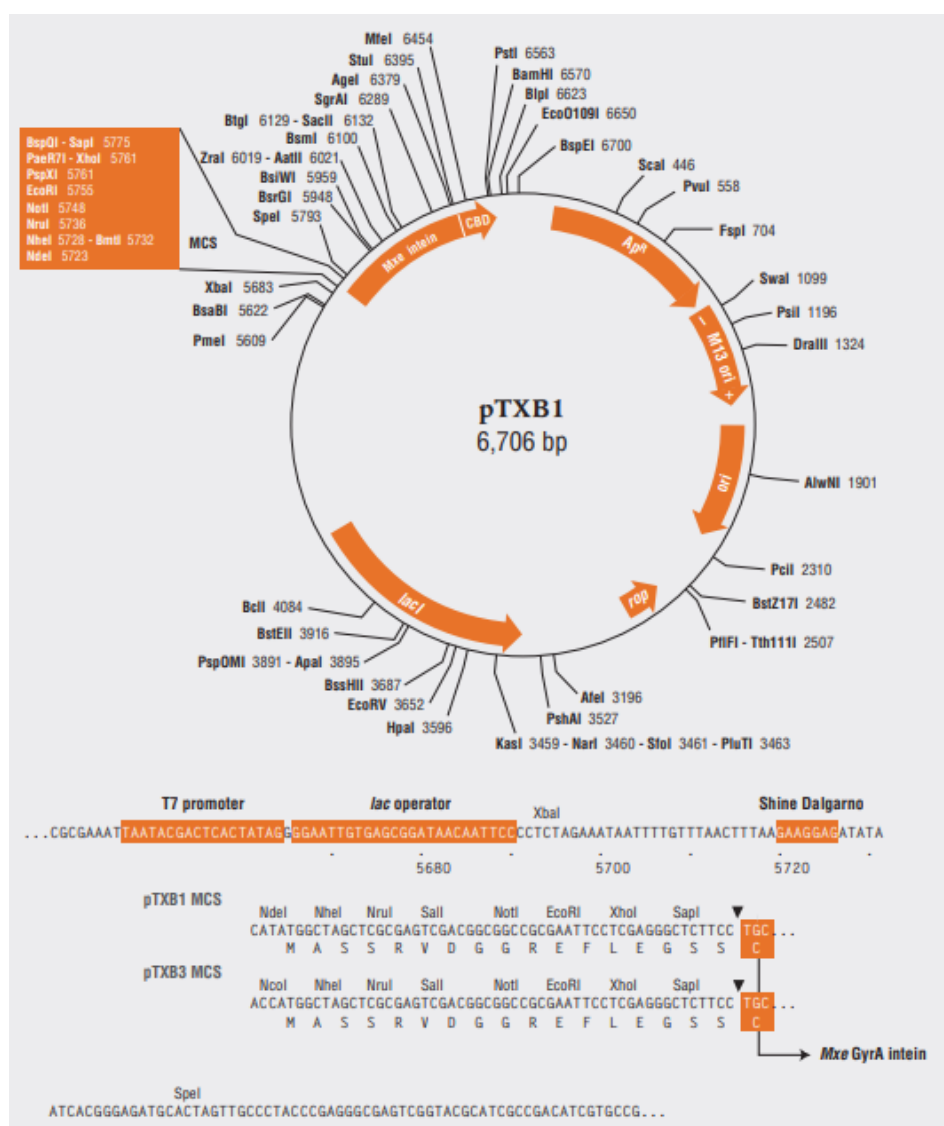
Figure 19: pTXB1 vector map including restriction sites.[212]
(New England Biolabs Inc., 2021)

89

7 Abbreviations

aa   amino acid

APS   ammonium persulfate

Boc   high performance liquid chromatography

BSE   Bovine Spongiform Encephalopathy

bvPrP   Bank vole prion protein

cAMP   cyclic adenine monophosphate

CBD   chitin binding domain

CCV   clathrin-coated vesicles

CD   circular dichroism

CDI   1,1-carbonyldiimidazole

CJD   Creuzfeldt-Jakob disease

CFC   Cell-free conversion

CME   clathrin mediated endocytosis

Cryo-EM   Cryo electron microscopy

DCC   dicyclohexylcarbodiimide

DCM   dichloromethane

DIC   Diisopropylcarbodiimide

DIPEA   N,N-diisopropylethylamine

DMF   N,N-dimethylformamide

DOPC   Dioleoylphosphatidylcholine

EGFP   enhanced green fluorescent protein

EPL   expressed protein ligation

ER   endoplasmic reticulum

ERK1/2   extracellular signal-regulated kinases 1/2

ESI-MS   Electrospray ionisation mass spectrometry

FFI   Fatal Familial Insomnia

Fmoc   fluoren-9-ylmethoxycarbonyl

FSE	Feline spongiform encephalopathy
FTIR	Fourier transform infrared
GABA	gamma-aminobutyric acid
Gdn·HCl	guanidine hydrochloride
GPI	glycosylphosphatidylinositol
GSS	Gerstman-Sträussler-Scheinker
HATU	N-{(Dimethylamino)-1H-1,2,3-triazolo [4,5-b]-pyridino-1-ylmethylene}-N-methylmethan-aminium hexa- fluorophosphate
HBTU	N-[(1H-Benzotriazol-1-yl)(dimethylamino)-methylene]-N-methylmethanaminium hexafluorophosphate N-oxide
HOBt	1-hydroxybenzotriazole
HPLC	high performance liquid chromatography
hPrP	human prion protein
IPTG	isopropyl-β-D-thiogalactoside
KA	kainic acid
LC-MS	Liquid chromatography mass spectrometry
LRP	laminin receptor precursor
LRP1	low-density lipoprotein receptor-related protein 1
LTP	long term potentation
MALDI	Matrix assisted laser desorption ionization
MBHA-resin	4-methylbenzhydrylamine resin
MESNA	sodium 2-mercaptoethanesulfonate
MPAA	4-mercaptophenylacetic acid
MSA	Multiple System Atrophy
Mtt	4-methyltrityl
MWCO	Molecular weight cut off
NCL	Native Chemical Ligation
NCAM	neuronal cell adhesion molecule
Ni-NTA	nickel-nitriloacetic acid
OG	N-Octyl-ß-D-Glucopyranoside

Abbreviations

PIRIBS	parallel in-register intermolecular beta-sheet
PK	proteinase K
PMCA	protein misfolding cyclic ampification
POPG	1-palmitoyl-2oleoyl-sn-glycero-3-phospho-(1'-rac-glycerol)
PPO	polyethyleneglycol polyamide oligomer
PRNP	prion protein gene
PrP	prion protein
PrP$^{\text{C}}$	cellular prion protein
PrP$^{\text{Palm}}$	palmitoylated prion protein
PrP$^{\text{Res}}$	protease resistent prion protein
PrP$^{\text{Sc}}$	scrapie prion protein
PTM	posttranslational modification
sAHP	slow after hyperpolarization
SDS-page	sodium dodedcyl sulfate polyacrylamide gel electrophoresis
SHa	Syrian hamster
SPPS	solid phase peptide synthesis
TCEP	tris(2-carboxyethyl)phosphine
TEMED	tetramethylethylenediamine
ThT-binding	Thioflavin T binding
TIS	triisopropylsilane
TSE	Transmissible Spongiform Encephalopathies
vCJD	variant Creuzfeldt-Jakob disease
VGCC	voltage-gated calcium channel